

ABSTRACT

Title of Dissertation: PURIFICATION AND CHARACTERIZATION OF THE
RECD PROTEIN-HOMOLOGUE FROM
DEINOCOCCUS RADIODURANS

Jianlei Wang, Doctor of Philosophy, 2004

Dissertation directed by: Professor Douglas A. Julin
Department of Chemistry and Biochemistry

In many gram-negative bacteria, RecBCD enzyme is found to be responsible for double strand DNA break repair through homologous recombination. The AddAB enzyme, a RecBCD analog, is found in some gram-positive bacteria and functions in a similar way as RecBCD. A few bacteria appear to lack both RecBCD and AddAB enzymes entirely. One such organism is the bacterium *Deinococcus radiodurans*. This remarkable organism is able to survive in the presence of very high levels of radiation or DNA-damaging chemicals, levels that would overwhelm the DNA repair capacity of most other organisms.

Interestingly, the *D. radiodurans* genome does have an open reading frame that would encode a protein that is homologous to the *E. coli* RecD protein. The amino acid

sequence of this *D. radiodurans* RecD-like protein suggests that it is a helicase and therefore could function in some aspect of DNA repair, as does its *E. coli* homologue. However, the RecD protein of *D. radiodurans* must serve a different and novel function compared to the *E. coli* RecD protein.

The *D. radiodurans* RecD protein can be expressed at high levels in *E. coli* and is readily purified by chromatography on a nickel column followed by single-stranded DNA-cellulose. The purified protein exhibits DNA-dependent ATPase and DNA helicase activities. The helicase activity requires at least a 10 nucleotide single strand overhang at the 5'-end of the double strand DNA substrate to start unwinding. The helicase assay shows that *D. radiodurans* RecD-like protein unwinds dsDNA substrates catalytically, but with low processivity, even with the help of single strand binding proteins (SSB) from either *E. coli* or *D. radiodurans*. These results show that *D. radiodurans* RecD-like protein is a DNA helicase that moves with 5'-3' polarity on single-stranded DNA. The *E. coli* RecD protein was shown recently to unwind dsDNA with the same 5'-3' polarity. The low processivity of the *D. radiodurans* RecD-like protein suggests that it may function in a complex with other proteins. The identity of these proteins is not known.

We have also generated insertion mutations that are likely to disrupt all of the *recD* gene copies in the *D. radiodurans* genome after multiple generations growing in media with antibiotics. The *in vivo* effects of the insertion mutation, such as the growth curve and the sensitivity to UV radiation and DNA damaging chemicals, were studied.

PURIFICATION AND CHARACTERIZATION OF THE RECD
PROTEIN-HOMOLOGUE FROM *DEINOCOCCUS RADIODURANS*

By

Jianlei Wang

Dissertation submitted to the Faculty of the Graduate School of the
University of Maryland, College Park in partial fulfillment
of the requirements for the degree of
Doctor of Philosophy
2004

Advisory Committee:

Professor Douglas Julin, Chair/Advisor
Professor Jeff DeStefano
Professor David Fushman
Professor Norman Hansen
Professor Jason Kahn

©Copyright by
Jianlei Wang
2004

ACKNOWLEDGMENTS

It's almost the end of my enjoyable and memorable journey in the Department of Chemistry and Biochemistry, University of Maryland. I would like to express my gratitude to all the people who have helped me get towards the completion of this degree.

First, I would like to thank the department and the University for giving me this wonderful opportunity five years ago to study here. The people, resources and facility have helped me through the hard time for a student studying abroad. Second, I would like to thank all my committee members Dr. Norman Hansen, Dr Jason Kahn, and Dr. David Fushman for their valuable advice and guidance through the five years. I would like to thank Dr. Jeff DeStefano for accommodating my request and making the time to serve as the dean's representative for my committee. Most importantly, I would like to thank my advisor Dr. Douglas Julin for his support, advice, and encouragement. He is always there whenever I need help. Everything I learnt from him is valuable and lasts lifetime.

Last but not least, I would like to thank my family and friends. The support from family and friends helps me through problems and able to achieve this end today.

TABLE OF CONTENTS

	Page
List of Figures	vii
List of Tables	xi
List of Abbreviations	xii
Chapter 1 INTRODUCTION	1
1.1 RecBCD in <i>E. coli</i>	2
1.1.1 The well-known double-stranded DNA break repair function	3
1.1.2 The recently-discovered helicase activity of RecD subunit	6
1.1.3 Studies of RecBCD mutants in <i>E. coli</i>	9
1.2 Properties of <i>Deinococcus radiodurans</i> that make it so interesting	10
1.2.1 Extreme DNA damage-resistance in <i>Deinococcus radiodurans</i> R1 strain	11
1.2.2 Previous work on <i>Deinococcus radiodurans</i>	12
1.2.3 What the genome project of <i>Deinococcus radiodurans</i> revealed	14
1.2.4 A RecD-like homologue is found in <i>Deinococcus radiodurans</i> , but no RecB and RecC	16
1.2.5 The possible functions the RecD-like protein might have by sequence alignment with other well-known proteins	17
1.3 Orthology of homologous RecD-like proteins in evolutionarily different species	19
1.3.1 Species group with RecBCD holoenzyme	19
1.3.2 Species group without RecBCD	21

1.4	The significance of this project	23
Chapter 2 CLONING RECD FROM <i>DEINOCOCCUS RADIODURANS</i> AND EXPRESSION OF THE PROTEIN IN <i>E. COLI</i>		25
2.1	Introduction	25
2.2	Materials and methods	26
2.2.1	Preparation of genomic DNA and PCR	26
2.2.2	Construction of the plasmid expressing the N-terminal His-tagged RecD protein	29
2.2.3	Construction of the plasmid expressing the C-terminal His-tagged RecD protein	29
2.2.4	RecD protein expression and solubility test	31
2.2.5	Purification of His-tagged RecD proteins	33
2.3	Results	36
2.3.1	Construction of the plasmids	36
2.3.2	Induction under different conditions	39
2.3.3	Solubility test	41
2.3.4	Purification behavior	43
2.3.5	The purified C-terminal His-tagged RecD protein	46
2.4	Discussion	48
2.4.1	The effect of His-tag location on its affinity	48
2.4.2	The significantly tight binding of RecD protein on ss-DNA cellulose column	48
2.4.3	Stability	49
2.4.4	Conclusion	49

Chapter 3	BIOCHEMICAL STUDY OF RECD <i>IN VITRO</i>	51
3.1	Introduction	51
3.2	Materials and methods	52
3.2.1	ATPase assay	52
3.2.2	Helicase assay	54
3.2.3	Gel mobility shift experiment	59
3.2.4	The assays with lower pH	60
3.3	Results	61
3.3.1	ssDNA-dependent ATPase	61
3.3.2	DNA helicase with low processivity	62
3.3.3	The binding of RecD to DNA substrates	73
3.3.4	Lower pH (pH 6.5) works better than pH 7.5	76
3.3.5	K_d for the binding at different pH	86
3.4	Discussion	89
3.4.1	Structure-related substrate preference	90
3.4.2	Unwinding in different conditions	91
3.4.3	The rates determined in our study	92
3.4.4	Monomer or dimer?	93
Chapter 4	BIOLOGICAL STUDY OF RECD FUNCTION <i>IN VIVO</i>	97
4.1	Introduction	97
4.2	Materials and methods	99
4.2.1	PCR-blunt plasmids with <i>recD</i> fragment insertions	99

4.2.2	The <i>Deinococcus radiodurans</i> mutants with different RecD truncations by homologous recombination	103
4.2.3	The phenotype of the mutants	104
4.3	Results	106
4.3.1	The five pCR-blunt plasmids with various insertions	106
4.3.2	The <i>recD</i> locus disrupted mutants of <i>Deinococcus radiodurans</i>	108
4.3.3	The phenotype changes of mutants (1) and (3)	113
4.4	Discussion	122
 Chapter 5 DISCUSSION AND CONCLUSION		 124
5.1	The RecD-like protein compared to RecD subunit	125
5.2	The Characteristics of C-terminal His-tagged RecD for its binding to resin and solubility may reveal some structural properties of RecD	126
5.3	Difference in helicase activities with short (20bp) and longer (52 or 76 bp) dsDNA substrates and the requirement for the ssDNA 5'-overhang	127
5.4	The lack of apparent difference in the phenotypes between wild type and <i>recD</i> mutants of <i>Deinococcus radiodurans</i>	129
5.5	Conclusion	130
 BIBLIOGRAPHY		 132

LIST OF FIGURES

		Page
Figure 1.1	Double-stranded DNA break repair model of homologous recombination by RecBCD	5
Figure 1.2	The bipolar DNA helicase translocation model of RecBCD	8
Figure 1.3	Schematic structure of RecD proteins	18
Figure 1.4	The Cluster of Orthologous Groups tree	20
Figure 1.5	Distribution of the RecBCD and AddAB enzymes in eubacterial genomes	22
Figure 2.1	The pair of primers used to amplify the <i>recD</i> gene from the <i>D. radiodurans</i> genome	28
Figure 2.2	The pair of primers used to change the location of His-tag to RecD C-terminus	30
Figure 2.3	PCR products with 1 kb DNA ladder on 1% agarose gel stained with ethidium bromide	37
Figure 2.4	Plasmid pDr-recD.ptz and its double digestion (<i>EcoR I</i> and <i>BamH I</i>) product on a 1% agarose gel with 1kb DNA ladder	38
Figure 2.5	The PCR to introduce an Xho I site right behind the last amino acid of the RecD protein	39
Figure 2.6	10 % SDS-PAGE gel for the time course expression of RecD protein at 1 mM IPTG and 37 °C	40
Figure 2.7	10 % SDS-PAGE gel for the time course expression of RecD protein at 0.5 mM IPTG and 30 °C	41
Figure 2.8	10 % SDS-PAGE gel for the solubility test of RecD proteins expressed in two different conditions	42
Figure 2.9	10 % SDS-PAGE gel for denatured purification of N-terminal His-tagged RecD protein	43
Figure 2.10	10 % SDS-PAGE gels for native C-terminal His-tagged RecD protein from a nickel column	44

Figure 2.11	10 % SDS-PAGE gels for native C-terminal His-tagged RecD protein from an ssDNA column	45
Figure 2.12	10 % SDS-PAGE gel of RecD proteins from the two-step purification with 10 kDa protein ladder	47
Figure 3.1	The eight oligomers designed for the helicase assay	55
Figure 3.2	The design for the 52 and 76 bp duplexes with a 5'-single-stranded 12 nt tail	58
Figure 3.3	The design for the three hairpin structures	59
Figure 3.4	ATP hydrolysis by RecD on TLC membrane	61
Figure 3.5	DNA unwinding by <i>D. radiodurans</i> RecD enzyme	63
Figure 3.6	Unwinding at various RecD concentrations for the 20 bp 5'-tailed substrate	64
Figure 3.7	The calculation of the reaction rate of the unwinding reactions of the 20 bp 5'-tailed substrate	65
Figure 3.8	Unwinding at various RecD concentrations for the 20 bp fork-shaped substrate	66
Figure 3.9	The calculation of the reaction rate of the unwinding reactions of the 20 bp forked substrate	67
Figure 3.10	Effect of 5'-single-strand length on DNA unwinding	69
Figure 3.11	The % unwound vs. time plots for the effect of 5'-single-strand extension length on DNA unwinding	70
Figure 3.12	Time-course unwinding of 52 bp duplex	71
Figure 3.13	Unwinding of 52 and 76 bp duplexes at pH 7.5	72
Figure 3.14	The binding between RecD and dsDNA hairpins with different ssDNA ends	74
Figure 3.15	The quantitation of the gel shift experiment shown in figure 3.14	75
Figure 3.16	pH dependence of 52 bp substrate unwinding	77

Figure 3.17	Time-course unwinding of 52 bp duplex at pH 6.5	78
Figure 3.18	Unwinding of 52 bp duplex	79
Figure 3.19	Unwinding of 52 bp duplex at pH 7.5, with SSB protein from <i>D. radiodurans</i>	81
Figure 3.20	ATP hydrolysis by RecD at different pHs	82
Figure 3.21	Effect of different pHs on DNA binding	85
Figure 3.22	The binding of RecD to 12 nt hairpin DNA at different pHs	87
Figure 3.23	Assessment of K_{dS} at different pHs	88
Figure 3.24	The equation used for the simulation of the data from reaction at pH 8.3	89
Figure 3.25	The schematic illustration of the possible role Pfh1 has in DNA replication	91
Figure 4.1	The schematic illustration of the method used to knockout targeted genes in <i>D. radiodurans</i>	98
Figure 4.2	The schematic structure of plasmid pCR-blunt and the partial restriction map	100
Figure 4.3	Part of the restriction map for plasmid pDR-recD.ptz	101
Figure 4.4	The <i>EcoR</i> I digestion products from the five newly constructed pCR- blunt plasmids	107
Figure 4.5	The four primers designed to verify the insertion of plasmid into genome of <i>D. radiodurans</i>	108
Figure 4.6	The locations of the four primers designed to verify the plasmid insertion	109
Figure 4.7	The lengths for the expected PCR products from mutant (1), (2) and (3) amplified by the designed two pairs of primers	110
Figure 4.8	5'-end PCR products from genomic DNAs of <i>D. radiodurans</i> wild type and mutants	111
Figure 4.9	3'-end and whole <i>recD</i> gene PCR products from genomic DNAs of <i>D. radiodurans</i> wild type and mutants	112

Figure 4.10	The growth curves for <i>D. radiodurans</i> wild type and mutants (1) and (3)	114
Figure 4.11	The logOD ₆₀₀ vs. time plot for the growth curves shown in figure 4.10	115
Figure 4.12	The comparison of UV-sensitivity of <i>E. coli</i> and <i>D. radiodurans</i> wild type and mutant (1)	117
Figure 4.13	The UV survival curves for <i>D. radiodurans</i> wild type, mutant (1) and (3) from exponential phase	118
Figure 4.14	The UV survival curves for <i>D. radiodurans</i> wild type and mutant (1) from stationary phase	119
Figure 4.15	The five pACYC184 plasmids prepared for the exogenous DNA uptake experiment	120

LIST OF TABLES

	Page
Table 1 Unwinding rates for 20 bp and longer substrates at different pHs	84
Table 2 Efficiencies of transformation with pCR-blunt and pACYC184 plasmid series	121

LIST OF ABBREVIATIONS

ATP	Adenosine triphosphate
BSA	Bovine serum albumin
DrSSB	<i>D. radiodurans</i> single-stranded DNA binding protein
DSB	Double stranded DNA break
dsDNA	Double stranded DNA
DTT	Dithiothreitol
EcSSB	<i>E. coli</i> single-stranded DNA binding protein
EDTA	Ethylenediaminetetracetic acid
HisRecD	His-tagged RecD
IPTG	Isopropyl- β -D-thiogalactopyranoside
kb	Kilo base pairs
kDa	Kilodalton
LB	Luria-Bertani
MOPS	3-(N-morpholino)-propanesulfonic acid
OAc	Acetate
PAGE	Polyacrylamide gel electrophoresis
PCR	Polymerase chain reaction
PEG	Polyethylene glycol
PIPES	1,4 piperazine bis-(2-ethanesulfonic acid)
PMSF	phenyl methyl sulfonyl fluoride
RDR	recombination-dependent-replication & replication-dependent-recombination

SDS Sodium dodecyl sulfate

ssDNA Single stranded DNA

TLC thin layer chromatography

UV Ultraviolet

Chapter 1 INTRODUCTION

RecBCD enzyme, also called exonuclease V, plays a very important role in both preventing exogenous DNA invasion and repairing a cell's own double-stranded DNA breaks¹. Although this enzyme is widely distributed in Gram-negative bacteria² (figure 1.5), it has been most thoroughly studied in *E. coli*. As a protective mechanism, exonuclease activity embodied in RecBCD can rapidly destroy up to several kilo base pairs of exogenous DNA in seconds so that RecBCD cannot do recombinational repair to breaks with only a few kilo base pairs terminal homology to an intact DNA molecule³. By this protective mechanism, bacteria can prevent exogenous DNA with some level of homology from invading into their genome. Most importantly, RecBCD is a well-known enzyme in homologous recombination. It functions in the first step of homologous recombination by generation of a 3'-single-stranded stretch of DNA, which is the substrate for RecA protein to initiate the chain invasion to one strand of an intact homologous recipient DNA⁴. The process of homologous recombination is important not only for the maintenance of genetic stability and integrity but also for the generation of genetic diversity and the proper segregation of chromosomes.

Interestingly, the genome project for the bacterium *Deinococcus radiodurans* done in 1999 revealed that even though this bacterium has outstanding DNA double strand break repair ability, it does not have the RecBCD holoenzyme. More specifically, only a *recD*-like gene was found in its chromosome I. Our interest here is to clone and express the *D. radiodurans recD*-like gene in *E. coli* and study the biochemical activities of the RecD-like protein *in vitro*. Further, its biological functions are studied by constructing *D. radiodurans* mutants with the *recD* gene knockout.

1.1 RecBCD in *E. coli*

The complex biochemical, genetic and molecular mechanistic studies of homologous recombination in *E. coli* have found at least 25 different gene products implicated in various aspects of this process^{4,5}. It was thought that homologous recombination was only responsible for repairing damaged DNA (DSBs) and for the generation of genetic diversity. However, new studies suggest that there is a more intricate connection between recombination and replication as well^{6,7}. The two processes employ the same biochemical machinery and work in conjunction to maintain the genome. Studies show that recombination is needed to initiate *oriC*-independent replication, which arises out of collapse of the replication fork due to imperfections in the DNA template⁸. The process is referred to as “recombination-dependent-replication” (RDR) and is proposed to occur in almost every replication cycle to repair collapsed or stalled replication forks^{9,10}. The interdependence of the two processes is further exemplified by the “replication-dependent-recombination” process, which is proposed to occur during conjugation or transduction whereby a linear DNA fragment is integrated into the bacterial host genome¹¹.

Homologous recombination in *E. coli* has multiple genetic pathways, including RecBCD, RecE and RecF pathways, and none of them is totally independent because of the significant overlap in the genetic requirements¹². The major pathway for recombination is the RecBCD pathway. Analogs of this enzyme, as well as its *cis*-regulatory element Chi sequence, have been found in both gram-positive and gram-negative bacteria¹³. The RecBCD enzyme is essential for 99% of the recombination

events occurring at DSBs in wild type *E. coli*. It is also responsible for >90% of the degradation of foreign DNA^{3, 14}.

The RecBCD enzyme possesses a number of seemingly disparate enzymatic activities¹, including ssDNA exonuclease, ssDNA endonuclease, dsDNA exonuclease, DNA-dependent ATPase and DNA helicase activities. The helicase shows a marked preference for blunt or nearly blunt dsDNA ends, further distinguishing it from other helicases, which typically prefer DNA substrates with ssDNA tails¹⁵.

1.1.1 The Well-Known Double-Stranded DNA Break Repair Function

A double-stranded DNA break (DSB) that remains unrepaired is lethal for any cell or its progeny. It can be produced directly by ionizing radiation, and indirectly as a natural consequence of DNA replication on a chemically flawed template. The homologous recombination repair by RecBCD in *E. coli* is largely responsible for repair of most DSBs⁹. The RecBCD enzyme is a 330 kDa heterotrimer composed of the RecB, RecC and RecD subunits, each with their distinct biochemical activities. As a holoenzyme it functions in the first step of homologous recombination, initiation of recombination by processing of blunt ended double-stranded DNA breaks to produce a 3'-single-stranded tail^{16, 17}. Its function and biochemical activities are regulated by the octameric regulatory DNA sequence called "Chi", which plays a critical role in RecBCD mediated recombination¹⁸. Reconstructed dsDNA substrates that are heteroduplex at the Chi site proved that an actively translocating RecBCD enzyme requires only the sequence information in the 5'-GCTGGTGG-3'-containing strand to recognize and to be regulated by Chi¹⁹. This implied that the recognition of Chi occurs following the unwinding of

DNA. Some other studies suggested the concept of Chi-like sequences which constitute a class of sequences that regulate the recombination function of RecBCD enzyme²⁰.

After RecBCD binds to a double-stranded DNA end, it unwinds dsDNA and its ssDNA endonuclease activity cleaves the ssDNA that it produces simultaneously. RecBCD enzyme binds tightly to the end of a dsDNA substrate ($K_m \sim 1$ nM), unwinds it at approximately 1000 (972 \pm 172) bp per second, translocates for about 30,000 (42,300 by individual molecule study) bp before dissociating⁵, and consumes 2-3 ATP molecules per bp unwound²¹. ATP hydrolysis is required to supply energy for DNA unwinding and the subsequent dsDNA hydrolysis and Chi-dependent cleavage. Single-strand DNA hydrolysis also requires ATP, possibly to activate the enzyme allosterically.

As shown in figure 1.1, upon binding to a DSB end, the helicase and nonspecific nuclease activities of RecBCD unwind the dsDNA and degrade the 3'-terminal strand more extensively than the 5'-terminal strand. After encountering Chi, the pause of RecBCD precisely at Chi enhances the probability that a cleavage occurs in the vicinity of Chi²³. The interaction with Chi causes a functional alteration in the RecBCD enzyme, leading to inactivation of the RecD subunit^{24, 25, 26, 27}. Overall, the enzyme's 3'-5' nuclease activity is attenuated, whereas a weaker 5'-3' activity is activated and its helicase activity remains unaltered^{17, 18}. Thus, Chi not only attenuates the overall nucleolytic activity of RecBCD enzyme, but it also switches the polarity of DNA-strand degradation²⁸, which produces a 3'-terminal ssDNA with the Chi sequence at the 3'-end^{29, 30}. This type of end is optimal for RecA-protein-dependent DNA strand invasion of dsDNA and needed to prime DNA replication. Following interaction with Chi, translocating RecBCD directs the loading of DNA strand exchange protein RecA onto the

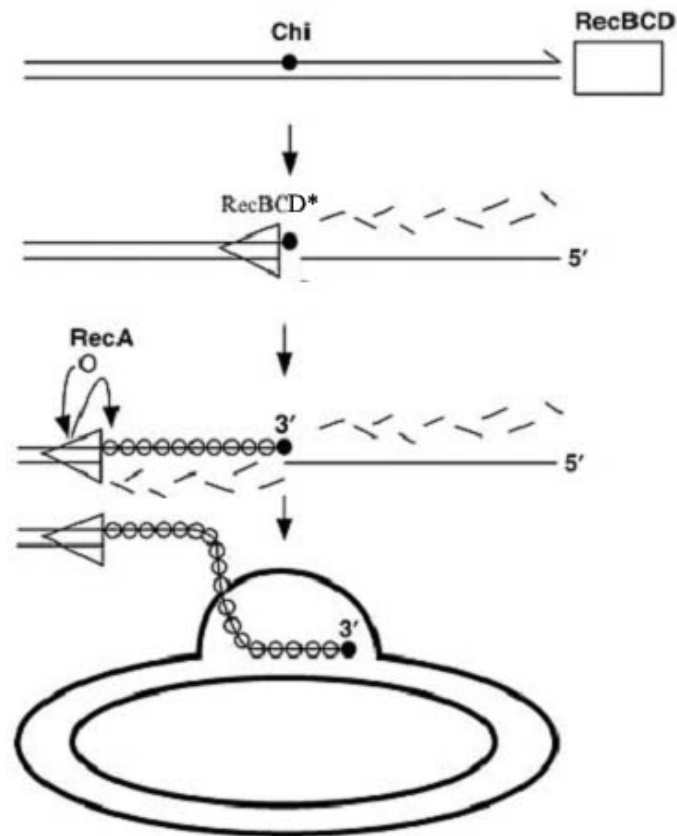


Figure 1.1 Double-strand break repair model of homologous recombination by RecBCD ²². The open box indicates RecBCD enzyme; solid dot, Chi; open triangle, RecBCD* enzyme after its encounters with Chi; small open circles, RecA protein; broken lines, DNA strands degraded by RecBCD or RecBCD* enzyme. The linear dsDNA molecule with Chi represents the donor DNA, and the circular dsDNA molecule represents the recipient DNA.

Chi-containing ssDNA ^{22, 31} and excludes the binding of inhibitory SSB protein ³².

Therefore, RecBCD contributes to the heightened invasiveness of that ssDNA. Studies showing that RecBC (lacking the RecD subunit) loads RecA protein constitutively onto

the 3'-terminal DNA strand, with no requirement for Chi suggested the inhibitory activity of RecD subunit on the RecA loading of RecBCD³³. At the completion of unwinding, the RecBCD holoenzyme is normally reactivated and can commence binding and unwinding on another DNA molecule.

1.1.2 The Recently-Discovered Helicase Activity of RecD Subunit

The RecB and RecC subunits that are encoded by *recB* and *recC* genes were previously thought to compose exonuclease V activity³⁴. Later, another polypeptide was found to be the third subunit, named RecD^{35, 36}. The *recB*, *recC*, and *recD* genes encode proteins with calculated molecular masses of 134, 129, and 67 kDa, respectively. Since the enzyme without RecD subunit (as in *recD* null mutant) promotes recombination efficiently but independently of Chi and has no nucleolytic activity, it was proposed that the products of the *recB* and *recC* genes are necessary for conjugal recombination and for repair of chromosomal DSBs in *E. coli*. The *recD* gene product with an ATPase activity is required for neither recombination nor repair. Instead, RecBCD enzyme is an exonuclease that inhibits recombination by destroying linear DNA.

In 2003, Dillingham, et al. suggested that besides the RecB subunit with a 3'-5' DNA helicase activity³⁹, which was thought to drive DNA translocation and unwinding in the RecBCD holoenzyme, purified RecD protein is also a DNA helicase with 5'-3' polarity⁴⁰. Their results showed that both of the RecB and RecD helicases are active in intact RecBCD, because the enzyme remains capable of processive DNA unwinding when either of them is inactivated by mutation. These findings suggested a bipolar translocation model for RecBCD in which the two helicases are complementary, traveling

with opposite polarities, but in the same direction, on each strand of the antiparallel DNA duplex. This bipolar motor organization helps to explain various biochemical properties of RecBCD, notably its exceptionally high speed and processivity, and offers a mechanistic insight into aspects of RecBCD function.

Later in the same year, Spies, et al.³⁰ found by observing translocation of individual enzymes along single DNA molecules that RecBCD enzyme pauses precisely at Chi, and then the enzyme continues translocating but at approximately one-half of the initial rate. They proposed that the interaction with Chi results in an enzyme in which one of the two motor subunits, likely the RecD motor, is inactivated to produce the slower translocase. Other experimental results such as a mutation in the consensus ATP-binding sequence of the RecD subunit that reduces the processivity of the RecBCD enzyme also support their proposal.

Helicases are molecular motors that move along and unwind double-stranded DNA¹⁵. As shown in figure 1.2, the RecBCD enzyme has two sets of helicase motifs in both RecB and RecD. The rapid, highly processive enzyme RecBCD unwinds DNA in an unusual manner: the 5'-ended strand forms a long single-stranded tail, whereas the 3'-ended strand forms an ever-growing single-stranded loop and short single-stranded tail. By studying individual molecules with electron microscopy it was found that RecD is a fast helicase acting on the 5'-ended strand and RecB is a slow helicase acting on the 3'-ended strand on which the single-stranded loop accumulates⁴⁰. Mutational inactivation of the helicase domain in RecB or in RecD, or removal of the RecD subunit, altered the rates of unwinding or the types of structures produced, or both⁴¹.

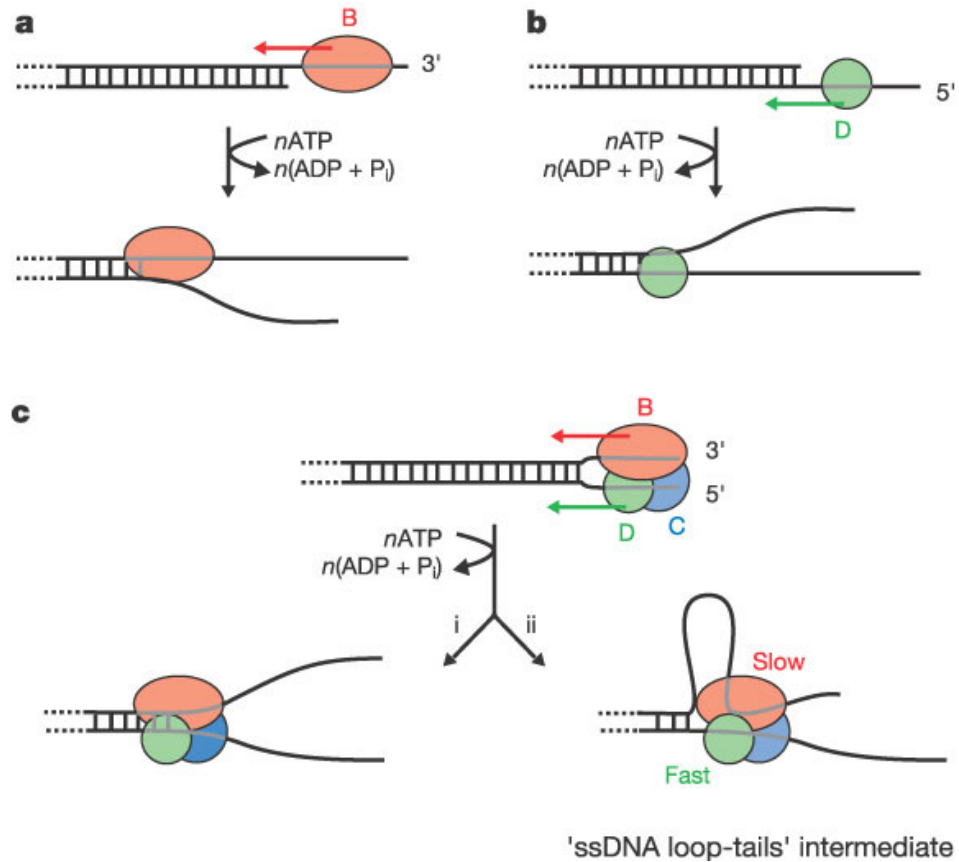


Figure 1.2 The bipolar DNA helicase translocation model of RecBCD⁴⁰. (a), RecB is a 3' -5' helicase; (b), RecD is a 5' - 3' helicase; (c), The RecB and RecD with opposite polarity complement the antiparallel DNA structure, producing cooperative movement. Pathway i: the two helicases move uniformly along the DNA, unwinding the duplex as they progress. Pathway ii: alternatively, if the motors move independently and at unequal speeds, then a bipolar translocation will generate the “ssDNA loop-tails” unwinding intermediates, which were observed by electron microscopy.

1.1.3 Studies of RecBCD Mutants in *E. coli*

The three individual subunits of RecBCD holoenzyme have been isolated, purified and characterized for their individual biochemical activities and contributions to the holoenzyme function. A large contribution in defining the function of RecBCD was the complementary data available from mutant studies.

Most mutations mapped to the *recB* and *recC* genes result in reduced recombination proficiency and some sensitivity to UV irradiation. The changes of enzymatic activities include (A) reduced helicase⁴², ds and ss exonuclease and endonuclease⁴³; (B) defect in Chi recognition, or interaction^{44, 45}; (C) defect in recombination and heteroduplex formation *in vivo*⁴⁶; (D) defect in ATP-binding and hydrolysis⁴⁷. The C-terminal 30 kDa domain of RecB is the only nuclease active site. The three residues RecB^{D1080}, RecB^{D1067} and RecB^{K1082} comprise a motif that is similar to one shown to form the active site of several restriction endonucleases^{48, 49, 50}. It suggested an unusual bipartite nature in the structural organization of RecB subunit, in which the DNA-binding and unwinding function is located in the N-terminal 100 kDa domain and the nuclease catalytic domain is located in the C-terminal 30 kDa domain⁵¹. The 30 kDa C-terminal domain of the RecB subunit also harbors a site that interacts with RecA protein, recruiting it to single-stranded DNA during unwinding - a function parallel to cellular motor proteins^{52, 53}.

Phenotypically, the mutations mapped to the *recD* gene are very similar to wild-type cells. They are fully viable, resistant to DNA-damaging agents, and recombination proficient⁴⁶. The strains with such mutations are also different from wild type by being susceptible to bacteriophage⁴⁶ and hyper-recombinogenic. The biochemical difference

between RecD mutants and wild-type RecBCD enzyme is that the mutant enzymes are devoid of any detectable ds- or ssDNA nuclease activities *in vivo* and *in vitro*^{26, 36, 54} even though the nuclease active site is located in RecB. These mutants also have either no, or a markedly lower, ability to produce a Chi-specific DNA fragment relative to the extent seen with the wild type enzyme⁵⁵ and do not promote Chi-dependent joint-molecule formation *in vitro*⁴. These findings led to the hypothesis that the RecBC enzyme, which lacks the RecD subunit, is functionally equivalent to the RecBCD enzyme after it has encountered a Chi sequence and is functionally Chi-activated⁵⁶. It reflects the regulation of RecBCD enzyme via the conformational change of the RecD subunit.

1.2 Properties of *Deinococcus radiodurans* that Make It So Interesting

Bacterium *Deinococcus radiodurans* strain R1 was the first of the *Deinobacteria* to be discovered and isolated in 1956, from canned meat that had spoiled following exposure to X rays⁵⁷. It is a red-pigmented, nonsporulating, gram-positive bacterium⁵⁸. All species in the genus *Deinococcus*, in particular *D. radiodurans*, are extremely resistant to a number of agents and conditions that damage DNA, including ionizing radiation (200 times as resistant as *E. coli*) and ultraviolet irradiation (UV) (20 times), hydrogen peroxide (about hundreds times higher compared to *E. coli*), and desiccation⁵⁹.⁶⁰ *D. radiodurans* is the most studied species in the *Deinococcus* genus since it is the only member of the family naturally transformable by homologous DNA - both high-molecular-weight chromosomal DNA and plasmid DNA^{61, 62, 63}, a property that has facilitated efforts at genetic characterization. However, characterization of this organism and the other *Deinococcaceae* has been limited by the lack of other applicable techniques,

including conjugation, protoplast fusion, or transduction for introduction of genetic markers ⁶⁴.

1.2.1 Extreme DNA Damage-Resistance in *Deinococcus radiodurans* R1 Strain

D. radiodurans exhibits an extraordinary ability to withstand the lethal and mutagenic effects of DNA damaging agents - particularly the effects of ionizing radiation. Of the many forms of damage imposed on DNA by ionizing radiation, DSBs are considered the most lethal due to the inherent difficulty in their repair, since no single-strand template remains in the double helix for accurate repair ⁶⁵. When exponential-phase cultures of *D. radiodurans* are exposed to a 5,000-Gray dose of gamma radiation, individual cells suffer massive DNA damage as shown by examining the chromosomal DNA on a pulsed-field gel ⁶⁴: the chromosomes of every *D. radiodurans* cell are cleaved into multiple, subgenomic fragments. For most species, this level of DNA damage is irreparable and lethal. However, *D. radiodurans* can reconstitute its genome from 1,000 to 2,000 DSB fragments compared to the maximum capability of *E. coli* of restoring its genome from 10 to 15 DSB fragments ^{58,66}. *D. radiodurans* can not only rebuild its genome from those DNA fragments in a short period time (90 min for 2 kGy and 180 min for 4 kGy) without loss of viability ⁶⁷ but also the survivors do not show any mutagenesis greater than that occurring after a single round of normal replication ⁶⁸. Relatively little is known about the biochemical basis for this phenomenon even though the genome of *D. radiodurans* has been released since 1999 ⁶⁹. Available evidence indicates that efficient repair of DNA damage is, in large part, responsible for its radioresistance ⁵⁹. Because

most of the DNA metabolism genes in *D. radiodurans*' genome were also found in other much more radiosensitive species, the DNA repair strategies found in other more radiosensitive organisms are not enough to explain its extreme DNA damage tolerance. The possibilities are (a) it had developed repair mechanisms that are fundamentally different from other prokaryotes, or that (b) it has the ability to utilize the conventional complement of DNA repair proteins with much higher efficiency⁶⁴, which is more likely.

Even though the multiplicity of genome in *E. coli* (four or five haploid chromosomes during vigorous exponential growth) has been shown to be necessary for the repair of double strand breaks⁷⁰, the facts that the number of genome equivalents of DNA per *D. radiodurans* cell are approximately 5 to 10⁷¹ and the sensitivity to ultraviolet light or gamma-ray was not different between the cells with different genome multiplicity⁷¹ suggest that the high efficiency of the DNA repair process in *D. radiodurans* does not totally depend on its multi-copy genome. Polyploid nature is common among prokaryotes and does not confer extreme resistance to DNA damage⁷². Thus, it is likely that *D. radiodurans* uses redundant genomic information in a manner that other organisms do not. The enzymatic basis for the radiation resistance is not well understood.

1.2.2 Previous Work on *Deinococcus radiodurans*

It has been reported that *D. radiodurans* has repair pathways of excision repair, mismatch repair, and recombination repair^{57, 59, 73}. There are changes in the cellular abundance of proteins after gamma-irradiation at 6 kGy as proved by sodium dodecyl sulfate-polyacrylamide protein gels^{74, 75}. There are at least nine proteins with enhanced

synthesis and more than thirteen proteins with reduced synthesis. Among the group of increased-synthesis proteins are probably RecA, elongation factor Tu, and KatA⁷⁶ proteins shown to be synthesized during post-irradiation incubation. While there are many predicted DNA repair genes and pathways in the *D. radiodurans* genome⁷⁷, only a few of its DNA repair enzymatic activities and/or genes have been evaluated for their biochemical activities.

It was found in 1975 that one *D. radiodurans* mutant, *rec30*, showed significant loss of DNA-damage tolerance and the ability of homologous recombination⁷⁸. Later the genome of this mutant was characterized. The result showed that the disruption of the *recA* locus was responsible for its phenotype. The sequence of *D. radiodurans* RecA protein shows greater than 50% identity to the *E. coli* RecA protein⁷⁹. Mutants with even single base pair change in this gene are highly sensitive to UV and ionizing radiation. Unlike UvrA and DNA polymerase I proteins⁸⁰, expression of *E. coli* RecA in *D. radiodurans* does not complement the RecA deficiency and appears to have no effect on *D. radiodurans*. Expression of *D. radiodurans* RecA in *E. coli* had been reported to be lethal⁸¹. However, recently it has been successfully expressed in *E. coli* with less toxicity, and it has been reported to partially complement *E. coli* RecA deficiency⁸². It is consistent with the suggestion that RecA protein from many bacterial species can functionally complement *E. coli recA* mutants. *In vitro* the *D. radiodurans* RecA protein has been shown to catalyze the spectrum of activities classically attributed to RecA proteins. However, *D. radiodurans* RecA is also distinct from other well-characterized RecAs (e.g., from the gram-negative *E. coli*) in its nucleoside triphosphatase and DNA strand exchange activities⁸³. Moreover, recent studies suggested that the co-protease

activity (RecA-based transcriptional regulation ⁵⁸) of RecA, instead of the recombination activity, actually contributes to the radiation resistance of *D. radiodurans* ⁸⁴. It has also been reported that unlike other organisms, *D. radiodurans* RecA is not present in the undamaged *Deinococcal* cell but is synthesized only following DNA damage and repair ⁸¹.

The existence of a very efficient *recA*-independent single-stranded DNA annealing repair pathway has been reported for *D. radiodurans* ⁸⁵. This pathway is active during and immediately after DNA damage and before the onset of RecA-dependent repair. It can repair about one-third of the 150 to 200 DSBs per chromosome following exposure.

It has been argued that *D. radiodurans* is endowed with enhanced repair systems that provide protection and stability. However, predicted expression levels of DNA repair proteins with the exception of RecA tend to be low and do not distinguish *D. radiodurans* from other prokaryotes ⁸⁶. Some researches attributed the capability to an unusually high number of PHX (predicted highly expressed) chaperone/degradation, protease, and detoxification genes ⁸⁷. The real reason underneath is still unknown.

1.2.3 What the genome project of *Deinococcus radiodurans* revealed

The *D. radiodurans* genome sequence was determined in 1999. There are four circular molecules in its genome: chromosome I, chromosome II, one megaplasmid, and one plasmid ⁷⁷. The gene-coding prediction by a statistical analysis program and phylogenetic studies suggested that the *Deinococci* are most closely related to the *Thermus* genus ⁸⁸, which means that the extreme DNA-damage resistance of the

Deinococci may have originated through modification of systems that evolved for resistance to heat ⁸⁹. It was proved by experiment that there is a time-dependent increase in DNA double-strand breaks in forty-one ionizing radiation-sensitive strains of *D. radiodurans* undergoing six weeks of desiccation ⁹⁰. All of the mutants exhibited a substantial loss of viability upon rehydration compared to wild type *D. radiodurans*.

The polyploid nature of *D. radiodurans* is likely an important component of its efficient homologous recombination-based repair of double-stranded DNA breaks. Another important component may be the presence of DNA repeat elements scattered throughout the genome ⁹¹. Those intergenic, ubiquitous repeats occur at a frequency comparable to the number of double-stranded DNA breaks that can be tolerated by *D. radiodurans*. A possible function of the repeats is in regulating DNA degradation after damage. DNA degradation after the introduction of double-strand breaks is an integral part of the DNA repair process in *D. radiodurans*. However, the extent of DNA degradation appears to be limited by an inhibitory protein (IrrI) that is activated shortly after DNA damage ⁹². This protein from soluble cell extracts was identified with specific recognition of the genomic repeat sequences. The binding of IrrI protein to the repeats may prevent exhaustive chromosomal degradation after radiation exposure ⁷⁷.

Other unique mechanisms in *D. radiodurans* may also contribute to its resistance to DNA damage. The damaged nucleotides can be transported out of the cell, which potentially prevents them reincorporating into the genome during repair ^{59, 93}. Some research suggested that *D. radiodurans* genome shows its redundancy in a special form that chromosomes exist in pairs, linked to each other by thousands of four-stranded (Holliday) junctions ⁹⁴. Thus, a DSB is not a lethal event when the identical undamaged

duplex is nearby, providing an accurate repair template. Some other study suggested that *D. radiodurans* genome assumes an unusual toroidal morphology⁹⁵. In this case, the diffusion of radiation-generated free DNA ends are restricted and held together within the tightly packed and laterally ordered DNA structures and the template-independent yet error-free joining of DNA breaks is facilitated.

1.2.4 A RecD-Like Homologue is Found in *Deinococcus radiodurans*, but no RecB and RecC

The proposal that *D. radiodurans* needs a DNA repair system which is different from the main RecBCD pathway in *E. coli* is verified by the accomplishment of the genome project of *D. radiodurans*. The *D. radiodurans* genome does have a predicted open reading frame that encodes a protein whose closest characterized homologues are other bacterial RecD proteins. The gene was thus annotated as the *D. radiodurans recD* gene. But neither around the putative *recD* locus nor in the whole genome are there genes in *D. radiodurans* that are homologous to *recB* and *recC* genes in *E. coli*. A *D. radiodurans recA* gene is found and the RecA protein has been characterized biochemically. Complete DSB rejoining in *D. radiodurans* is *recA* dependent, as demonstrated by the requirement for *recA* to restore chromosomal integrity from many hundreds of DNA fragments. Since the RecBCD enzyme and RecA protein play the two most important roles in the homologous recombination and repair pathway in *E. coli*, how the RecA-dependent DSB repair pathway works in *D. radiodurans* is an interesting question.

1.2.5 The Possible Functions the RecD-Like Protein Might Have by Sequence Alignment with Other Well-Known Proteins

The function of the putative *D. radiodurans* RecD protein and its close relatives is unknown. The only known function of RecD in other bacteria is as a RecD subunit of a RecBCD enzyme. The greatest amino acid sequence similarity between *D. radiodurans* RecD and the other RecD family members is in regions that are similar to the Superfamily I helicases, of which RecD and RecB are considered members. The helicase superfamily is defined by seven conserved helicase motifs (colored bars, as shown in figure 1.3), sequences that align most strongly among the RecD family members. The sequence alignment reveals the seven functional motifs located on the C-terminal half of the whole 715 amino acids of the *D. radiodurans* RecD-like protein. It suggests that this putative exodeoxyribonuclease V subunit RecD should have similar function as the RecD subunit of RecBCD in *E. coli*. The RecD protein from *D. radiodurans* should also have some difference from RecD subunit since they are different in the region preceding the first helicase motif at the N-terminus. The *D. radiodurans*-RecD type of proteins are larger than the RecD subunit proteins (715-865 and 493-721 amino acid residues, respectively). The long N-terminal region, which is almost half of the whole sequence (360-389 residues in the *D. radiodurans* RecD-like proteins), precedes the first helicase motif (the “Walker A” ATP-binding motif). These N-terminal regions are less conserved among the *D. radiodurans* RecD-like proteins and do not contain sequences found in other helicases. It suggested that some novel functions might locate in this region and function with the C-terminal helicase domain.

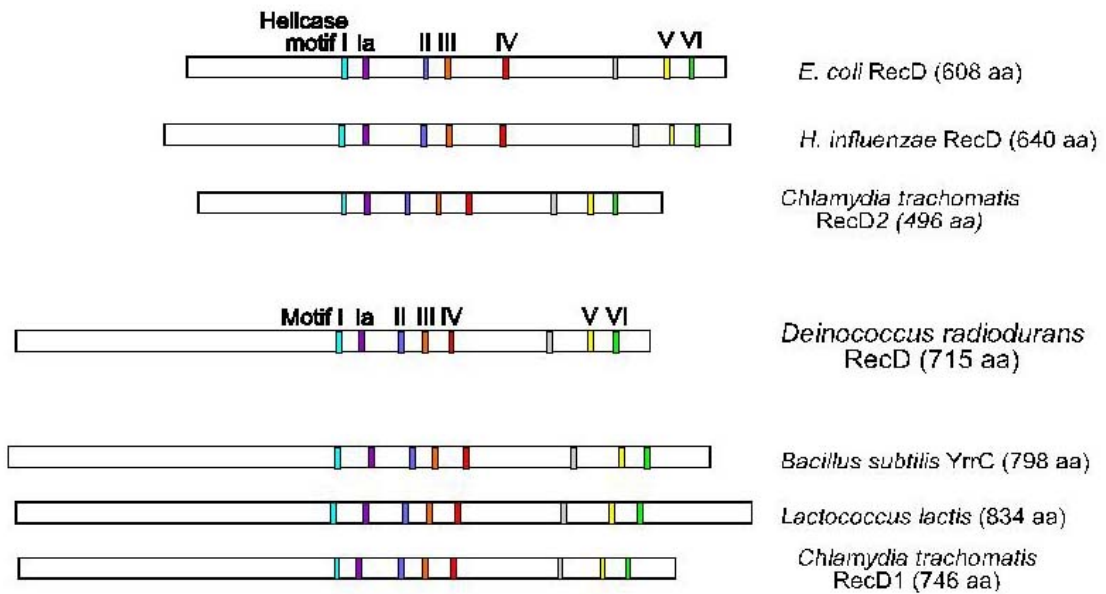


Figure 1.3 Schematic structure of RecD proteins. The top three rectangles represent the RecD subunit of *E. coli* RecBCD enzyme and the close relatives from *H. influenzae* and *Chlamydia trachomatis* (RecD2). The bottom four rectangles represent the RecD protein from *Deinococcus radiodurans* and the close relatives from *Bacillus subtilis* (YrrC), *Lactococcus lactis*, and *Chlamydia trachomatis* (RecD1). Amino terminus is on the left. Vertical bars represent the seven amino acid motifs that are conserved among Superfamily I helicases.

1.3 Orthology of Homologous RecD-like Proteins in Evolutionarily Different Species

Based on amino acid sequence analysis, as reported in the Cluster of Orthologous Groups (COG) database^{96,97} (see <http://www.ncbi.nlm.nih.gov/COG/new>), the putative *D. radiodurans* RecD protein was included in a RecD protein family (COG0507). Many other members of this family are clearly RecD subunits of a RecBCD enzyme. However, the predicted *D. radiodurans* RecD protein is more similar to a sub-group of this family, which includes predicted proteins in genomes of several other Gram-positive bacteria, including *B. subtilis*, *Lactococcus lactis*, *Streptococcus pyogenes*, and several *Chlamydia* species (figure 1.3). Interestingly, *B. subtilis*, *L. lactis*, and several other bacteria in this sub-group have the two-subunit AddAB-like enzyme (which lacks a RecD-like subunit), while the *Chlamydia* genomes have two so-called *recD* genes⁹⁸: one encodes a likely subunit of the *Chlamydial* RecBCD enzyme while the second *Chlamydial* RecD-like protein groups with the *D. radiodurans* RecD protein. The two subgroups are listed as separate families in the TIGR Protein Families database (see <http://www.tigr.org/TIGRFAMs/>). The RecD subunits are grouped in the TIGR01447 family, while the RecD-like proteins from organisms that do not have RecB and RecC, including *D. radiodurans*, are grouped in the TIGR01448 family.

1.3.1 Species Group with RecBCD Holoenzyme

As shown in figure 1.4, a large sub-group is for bacteria (including *E. coli* and *Chlamydia trachomatis RecD2*) that have easily identifiable *recB* and *recC* genes – these are likely to be true RecD subunits of a RecBCD enzyme.

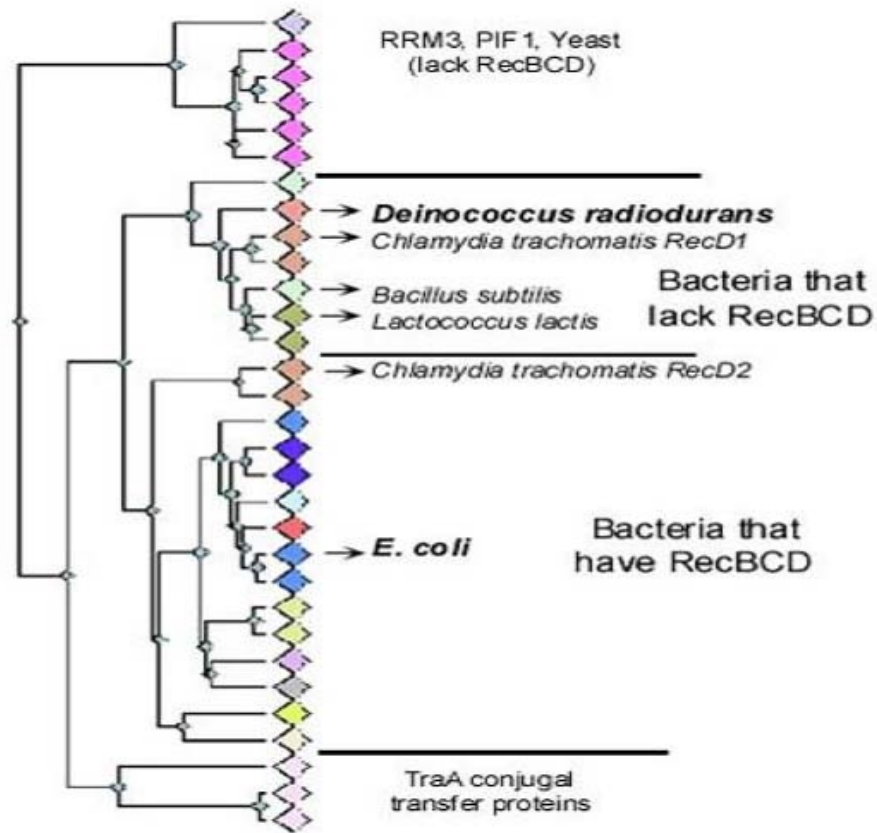


Figure 1.4 The Cluster of Orthologous Groups tree. COGs of proteins were delineated by comparing protein sequences encoded in complete genomes, representing major phylogenetic lineages. The tree (taken from the COG web-site) shows the relationship among the RecD proteins based on their amino acid sequences (this is not necessarily the true phylogenetic relationship among the organisms).

1.3.2 Species Group without RecBCD

The *D. radiodurans* RecD is grouped in a sub-family along with ORF's from other bacteria that do not have a heterotrimeric RecBCD enzyme. Instead, most of these bacteria have a two-subunit enzyme (called AddAB in *Bacillus subtilis* or RexAB in *Lactococcus lactis*), which is enzymatically similar to the RecBCD enzyme with AddA subunit as the RecB homologue and the AddB subunit as neither RecC nor RecD. This enzyme appears to function in a largely similar way as RecBCD, using the cognate RecA protein and organism-specific Chi-sequence^{99, 100}. Direct homologues of the *B. subtilis* AddAB complex have now been identified by sequence homology and/or direct function in at least 12 different bacterial species, including three other bacilli⁸ (as shown in figure 1.5). It is very interesting to note that the AddB subunits among those species show a relatively low level of homology (25-40% identity) to each other when compared with other conserved proteins such as RecA.

In *B. subtilis*, *addA* and *addB* genes encode the two subunits of the AddAB enzyme (135 and 141 kDa respectively). Inactivation of *addA* or *addB* leads to increased sensitivity to DNA-damaging treatments, lower viability and reduced frequencies of homologous recombination. Those phenotypes are similar to *E. coli recBC* cells. The fact that AddAB is fully functional in *E. coli* suggests that they are performing largely overlapping functions and share the same evolutionary origin⁸. *D. radiodurans* appears to be the only one that lacks both the RecBCD enzyme and AddAB in this subgroup.

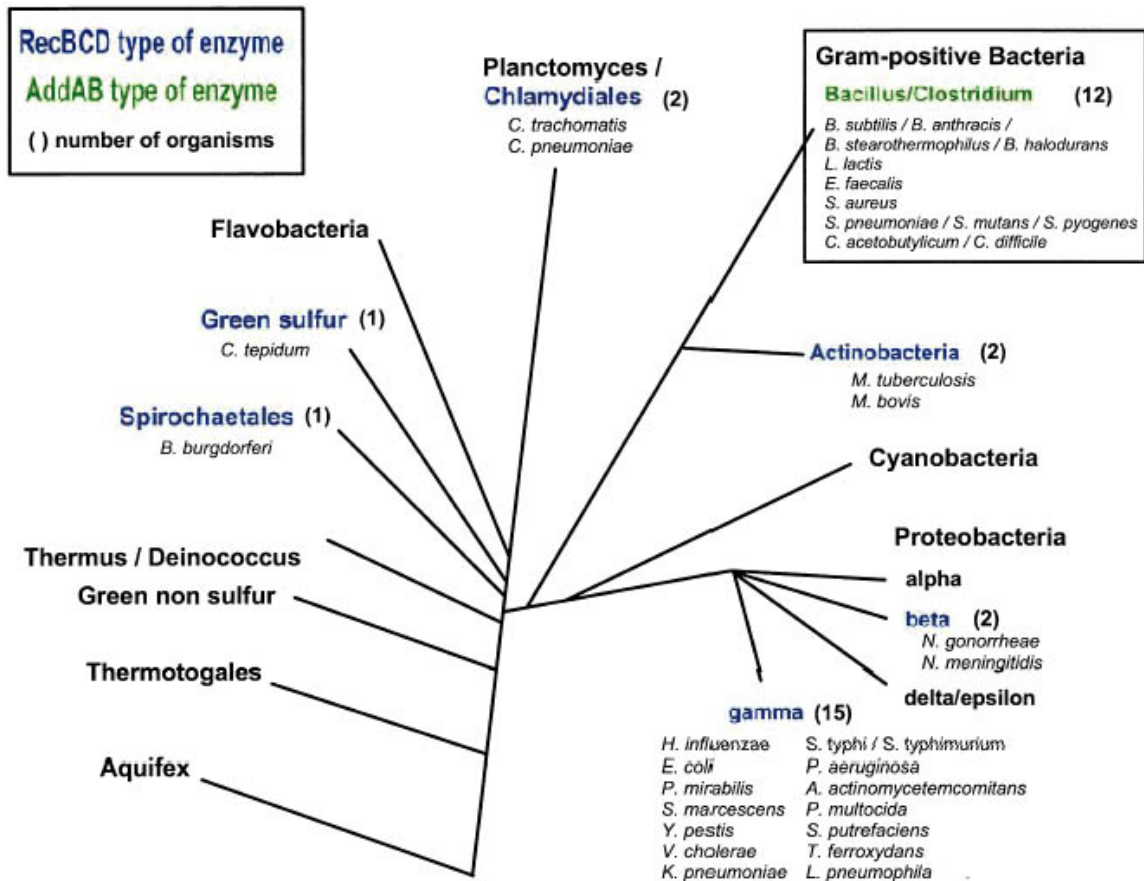


Figure 1.5 Distribution of the RecBCD and AddAB enzymes in eubacterial genomes². Groups containing RecBCD homologues are indicated in blue, while groups containing AddAB homologues are indicated in green. The schematic tree was based upon 16S ribosomal RNA sequence comparisons. Numbers in parentheses indicate the number of species containing a RecBCD or AddAB homologue in each group.

1.4 The Significance of This Project

Deinococcus radiodurans is remarkable for its extraordinary resistance to ionizing and UV irradiation, and to many other agents that damage DNA. Recent inspection of the *B. subtilis* genome revealed the presence of a putative homologue of the *E. coli* RecD protein (encoded by the gene *yrnC*)⁸. No evidence yet has shown that the *yrnC* gene is functionally related to the AddAB enzyme in its homologous recombination.

Besides horizontal gene transfer event, the lineage-specific gene loss also plays a very important role in evolution. Actually on many occasions, it is difficult to distinguish the one from the other, especially when an episodic distribution of a gene or a whole system is observed. The RecBCD enzyme is a good example of such situation¹⁰¹. What happened for the history of RecBCD repair pathway during evolution was likely that both horizontal gene transfer and differential gene loss occurred. Even though the RecBCD pathway is essential for repair of double strand breaks, it can be inactivated without an immediate lethal effect because of multiple pathways of DNA repair in nature.

The *recA* gene was shown to be essential in nearly every type of homologous recombination event, and subsequent biochemical analysis uncovered a unique and centrally critical enzymatic activity: the RecA protein could homologously pair DNA molecules, both single and double stranded, and promote the reciprocal exchange of DNA strands. Some researches proved that the unusual DNA damage resistance of *D. radiodurans* is *recA* dependent and mutation of this *recA* in strain R1 causes marked radiosensitivity^{81, 85}. It was found that the accumulation of the active *S. flexneri* RecA (protein sequence identical to that of *E. coli* RecA) in *recA*-defective *D. radiodurans* does not complement the *D. radiodurans recA* phenotype - including DNA damage

sensitivity, inhibition of natural transformation, nor ability to support a plasmid that requires RecA for replication⁸¹. These results suggested that neither *D. radiodurans* nor *S. flexneri* RecA is functional in the other species. The different kinetics of induction and suppression between them indicates that they employ different modes of action or interact differently with other proteins for function.

Keeping in mind that the *S. flexneri* (same as *E. coli*) RecA protein plays a very important role in the RecBCD repair pathway and there is no *recB* and *recC* genes found in *D. radiodurans*, this bacterium has to employ another more effective DNA repair pathway than the RecBCD in *E. coli* and RecA also plays a very important role in this pathway. Does this pathway involve the RecD-like protein found in *D. radiodurans*' genome or is it just debris through evolution? We might solve this question by finding out its biochemical activities *in vitro* and biological functions *in vivo*.

Chapter 2 CLONING RECD FROM *DEINOCOCCUS RADIODURANS* AND EXPRESSION OF THE PROTEIN IN *E. COLI*

2.1 Introduction

To study the RecD protein biochemically *in vitro*¹⁰², we first used PCR¹⁰³ to amplify the *recD* gene and cloned it into a pTZ19R plasmid. We then inserted the *recD* gene into an expression vector pET15b, which adds a twenty amino acid polypeptide tag with six tandem histidine at the N-terminus of the RecD protein, and expressed it in *E. coli*. The following expression tests showed that the N-terminal His-tagged recombinant RecD protein was not very soluble, especially when the expression level was high under high IPTG concentration and incubation temperature. Moreover, it doesn't bind to the nickel column very well which brings the problem of how to purify it under native condition.

Next, we adjusted the structure of the recombinant protein by putting a short eight amino acid peptide with six-histidine tag on its C-terminus. This time, the C-terminal His-tagged recombinant protein, in another expression vector pET21a, has quite high solubility, especially when we induced it with lower IPTG concentration and incubated the host *E. coli* cells in lower temperature. Another advantage of the C-terminal His-tagged RecD protein is that it binds to the nickel column very tightly under native condition and can only be washed off by native wash buffer with high imidazole. This property of the RecD protein significantly simplifies the protein purification process since only a small amount of other proteins can bind to the nickel column so tightly and be washed off with the RecD protein. After the nickel column, only one more column (ssDNA cellulose) was needed to get the RecD protein with higher than 90% purity.

2.2 Materials and Methods

2.2.1 Preparation of Genomic DNA and PCR

D. radiodurans strain R1 was obtained from the American Type Culture Collection, Manassas, VA. The cells were grown in TYG (0.8 g Tryptone, 0.4 g yeast extract and 0.1 g glucose in 100 ml distilled water and autoclaved) media and incubated at 30 °C for about 48 hours to reach the stationary phase. The DNA isolation from *D. radiodurans* was done as described previously with some modifications^{104, 105}. (A) 10 ml saturated cultures were harvested by centrifugation at 3,000 × g, 4 °C for 15 min. (B) The pellet was resuspended in 2 ml of absolute ethanol in room temperature for 30 min to remove the outer membrane of the *D. radiodurans*. (C) The ethanol-stripped cells were collected by centrifugation at 3,000 × g, 4 °C, for 15 min, and the resulting pellet was resuspended in 1 ml of TE buffer (10 mM Tris-HCl, 0.1 mM EDTA, pH 8.0). (D) Two milligrams of lysozyme was added to the stripped cells, and the mixture was incubated at 37 °C for 30 min. (E) 100 µl of 25 % SDS was added and the mixture was placed in a 60 °C water bath for 10 min, then cooled down to room temperature. (F) 3 M NaOAc was added to a final concentration of 1 M to the viscous, lysed suspension. (G) Equal volume of phenol-chloroform-isoamyl alcohol (25:24:1) was added into the mixture and gently shaken for 5 min. (H) The mixture was centrifuged at 5,000 × g, 4 °C, for 15 min, and the upper aqueous layer was removed into a clean and sterile tube. Steps (G) and (H) were repeated three times until the white precipitate in the interface was gone. At this point, the deproteination is finished. (I) The upper layer was transferred to an eppendorf tube, and 0.6 volumes of isopropanol was added to precipitate the DNA. (J) The string-like white DNA precipitate was spooled out using a small tip and put in 10 % 3 M NaOAc

and 70 % ethanol solution to wash the DNA. (K) The mixture was spun in a microcentrifuge at $8,000 \times g$, $4\text{ }^{\circ}\text{C}$ for 15 min. The supernatant was removed and the pellet was washed three times with 70% ethanol and then air-dried. The genomic DNA was then redissolved in TE buffer (10 mM Tris-HCl, pH 8.0, and 1 mM EDTA) and the DNA concentration was determined by its absorption at 260 nm.

PCR reaction was carried out in 100 μl /each tube with 0.5 μg genomic DNA as template, 0.2 mM/each dNTP, 1 μM /each of the two primers RecD1 and RecD2 in $1\times$ Pfu Turbo polymerase (Stratagene) buffer. 2.5 units of the Pfu Turbo polymerase were added to start the PCR reaction. Incubation for 4 min at $96\text{ }^{\circ}\text{C}$ was used as the initial step, followed by 25 cycles of 1 min at $96\text{ }^{\circ}\text{C}$ for template DNA denaturation, 1 min at $61\text{ }^{\circ}\text{C}$ for primer annealing, and 6 min at $72\text{ }^{\circ}\text{C}$ for the primer extension. An extra 10 min at $72\text{ }^{\circ}\text{C}$ was added to the end of 25 cycles to make sure the extension was completed. Then, the PCR product was directly loaded onto a 1 % agarose gel and the *recD* gene bands with correct size were cut out and recovered from the 1 % agarose gels with QIAEX[®] II Gel Extraction Kit (Qiagen), as described in the kit. The primers that we designed include three restriction enzyme sites so that the PCR product can be digested and inserted into plasmid vectors pTZ19R and pET15b as shown in figure 2.1. Thus, the 2192 bp *recD* gene fragment was eluted from the resin in TE buffer, double-digested with *EcoR I* and *BamH I* and ligated to the plasmid pTZ19R cut with the same enzymes. The ligation product was used to transform the HB101 competent cells.

Several colonies from the ampicillin selective plates were picked to inoculate 5ml/each LB medium with the same antibiotic. The QIAprep[®] Spin Miniprep Kit was used to isolate the plasmids. The *recD* gene was verified both by restriction digestion

followed by electrophoresis on 1.0 % agarose gel and sequencing. Dye-terminated sequencing was done by the DNA Sequencing Facility at UMCP. The restriction map and sequence alignment analysis were determined by using Web tools (<http://www.firstmarket.com/cutter/cut2.html> and <http://pbil.univ-lyon1.fr/lfasta.html>, respectively).

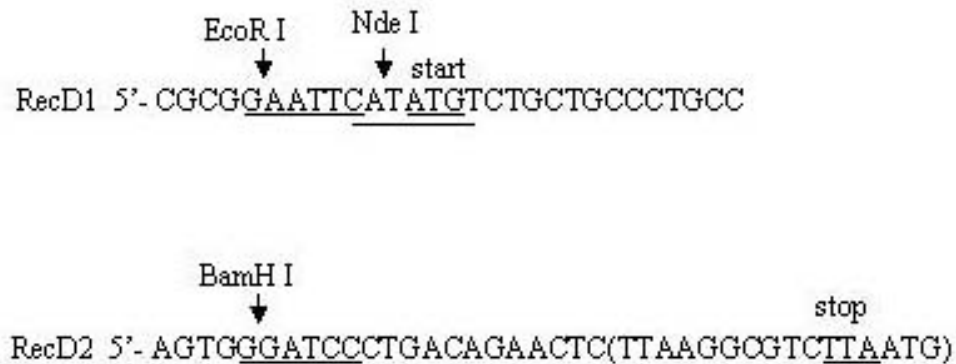


Figure 2.1 The pair of primers used to amplify the *recD* gene from the *D. radiodurans* genome. The upstream primer RecD1 annealing at the 5'-end of the gene has an *EcoR I* and an *Nde I* site before the RecD coding region. The downstream primer RecD2 annealing at the 3'-end of the gene has a *BamH I* site after the RecD stop codon. Both primers are partially complementary to the *recD* gene.

2.2.2 Construction of the Plasmid Expressing the N-terminal His-Tagged RecD Protein

The plasmid with correct sequence (named pDr-recD.ptz) was used in the next steps. Both vector pET15b-30 (Novagen Corp) and pDr-recD.ptz were double digested with *Nde I* and *BamH I*. The two fragments (5698-base pair vector and 2180-base pair *recD* gene) recovered from 1.0 % agarose gel were ligated together in a ratio of 3:1 = vector: *recD* gene by T4 ligase in 1 × ligation buffer and 10 % PEG. The addition of polyethylene glycol (PEG) in the ligation buffer promotes the performance of the reaction at low enzyme and DNA concentrations. The reaction product was then used to transform Amp^s host cell BL21 (DE3). The colonies on the selective plates have the recombinant plasmid pDr-recD-pET15b. After the sequence and orientation of the insertion were verified, one single colony was stored in -80°C freezer in 15 % glycerol and also used in the next purification steps.

2.2.3 Construction of the Plasmid Expressing the C-terminal His-Tagged RecD Protein

C-terminal His-tagged RecD protein was brought to consideration because the N-terminal His-tagged RecD protein has problems of low solubility and low affinity to the nickel column. Another two primers were designed to amplify the 3'-end region 1500-base-pair fragment of *recD* gene from plasmid pDr-recD.ptz. The upstream primer annealing inside the gene includes the *Sac II* site (648 bp) and the downstream primer annealing at the 3'-end of the gene has *Xho I* and *BamH I* sites right behind the last

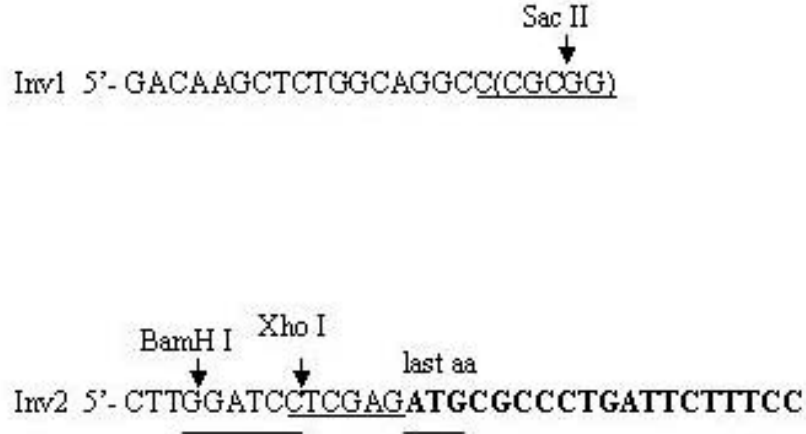


Figure 2.2 The pair of primers used to change the location of His-tag to RecD C-terminus. Inv1 is complementary to the *Sac II* restriction site at bp # 648 inside the gene. Right region (bold) of Inv2 is complementary to the end of the gene and the left region is used to introduce new *Xho I* and *BamH I* sites after the last codon of the *recD* coding region, and replace the natural stop codon.

amino acid of RecD protein, as shown in figure 2.2. The web tool used to design primers is: <http://www.williamstone.com/primers/calculator/calculator.cgi>

The HB101 cells with plasmid pDr-recD.ptz were grown in LB media with 100 µg/ml ampicillin overnight. The plasmid was isolated with the QIAprep® Spin Miniprep Kit and eluted in TE buffer. PCR reaction was carried out in 100 µl/each tube with 0.2 µg plasmid DNA as template, 0.2 mM/each dNTP, 1 µM/each of the two primers (Inv1 and Inv2) in 1× Pfu Turbo polymerase (Stratagene) buffer. 2.5 units of the Pfu Turbo

polymerase were added to start the PCR reaction. Incubation for 4 min at 94 °C was used as initial step, followed by 25 cycles of 1 min at 94 °C for template DNA denaturation, 1 min at 57 °C for primer annealing, and 2.5 min at 72 °C for the primer extension. Extra 10 min at 72 °C was added to the end of 25 cycles to make sure the extension was completed. Then, the PCR product was directly loaded onto a 1 % agarose gel, the *recD* fragment bands were cut out and recovered with the QIAEX[®] II Gel Extraction Kit (Qiagen).

The purified 1535-base pair PCR product and pDr-recD.ptz were double digested with *Sac II* and *BamH I* enzymes. The 3'-three quarters of *recD* gene (1535-base pair) fragment from PCR product and vector with 5'-one quarter of *recD* gene (648-base pair) fragment from plasmid pDr-recD.ptz were recovered from 1.0 % agarose gels and ligated with T4 ligase to introduce a new *Xho I* restriction site. The ~1600 bp *recD* sequence after modification in the new version of plasmid pDr-recD.ptz(C) was verified both by restriction digestion followed by electrophoresis on 1.0 % agarose gel and sequencing. Then, the plasmid pDr-recD.ptz(C) and vector pET21a (Novagen Corp) were double digested with *Nde I* and *Xho I*. The corresponding digestion pieces were religated to construct a plasmid pDr-recD-pET21a that expresses RecD protein with the six-histidine tag on its C-terminus.

2.2.4 RecD Protein Expression and Solubility Test

The C-terminal His-tagged RecD protein was expressed in *E. coli* strain BL21 (DE3) transformed with pDr-recD-pET21a. The overnight culture was grown in LB media with 100 µg / ml ampicillin at 37 °C. A 1:200 ratio of the overnight culture was

used to inoculate fresh media with 100 $\mu\text{g} / \text{ml}$ ampicillin by centrifugation at $5,000 \times g$, $4\text{ }^\circ\text{C}$ for 5 min to collect the cells. Then, the cells were resuspended in a small volume of fresh LB media and added into a large volume of media in a flask. The cells were grown at $37\text{ }^\circ\text{C}$ until the $\text{OD}_{600} = 0.5$. IPTG was then added to 0.5 mM or 1 mM final concentration and incubation at $30\text{ }^\circ\text{C}$ or $37\text{ }^\circ\text{C}$ was continued. The cells were sampled every half hour. The cell pellet from 200 μl of culture at each time point was collected and 30 μl 1 \times SDS loading buffer (50 mM Tris-HCl, pH 6.8, 100 mM DTT, 2 % SDS, 0.1 % bromophenol blue and 10 % glycerol) and 3 μl 1 M DTT were added to resuspend the cell pellet. The mixture then was heated to $90\text{ }^\circ\text{C}$ for 2 min, centrifuged at $12,000 \times g$ at room temperature for 1 min and 15 μl supernatant was used to run the gel. All of the samples from up to 4 hours incubation were run on a 5 % stacking and 8 % resolving SDS-PAGE gel to see the time course of expression level.

The solubility test and protein location experiment were conducted to determine the optimal conditions for the RecD expression and where the RecD proteins locate in cells. The cultures with 1 mM IPTG at $37\text{ }^\circ\text{C}$ for two hours and 0.5 mM IPTG at $30\text{ }^\circ\text{C}$ for three hours were used in this experiment. The sample of periplasmic protein was the supernatant made from cell pellet from 1 ml culture treated in 100 μl freshly prepared solution of lysozyme (1 mg/ ml), 20 % (w/v) sucrose, 30 mM Tris-HCl pH 8.0, and 1 mM EDTA. The cell solution was then placed on ice for 10 min and centrifuged at $4\text{ }^\circ\text{C}$, $12,000 \times g$ for 1 min to collect the “naked” cells. The “naked” cell pellet was resuspended in 100 μl 0.1 M Tris-HCl, pH 8.0 buffer. The step of freezing the cells on dry ice and thawing it at $37\text{ }^\circ\text{C}$ was repeated three times to break the cell membrane. The supernatant after centrifugation at $4\text{ }^\circ\text{C}$, $12,000 \times g$ for 5 min was the soluble portion of the proteins.

The pellet containing the membrane fraction and insoluble inclusion bodies was solubilized with 1 % Triton X-100 and incubated at 4 °C for 10 min. All three types of samples were used to run SDS-PAGE gel.

2.2.5 Purification of His-Tagged RecD Proteins

First, the RecD protein was expressed in *E. coli* strain BL21 (DE3) transformed with plasmid pDr-recD-pET15b. The N-terminal His-tagged RecD protein could be purified only under denaturing condition. A small scale purification was done as follows: cells from 200 ml culture with 0.5 mM final IPTG concentration induced for three hours at 30 °C were collected by centrifugation at $5,000 \times g$, 4 °C for 5 min. 10 ml of 37 °C preincubated guanidinium lysis buffer (6 M guanidine hydrochloride, 20 mM sodium phosphate, 500 mM sodium chloride, pH 7.8) were added to resuspend the cell pellet and the denatured protein solution was obtained by following the procedure on the ProBond™ Resin purification manual (version C, Invitrogen). The cells were slowly rocked for 5-10 min at room temperature to assure thorough cell lysis, and then sonicated on ice-salt bath with six 10-second pulses at a high intensity setting (power level 5, at 50% duty cycle, Branson Sonifier 450) to shear the DNA and RNA. The insoluble debris was removed by centrifugation at $3,000 \times g$, 4 °C for 15 min and the supernatant lysate was transferred to a clean 15 ml plastic tube. 5 ml of the denatured protein solution was loaded onto a 2 ml Ni²⁺-NTA column (ProBond resin, Invitrogen Corp.), followed by 10 ml of denaturing binding buffer (8 M urea, 20 mM sodium phosphate, 500 mM sodium chloride, pH 7.8) to wash off the unbound proteins. 20 ml denaturing wash buffer (8 M urea, 20 mM sodium phosphate, 500 mM sodium chloride, pH 6.0), 15 ml denaturing

wash buffer (8 M urea, 20 mM sodium phosphate, 500 mM sodium chloride, pH 5.3), and 10 ml denaturing elution buffer (8 M urea, 20 mM sodium phosphate, 500 mM sodium chloride, pH 4.0) were used to elute the column. All the elution samples were collected and used to run SDS-PAGE gels.

Then, the C-terminal His-tagged RecD protein was expressed in *E. coli* strain BL21 (DE3) transformed with pDr-recD-pET21a in large scale. All cells from 10 ml overnight LB media culture containing 100 µg / ml ampicillin were collected by centrifugation for 5 minutes at 4,000 ×g, 4 °C in a 15 ml plastic tube. 2 ml fresh LB media were added to the plastic tube to resuspend the cell pellet. The cell suspension (1:200 inoculation ratio) then was transferred to a 6 liter flask with 2 liter autoclaved LB media (100µg/ml ampicillin). The cells were grown in 37 °C with vigorous shaking (250-300 rpm) for about 2-2.5 hours until the OD₆₀₀ = 0.5. IPTG was then added to 0.5 mM final concentration and the cells were incubated in 30°C for another three hours before the cells were harvested. After collecting the cell by centrifugation at 6,000 ×g, 4 °C for 15 minutes, the cell pellets were stored in the -80°C freezer overnight. The next day the cell pellets (~4 g) were thawed on ice and 50 ml of native binding buffer (20 mM sodium phosphate, 500 mM NaCl, pH 7.8) were added. Meanwhile, 600 µl 1M PMSF and 300 µl protease inhibitor cocktail for polyhistidine-tagged proteins (Sigma, Inc.) were also added into the cell suspension. The mixture was sonicated on an ice-salt bath with a microtip using 10-second bursts and 30-second breaks (power level 5, at 50% duty cycle, Branson Sonifier 450) for either a total of 100 seconds of bursts per gram or until it was no longer viscous. The cell debris was removed from the lysate by centrifugation at 16,000 ×g, 4 °C for 30 minutes.

The crude cell extract (about 50 ml) was applied to a 10 ml Ni²⁺-NTA column pre-washed with native binding buffer. The column was then washed with 30 ml of native binding buffer followed by 100 ml of native wash buffer (20 mM sodium phosphate, pH 6.0, 500 mM sodium chloride, 60 mM imidazole). Finally, the RecD protein was eluted in a 140 ml gradient of 60 mM to 400 mM imidazole in elution buffer (20 mM sodium phosphate, pH 6.0, 500 mM sodium chloride), followed by 10 ml elution buffer with 500 mM imidazole to make sure all RecD was off the column.

The fractions containing the RecD protein, based on SDS-PAGE gel results, were pooled and dialyzed against dialysis Buffer A (20 mM potassium phosphate, pH 7.5, 1 mM EDTA, 1 mM DTT, 10 % (w/w) glycerol). The dialyzed pool was then applied to a 5 ml ssDNA cellulose column (Sigma) in Buffer A. The ssDNA cellulose column was washed with ten volumes of Buffer A containing 50 mM NaCl and the RecD protein was eluted by 30 ml Buffer A with 0.6 M NaCl, 30 ml Buffer A with 1 M NaCl, and 30 ml Buffer A with 1.5 M NaCl. The fractions containing RecD were pooled and dialyzed against Buffer A with 10% (v/v) glycerol and then concentrated by ultrafiltration (Amicon). The resulting protein solution was then dialyzed against Buffer A with 50% (v/v) glycerol and aliquoted into small volume (50µl/each) and stored in -80 °C freezer.

The single-stranded deoxyribonucleic acid-cellulose came as a white powder. The column was prepared as follows: 2 g of the cellulose powder was soaked in buffer (50 mM sodium chloride, 1 mM trisodium salt of EDTA, 1 mM β-mercaptoethanol, 10 % (w/w) glycerol, 20 mM Tris.HCl, pH 7.6) overnight. The floating tiny particles were removed by pouring away the upper solution after being stirred to prevent extremely low flow rate.

2.3 Results

2.3.1 Construction of the Plasmids

The PCR reaction we used can specifically amplify the *recD* gene region from the genome of *D. radiodurans*, as shown on the left gel of figure 2.3. The nonspecific reactions on the right gel can be limited by lowering the template concentration and avoiding any physical shearing during purification of genomic DNA. This PCR product was used to construct a storage plasmid pDr-recD.ptz.

The correct insertion of *recD* into the recombinant plasmid pDr-recD.ptz was verified both by the restriction digest, as shown in figure 2.4, and DNA sequencing. The same plasmid was used as template to amplify the 3'-end three quarters of the *recD* gene to introduce a new *Xho I* site right behind the last amino acid, as shown in figure 2.5. This PCR product was used to construct a new version of the storage plasmid, pDr-recD.ptz(C).

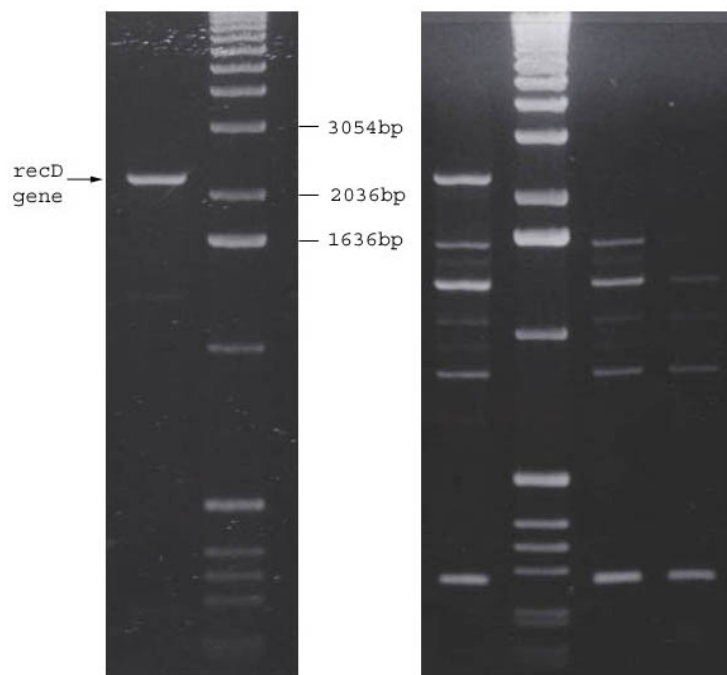


Figure 2.3 PCR products with 1 kb DNA ladder on 1% agarose gel stained with ethidium bromide. Left: one lane directly loaded with PCR product. 100 μ l/each reaction has 0.5 μ g genomic DNA as template, 0.2 mM/each dNTP, 1 μ M/each of the two primers in 1 \times Pfu Turbo polymerase (Stratagene) buffer. 2.5 unit of the Pfu Turbo polymerase was added to start PCR reaction. Reaction cycles were described as in materials and methods. Right: three lanes of PCR products with many non-specific bands. The differences between the PCR reaction conditions in the left and right lanes were the template concentration and quality of the genomic DNA.

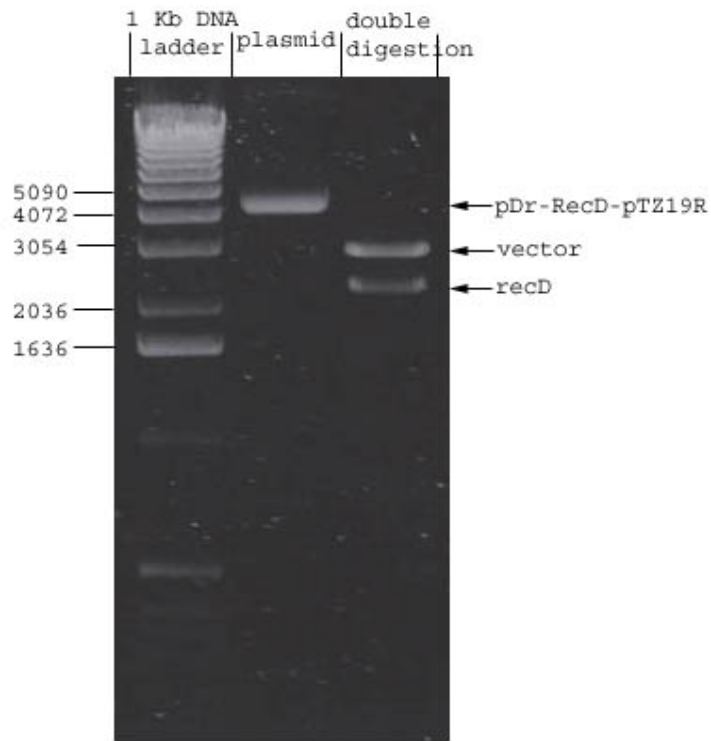


Figure 2.4 Plasmid pDr-recD.ptz and its double digestion (*EcoR I* and *BamH I*) product on a 1% agarose gel with 1kb DNA ladder. Left lane: the 1 kb DNA ladder; middle lane: the plasmid purified with the QIAprep® Spin Miniprep Kit; right lane: its *EcoR I* and *BamH I* double-digested product.

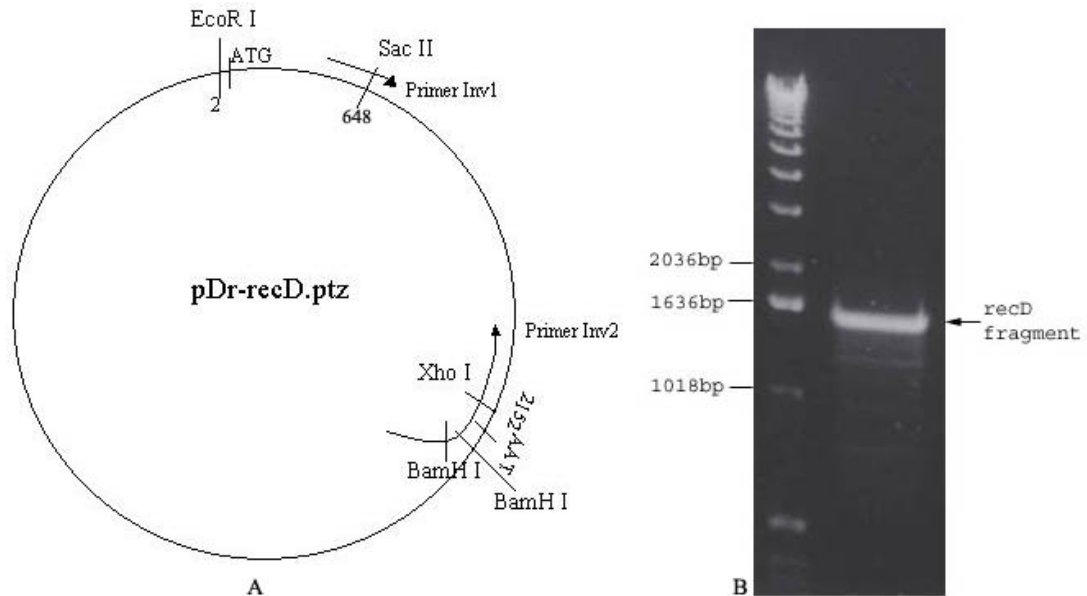


Figure 2.5 The PCR to introduce an *Xho I* site right behind the last amino acid of the RecD protein. A. The schematic model of the PCR using the primers shown in figure 2.2. The reaction amplifies the 3'-terminal three quarters of the *recD* gene. B. ~1500-base pair *recD* gene fragment from PCR on 1% agarose gel with 1 kb DNA ladder. 100 μ l/each reaction has 0.2 μ g plasmid DNA as template, 0.2 mM/each dNTP, 1 μ M/each of the two primers (Inv1 and Inv2) in 1 \times Pfu Turbo polymerase (Stratagene) buffer. 2.5 unit of the Pfu Turbo polymerase was added to start PCR reaction. Reaction cycles were described as in materials and methods.

2.3.2 Induction Under Different Conditions

A protein band of about 80 kDa was observed by SDS-PAGE analysis of the lysate of cells transformed with pDr-recD-pET21a, the RecD over-expression plasmid, after induction with IPTG at different time points. The production of total cellular RecD protein started to accumulate after half-hour induction and reached the peak after one-

hour induction with 1 mM IPTG at 37 °C. Almost none of this band was present in the same cells without induction, as shown in the figure 2.6. The same test with lower incubation temperature (30 °C), lower IPTG concentration (0.5 mM) and longer induction time was done. The production of the RecD protein accumulated after one-hour induction and reached the peak after three hours, as shown in figure 2.7.

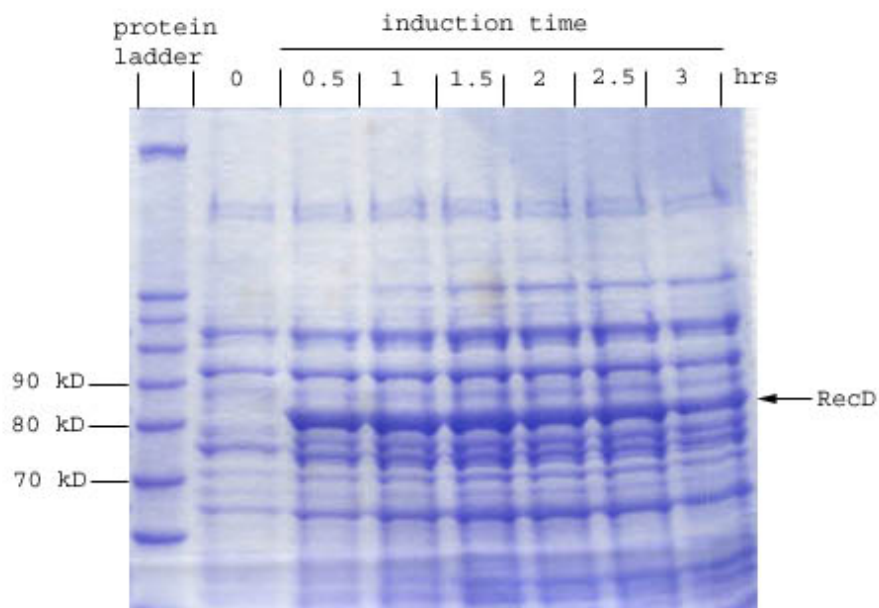


Figure 2.6 10 % (29:1=acrylamide:bis-acrylamide) SDS-PAGE gel for the time course expression of RecD protein at 1mM IPTG and 37 °C. The cells from 200 µl culture at each time point were collected and 30 µl 1 × SDS loading buffer and 3 µl 1 M DTT were added. 15 µl / each sample of the supernatant after the samples were heated at 90 °C for 2 min and centrifuged was loaded onto a SDS-PAGE gel as described in the materials and methods, and stained with Coomassie brilliant blue.

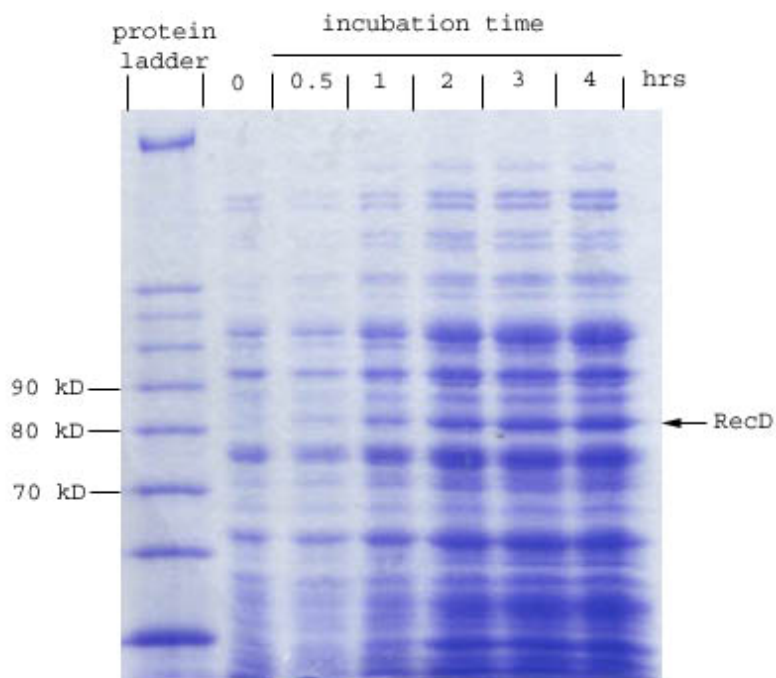


Figure 2.7 10 % SDS-PAGE gel for the time course expression of RecD protein at 0.5 mM IPTG and 30 °C. The cells from 200 μ l culture at each time point were collected and 30 μ l 1 \times SDS loading buffer and 3 μ l 1 M DTT were added. The samples were heated at 90 °C for 2 min, centrifuged, and 15 μ l / each sample of the supernatant was loaded onto a SDS-PAGE gel as described in the materials and methods, and stained with Coomassie brilliant blue.

2.3.3 Solubility Test

The protein solubility and location experiments showed the biggest difference between the two induction conditions. Most of the total cellular RecD protein that accumulated under 37 °C and 1 mM IPTG was insoluble. Under this condition, most of the synthesized RecD protein formed into insoluble inclusion bodies because new translated peptides don't have enough time to assemble into correct conformation. Even

though the yield of the total cellular RecD protein under 30 °C and 0.5 mM IPTG was lower, most of it was soluble, as shown in figure 2.8. It can be explained that when the protein accumulated much slower, the new-synthesized peptides had enough time to fold correctly. Some of the soluble RecD protein was hydrolyzed in the induced cells after four to five-hour induction. The three-hour induction at 30 °C with 0.5 mM IPTG was used for the following purification procedure.

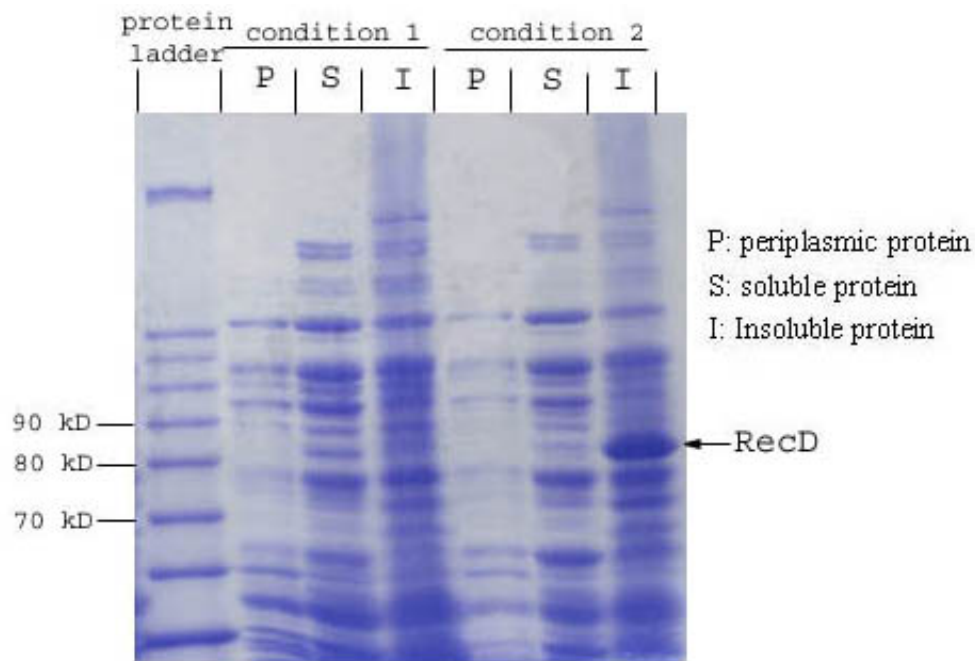


Figure 2.8 10 % SDS-PAGE gel for the solubility test of RecD proteins expressed in two different conditions. Condition 1 was at 0.5 mM IPTG and 30 °C for three hours. Condition 2 was at 1 mM IPTG and 37 °C for two hours. The preparations of the periplasmic, soluble and insoluble protein samples were as described in the materials and methods, 1/3 volume of 3 × SDS loading buffer were added into all liquid samples and 30 µl 1 × SDS loading buffer were added to all solid samples. 15 µl/each supernatant after the samples were heated at 90 °C for 2 min and centrifuged was loaded onto a SDS-PAGE gel as described in the materials and methods, stained with Coomassie brilliant blue.

2.3.4 Purification Behavior

The N-terminal His-tagged recombinant RecD protein can only bind to the nickel-column tight enough to distinguish itself from other proteins in host cells under denaturing condition, as shown in figure 2.9. When under native condition, it was washed off with very low imidazole (60 mM) in the wash buffer.

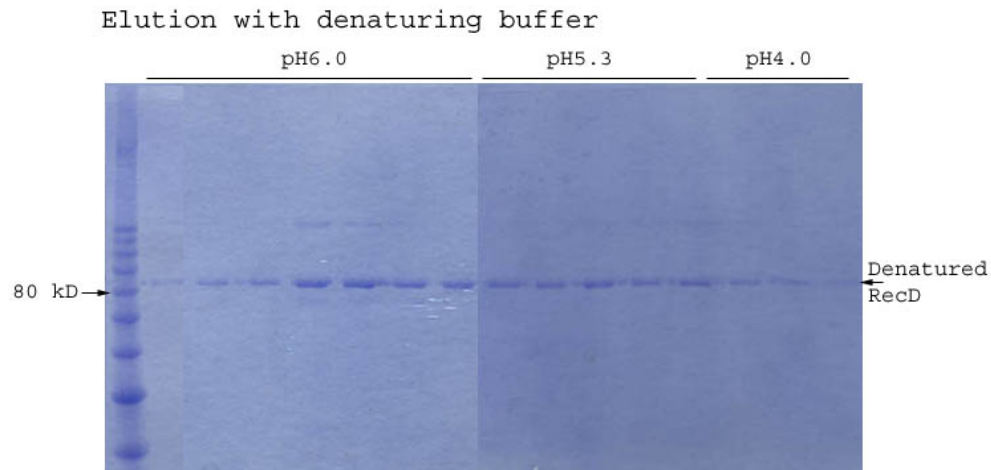


Figure 2.9 10 % SDS-PAGE gel for denatured purification of N-terminal His-tagged RecD protein. Cells from 200 ml culture were treated as described in the materials and methods, procedure coming with the ProBond Resin purification manual. 20 ml denaturing washing buffer, pH 6.0, 15 ml denaturing washing buffer, pH 5.3 and 10 ml denaturing elution buffer, pH 4.0 were used to elute the denatured RecD protein from the column. 30 μ l / each sample was taken out and added to 10 μ l 3 \times SDS loading buffer. After heating at 90 $^{\circ}$ C for 2 min and centrifugation at 12,000 \times g, room temperature for 5 min, 15 μ l supernatant / each sample was loaded to run gels as described in materials and methods, stained with Coomassie brilliant blue.

In contrast, as shown in the figure 2.10, the C-terminal His-tagged RecD protein binds very tightly to the nickel column in native condition. The bulk of the RecD protein was washed off by the native wash buffer with about 200 mM imidazole, under which condition most of the proteins from the host *E. coli* cells cannot bind to the column. This one step purification can give us the RecD protein with high purity.

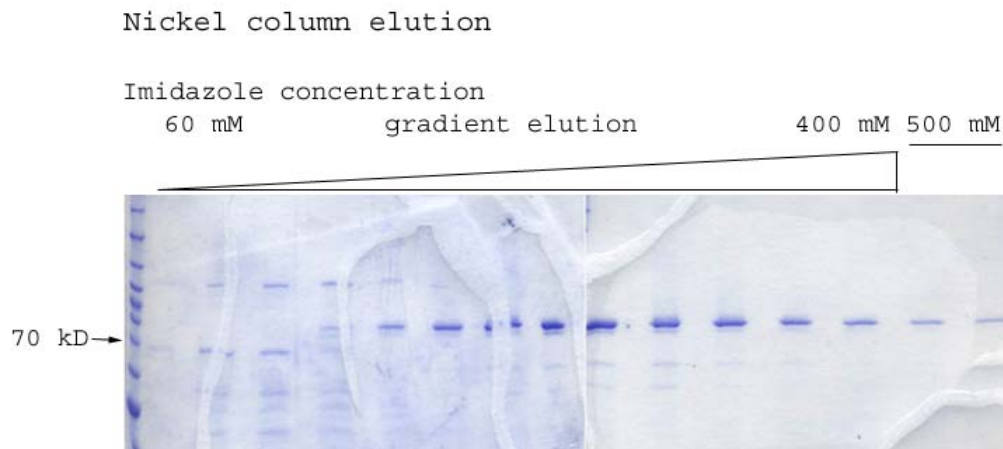


Figure 2.10 10 % SDS-PAGE gels for native C-terminal His-tagged RecD protein from a nickel column. Cells from 2L culture were treated as described in the materials and methods. The crude cell extract was applied to a 10 ml Ni²⁺-NTA column in native binding buffer. The column was washed with 30 ml of native binding buffer, 100 ml of native wash buffer with 60 mM imidazole (not shown in the gels), and the RecD protein was eluted in a 140 ml native wash buffer with gradient imidazole concentrations of 60 to 400 mM, followed by 10 ml native wash buffer with 500 mM imidazole. 15µl / each sample was taken out and added to 5 µl 3 × SDS loading buffer. After heating at 90 °C for 2 min and centrifugation at 12,000 × g, room temperature for 5 min, 10 µl supernatant / each sample was loaded to run gels as described in materials and methods, and stained with Coomassie brilliant blue.

The partially purified RecD protein from the nickel column was then run on a single-stranded DNA cellulose column. As shown in figure 2.11, the RecD protein binds to the ssDNA on the column very tightly so that it can only be washed off with high (1 M) salt concentration, which matches the expectation that it is a putative helicase. All other contaminant proteins from the nickel column and the partially proteolysed RecD were easily washed off with low (0.4 M) salt concentration.

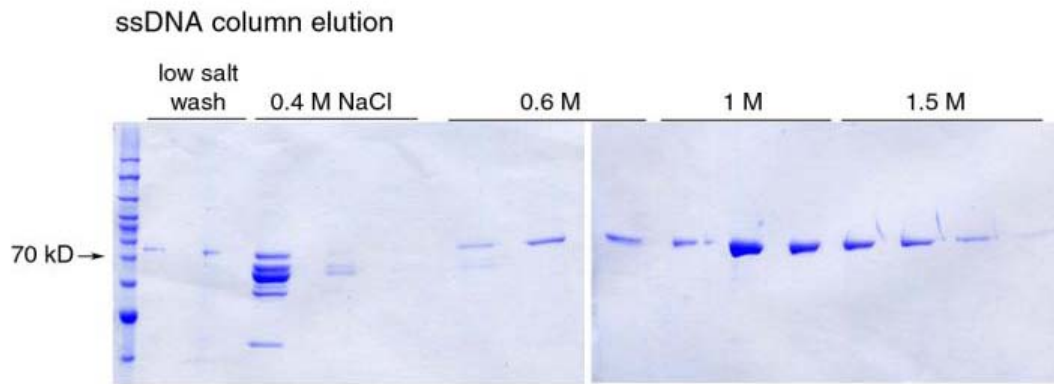


Figure 2.11 10 % SDS-PAGE gels for native C-terminal His-tagged RecD protein from an ssDNA column. The fractions containing RecD protein from nickel column were collected and dialyzed against Buffer A (20 mM potassium phosphate, pH 7.5, 1 mM EDTA, 1 mM DTT, 10% (v/v) glycerol) and applied to a 5 ml ssDNA cellulose column. The column was washed with 50 ml Buffer A containing 0.4 M NaCl, followed by 30 ml each of Buffer A with 0.6 M, 1 M, and 1.5 M NaCl. 15 μ l / each sample was taken out and added to 5 μ l 3 \times SDS loading buffer. After heating at 90 $^{\circ}$ C for 2 min and centrifugation at 12,000 \times g, room temperature for 5 min, 10 μ l supernatant / each sample was loaded to run gels as described in materials and methods, and stained with Coomassie brilliant blue.

2.3.5 The Purified C-Terminal His-Tagged RecD Protein

The RecD sample from the nickel column after storage in 4 °C for a couple of days contains more of the smaller bands, as shown in the figure 2.12, than the samples run on a gel right after the protein was washed off the column, as shown in figure 2.10. This is because either the hydrolysis or the proteolysis of the RecD protein happened during the storage in 4 °C. Since the RecD protein shows the properties of both resistance to hydrolysis and maintenance of its biochemical activity after the ssDNA column, the degradation is most probably because of proteolysis. It can be explained by the fact that a small amount of other protein contaminants, some of which can be proteases, were co-eluted with the RecD protein in the nickel column purification step.

After elution from the ssDNA cellulose column, the fractions containing RecD were pooled, concentrated, and followed by dialysis against Buffer A (20 mM potassium phosphate, pH 7.5) to get rid of the salt, or dialysis first followed by concentrating. The RecD protein began to precipitate beyond a certain concentration so that we could not get highly concentrated RecD protein. So the concentrating process was stopped right before RecD precipitated and the resulting RecD solution was then dialyzed against Buffer A (20 mM potassium phosphate, pH 7.5, 1 mM EDTA, 1 mM DTT) with 50% glycerol. This last dialysis step increased the protein concentration significantly.

The two-step chromatography on a Ni²⁺-NTA column followed by an ssDNA cellulose column can purify the C-terminal His-tagged RecD protein easily under native condition. The RecD protein concentration was determined from the absorbance at 280 nm, using an extinction coefficient $\epsilon_{280} = 52,060 \text{ M}^{-1}\text{cm}^{-1}$ (0.681 g/l) calculated for RecD using the program ProtParam (<http://ca.expasy.org/tools/protparam.html>). The typical

yield was about 1.2 mg from 4 liters of culture. The purified RecD protein (~8 μ M) is very stable, stored in -80 °C freezer for more than two years with no obvious loss of activity.

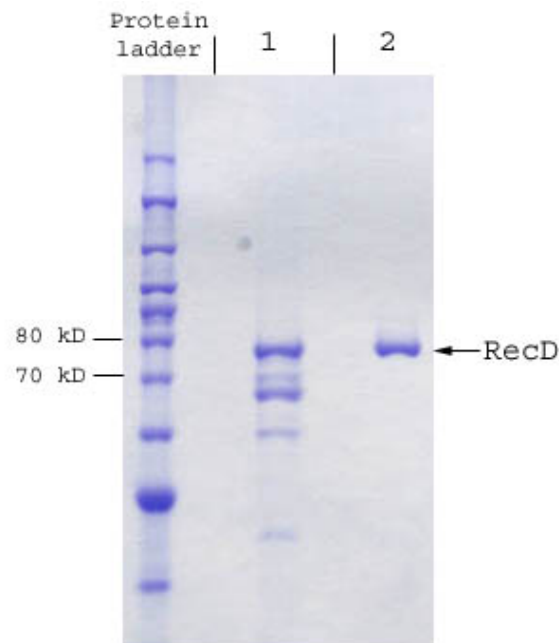


Figure 2.12 10 % SDS-PAGE gel of RecD proteins from the two-step purification with 10 kDa protein ladder. Lane 1 was protein sample after nickel column. Lane 2 was protein sample after ssDNA cellulose column. 5 μ l / each sample was taken out and added to 2 μ l 3 \times SDS loading buffer. After heating at 90 °C for 2 min and centrifugation at 12,000 \times g, room temperature for 5 min, 2 μ l supernatant / each sample was loaded to run gels as described in materials and methods, and stained with Coomassie brilliant blue.

2.4 Discussion

2.4.1 The Effect of His-Tag Location on Its Affinity

The N-terminal or C-terminal location of the six-histidine tag is very important for the recombinant RecD protein to bind to the nickel affinity column. The sequence alignment of RecD protein shows that the seven helicase-motifs are clustered relatively close to the C-terminus and a long region (almost half) with unknown function occupies the N-terminus. The fact that the recombinant RecD protein has a very low affinity to the nickel-column when the His-tag is attached to its N-terminus suggests that the N-terminal region is folded inside the protein in the native conformation. The twenty amino acid His-tag region cannot stick out from the interior side of the protein and have the chance to bind to the nickel-column. Another possibility is that the N-terminus forms a hydrophobic interface involved in the interaction with another copy of RecD or other protein subunit to work together as a holoenzyme. Can the RecD protein also employ a bipartite structure as RecB does in *E. coli*? If so, the DNA-binding and unwinding function in the RecD protein is located in the C-terminus about 40 kDa region, which is opposite to the N-terminal location in *E. coli* RecB, and another unknown function is located in the N-terminal 40 kDa domain.

2.4.2 The Significantly Tight Binding of RecD Protein on ss-DNA Cellulose Column

The binding between RecD protein and ssDNA cellulose is very tight so that RecD can only be washed off in buffer with very high (~ 1.0 M) salt concentration. It suggests that the binding between RecD protein and ssDNA is not a random interaction.

Instead, ssDNA must be involved in the biochemical function of RecD, e.g. either the substrate or product of RecD. The fact that C-terminal His-tagged RecD has high ssDNA affinity is consistent with the predicted C-terminal domain for its helicase activity that requires the easy access for dsDNA substrate and ATP.

2.4.3 Stability

The *E. coli* RecD protein is largely insoluble when overexpressed and must be purified in denatured condition and then renatured in order to detect its enzymatic activity. The denaturing and renaturing process may result in significant loss of its activity. The C-terminal His-tagged RecD-like protein from *D. radiodurans*, in contrast, can be fairly easily overexpressed and purified in native condition and retain activity during prolonged storage.

2.4.4 Conclusion

The high-level expression of recombinant gene products in the Gram-negative bacterium *E. coli* often results in the misfolding of the protein of interest. The misfolded protein is the target of the subsequent degradation by cellular proteases. It can also deposit into biologically inactive aggregates known as inclusion bodies¹⁰⁶. To avoid this from happening, we can decrease both the concentration of IPTG and the temperature of incubation to slow down the protein synthesis in the host cells so that the newly-translated polypeptides will have enough time and energy supply to adapt the correct folding.

The fact that most of the expression vectors produce fusion proteins might at first seem a disadvantage because the natural product of the inserted gene is not made. However, the extra amino acids on the fusion protein can be a great help in purifying the protein product. Expressing His-tagged recombinant protein, for an example, is a good way to study protein function *in vitro*. The attached stretch of six histidine sequence with a very short linker on one end (usually N-terminus) of the protein usually does not affect its conformational structure, as well as its function, but makes the purification process much easier. Oligo-histidine region has a high affinity for metals like nickel so that the proteins that have such region can be purified using nickel affinity chromatography because very few if any natural proteins have oligo-histidine region and can bind to the column tightly. The biochemical study of our recombinant RecD protein later showed a fairly high biochemical activity, suggesting that the effect of the eight amino acid tag on its C-terminus is not significant.

Chapter 3 BIOCHEMICAL STUDY OF RECD *IN VITRO*

As shown in figure 1.3, the sequence alignment of RecD protein from *D. radiodurans* revealed the seven conserved helicase motifs shared among the Superfamily I helicases. Both the RecBCD-subunit type RecD and the *D. radiodurans*-type RecD belong to this Superfamily. The difference between the two types is in their N-terminal regions. We predicted that the RecD protein from *D. radiodurans* is a single-stranded DNA-dependent ATPase and DNA helicase according to the biochemical activities of the well-known RecD subunit in *E. coli* RecBCD enzyme. Then, we designed a series of assays to test our prediction. With a longer N-terminal extension (> 300 residues), the RecD protein from *D. radiodurans* should also have some difference from RecBCD type RecD. It is enticing to think that the N-terminal region could represent a separate functional domain.

3.1 Introduction

Most of the biochemical assays used here were designed to study the C-terminal helicase domain of the RecD protein. The > 300 amino acid sequence preceding the first helicase motif in N-terminus is less conserved among the *D. radiodurans* RecD-like proteins and does not contain sequences found in other helicases. There has been no study of this region available so far. We predicted that the N-terminal region of the RecD protein (almost half of the protein) forms a structurally independent domain with some novel functions, based on the study of the properties of both N- and C-terminal His-tagged recombinant proteins binding to the nickel affinity column.

An ATPase assay carried out on TLC membrane was designed to test the ATPase activity of RecD by adding different types of DNA: ssDNA oligonucleotide, linearized plasmid and circular plasmid. Four types of DNA substrates with different end structures of blunt, 3'-, 5'-overhang, and fork-shape were designed to test the suitable substrates for the helicase activity. DNAs with different lengths (20, 52, and 76 bp) were used to test the processivity. The single strand binding (SSB) protein from either *E. coli* or *D. radiodurans* was used in the helicase assay with the 52 bp substrate. Their effects in unwinding at both pH 6.5 and pH 7.5 were evaluated. The gel mobility shift experiment was designed to test the possibility of dimerization of RecD upon binding to DNA substrate by using hairpin dsDNAs with different end structures.

Since there is no functional model available so far for the RecD-like protein found in *D. radiodurans* and some gram-positive bacteria, all of the conditions in the biochemical assays used here were those that worked well for the RecBCD enzyme from *E. coli*. Are those conditions also optimal for the RecD from *D. radiodurans*? Several adjustments were made toward the conditions for the helicase assay. Those adjustable conditions are: reaction temperature, Mg^{2+} concentration, ATP concentration, salt (such as NaCl and KCl) concentration, and reaction pH.

3.2 Materials and Methods

3.2.1 ATPase Assay

The ATPase assay was carried out by thin layer chromatography on polyethyleneimine (PEI)-cellulose plates (J. T. Baker). ATP, ADP, and inorganic phosphate group in solution have different negative charges so that they can be easily

separated and visualized on fluorescence-coated TLC plates. The polyethyleneimine-cellulose plates used here were pretreated with 10 % NaCl solution and pre-spotted at the origin with marker (0.5 μ l of 40 mM ATP and 40 mM ADP mixture), to act as a carrier and enhance the separation of [γ - 32 P]ATP and non-radioactive ADP.

Standard reaction (20 μ l total volume) contained: 50 mM Tris-HCl, pH 7.5, 10 mM MgCl₂, 10 μ M DNA (no DNA as control, single-stranded oligonucleotide, circular double-stranded DNA, or linear double-stranded DNA), 1 mM DTT, 5 % glycerol, 0.1 mg/ml BSA, and 10 μ M ATP (with 1 % [γ - 32 P]ATP). Enzyme dilutions were prepared by adding small aliquots of concentrated stock to enzyme dilution buffer (25 mM potassium phosphate, pH 7.5, 0.1 mM EDTA, 0.1 mM DTT, 0.1 mg/ml BSA and 10 % glycerol). The reactions were mixed and incubated in a 37 °C water bath for 5 min. A small aliquot (0.5 μ l) was taken out (zero time point) and the reactions were started by adding the same volume of RecD enzyme with different concentrations. Aliquots were taken and spotted on a TLC plate at various time points. The TLC plates were then developed in 0.5 M LiCl and 1 M formic acid buffer, dried, and exposed to the PhosphorImager screen (Molecular Dynamics) followed by scanning the screen (Amersham Biosciences Storm Scanner). An ellipse object was created using the ImageQuant software (Amersham Biosciences) for every radioactive spot corresponding to the [γ - 32 P]ATP or [32 P]Pi group migrating differently in the resulting image. The background for each exposure was corrected with its local average by the ImageQuant program. The percent ATP hydrolysis was determined by quantitating the relative amount of [γ - 32 P]ATP and [32 P]Pi group in each lane, and then calculated as % hydrolysis = Pi / (Pi + ATP), where Pi and ATP are integrated amounts of radioactivity in the Pi and ATP spots in that lane.

3.2.2 Helicase Assay

Synthetic DNA oligonucleotides were purchased from Invitrogen Corp. and were purified from denaturing polyacrylamide gels using a MERmaid kit (BIO101 Corp.). *E. coli* single-stranded DNA binding protein (EcSSB) was purchased from US Biochemicals Corp. or was purified before¹⁰⁷. Purified *D. radiodurans* SSB protein¹⁰⁸ was a generous gift from Professor Mike Cox, University of Wisconsin.

First, the helicase assay was done using short oligomers with 20-base pair dsDNA regions, as shown in figure 3.1. These four oligomers can be annealed in pairs to make the following four structures: a. 20 bp full duplex with blunt ends (II + III); b. 20 bp with a 12 nt single-stranded tail at the 5'-end (III + IV); c. 20 bp with a 12 nt single-stranded tail at the 3'-end (I + II); and d. 20 bp with a forked end of 12 nt single-stranded DNA (I + IV). Oligomers I and III were labeled at the 5'-end with [γ -³²P]ATP and polynucleotide kinase so that each of the four structures has one single strand labeled.

The 20 μ l labeling reactions had: 1 \times T4 polynucleotide kinase buffer, 0.5 μ M oligomer I or III, 10 units of T4 polynucleotide kinase, and 0.5 μ M [γ -³²P]ATP. The reaction was incubated at 37 °C for 60 min. The labeled oligomers were purified from unreacted [γ -³²P]ATP with QIAquick® Nucleotide Removal Kit (Qiagen Corp), and eluted in 100 μ l TE buffer. 0.5-1.0 μ l sample at each step during purification was taken out for scintillation counting to trace the radioactivity. The average recovery yield (= radioactivity of eluted oligomer / radioactivity of total labeling product) for the labeling was 40~50%. The final concentration of each 5-³²P-labeled oligomer was calculated from the starting [γ -³²P]ATP concentration, yield, and the final eluted volume (= 0.5 μ M * 20 μ l * yield / 100 μ l). The labeled oligomers were checked by thin layer

A		Helicase substrates:	
I	32	GCCGTAGIATGCACATCGACATCCAATCGACAT	
II	20	GTCGATGIGCATACTACGGC	
III	20	GCCGTAGIATGCACATCGAC	
IV	32	TACAGCTACCTAGTCGATGTGCATACTACGGC	
V	28	GCCGTAGIATGCACATCGACTAGGTAGC	
VI	26	TACCTIAGTCGATGTGCATACTACGGC	
VII	28	GCTIACCTIAGTCGATGTGCATACTACGGC	
VIII	30	CAGCTIACCTIAGTCGATGTGCATACTACGGC	
B		Substrate structures:	
I + II	20 bp, 12 nt 3'-tail		I II
II + III	20 bp, blunt ends		II III
III + IV	20 bp, 12 nt 5'-tail		III IV
I + IV	20 bp, 12 nt forked end		I IV
V + IV	28 bp, 4 nt 5'-tail		V IV
VI + III	20 bp, 6 nt 5'-tail		III VI
VII + III	20 bp, 8 nt 5'-tail		III VII
VIII + III	20 bp, 10 nt 5'-tail		III VIII

Figure 3.1 The eight oligomers designed for the helicase assay. (A). Each of the oligomers has a region complementary to other oligomer(s) in the group. (B). The paired oligomers shown on the right side are dsDNA substrates with different end structures.

chromatography on PEI TLC plates developed in 1 M NaH₂PO₄, pH 3.5, followed by exposure in the Phosphorimager and scanning of the screen.

The four ds DNA substrates were prepared by mixing 1 nM radio-labeled oligomer (I or III) with 19 nM of the same, but unlabeled oligomer and 20 nM of its unlabeled complementary strand (II or IV) in buffer containing 50 mM NaCl, 20 mM Tris-OAc, pH 7.5, 1 mM MgOAc. The mixtures were heated at 95°C for 2 min and then cooled down slowly at room temperature to allow the two complementary oligomers to anneal together.

The unwinding reaction mixture contained: 25 mM Tris-OAc, pH 7.5, 10 mM MgOAc, 1 mM ATP, 1 mM DTT, 0.1 mg/ml × BSA, and 1 nM of duplex substrate. 1 nM substrate concentration was proven to be low enough by a control experiment of 90 °C heat denaturing and 30 °C reannealing. The reannealing of single strand products can be ignored when calculating the reaction rates at this concentration. The reaction mixtures were incubated at 30°C for 5 min and 5 µl aliquots were taken (zero time point) and the reactions were started by adding RecD enzyme. 5 µl aliquots were taken and quenched on ice with 1.5 µl 4 × quenching buffer (40 % glycerol, 2.4 % SDS, 100 mM EDTA, 0.12 % bromophenol blue, and 15 nM of unlabeled oligonucleotide corresponding to the labeled strand in the double-stranded substrate) at the indicated time points.

After collecting all samples, non-denaturing 15 % polyacrylamide gels were run in 1 × TBE buffer (90 mM Tris, 89 mM boric acid, 1.98 mM EDTA, pH 8.3), under 150 volts constant power supply. The gels were then dried and exposed to the PhosphorImager screen followed by scanning the screen. The percent DNA unwound was determined by quantitating the relative amount of ³²P-labeled ds and ss DNA in each lane,

and then calculated as $\% \text{ unwound} = 100 \times [\text{ss} / (\text{ss} + \text{ds})]$, where ss and ds are the integrated amounts of radioactivity in the ss and ds bands in that lane. The background of ssDNA present in the zero time point (usually <5% of the total DNA) was subtracted out. DNA unwinding rates were calculated from the slope of the initial, nearly linear, part of the reaction time course.

The unwinding rates for the two types of substrates were calculated by using different concentrations of RecD protein in four reactions for each substrate. Depending on the structures of the ends in the substrates for RecD binding and reaction, the difference of reaction rates were almost ten-fold. 0.01, 0.03, 0.06, and 0.12 nM RecD concentrations were used in the four reactions for 20 bp 5'-overhang substrate. 0.001, 0.003, 0.006, and 0.012 nM RecD concentrations were used in the four reactions for 20 bp fork-shaped substrate.

Several substrates with 5'-overhang of 4, 6, 8, and 10 nucleotides respectively were used to test the minimum length of ssDNA overhang required by RecD for unwinding. The experiment was done as standard helicase assay, using 1 nM of each substrate and 0.25 nM RecD in each reaction.

After 20 bp short dsDNA substrates were tested, two longer substrates were designed with a 52 or 76 bp dsDNA region respectively plus a 12nt 5'- ssDNA tail, as shown in figure 3.2. These two substrates were used to do the same helicase assay to test the processivity of RecD protein. Since the unwinding efficiency of the longer substrates was very low, the SSB proteins from either *E. coli* or *D. radiodurans* were added in the helicase assays with 52 bp dsDNA substrates to prevent the rewinding of the unwound ssDNA product. The helicase assay with SSB protein was basically the same with the

following alternations: (1) The reaction was started by adding ATP, instead of RecD, to the pre-incubated mixture. This was because the SSB increased the ssDNA background at zero time point. (2) 1.5 μ l 4 \times dye buffer (40 % glycerol, 100 mM EDTA, and 0.12 % bromophenol blue), instead of quenching buffer (with SDS and corresponding unlabeled oligomer), was used to quench the reaction samples at each time point.

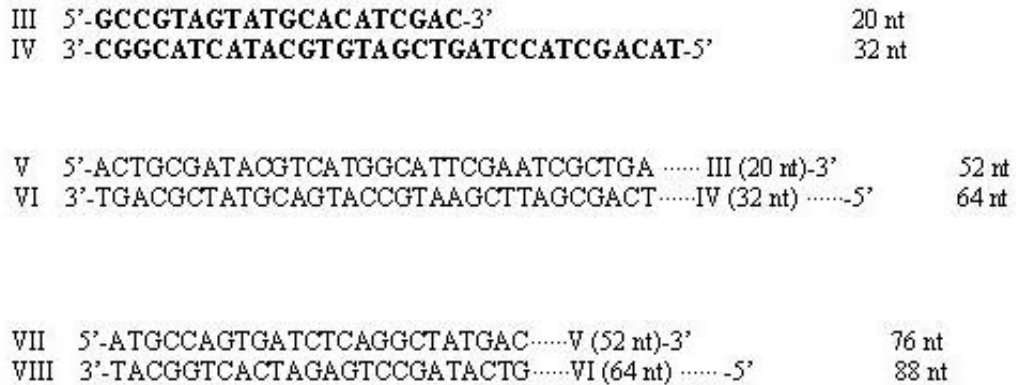


Figure 3.2 The design for the 52 and 76 bp duplexes with a 5'-single-stranded 12 nt tail. The 52 bp ds DNA V-VI is 20 bp III-IV ds DNA with a 32 bp double-stranded region added to its blunt end and the 76 bp ds DNA VII-VIII has a 24 bp double-stranded region added to the blunt end of 52 bp ds DNA V-VI.

3.2.3 Gel Mobility Shift Experiment

Three oligomers (Invitrogen) were designed with hairpin structures as shown in figure 3.3. A small three-nucleotide loop and a single-stranded region (a 6 nt or 12 nt 5'-single-stranded tail, or a 12 nt forked end) are connected by a 20 bp double-stranded DNA region. The 20 bp ds DNA region is formed by intra-molecular annealing to avoid the incomplete annealing between two complementary oligonucleotides (intermolecular) under the low DNA concentrations used.

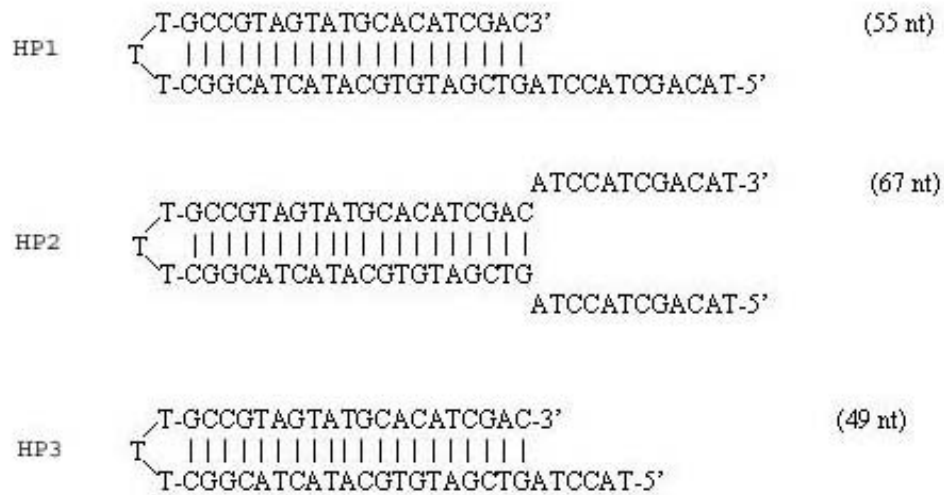


Figure 3.3 The design for the three hairpin structures. All of them share a common structure of a 20 bp double-stranded region that connects a three-T loop on one end and a single-stranded region at the other. HP1 has a 12 nt 5'-overhang. HP2 has a fork-shape of 12 nt at both 3'- and 5'-ends. HP3 has a 6 nt 5'-overhang.

The radio-labeling step of the three oligomers were the same as described in helicase assay. The binding experiment was carried out in a series of small aliquots with different final RecD concentrations. Each sample contained 5 μ l volume of 1 nM hairpin DNA (with 5 % radio-labeled) in 25 mM Tris-OAc, 10 mM MgOAc, and 1 mM DTT solution and 1.25 μ l appropriately diluted RecD. All of the samples were kept on ice for 30 minutes before 1.5 μ l of 30 % (v:v) glycerol (containing 0.25 % (w:v) bromophenol blue dye for samples without RecD as marker) was added to each sample. Then, the samples were quickly loaded onto 10 % (37.5:1 = acrylamide: bisacrylamide, 0.1% ammonium persulfate, and 0.035 % TEMED), 1 \times TBE, non-denaturing PAGE gels pre-chilled in the cold room and pre-run under 10 mA current for 30 minute. High voltage (~500 volt) was applied to run the gels for a short time (15~20 min) in the cold room. The gels were then dried and followed by analysis with the Storm PhosphorImager.

3.2.4 The Assays with Lower pH

Preliminary helicase assays with four different pHs of 6.8, 7.5, 8.0, and 9.0 were done by using Tris-HCl buffers with these pHs. The unwinding at pH 6.8 is the fastest (data not shown). More helicase assays with a range of pHs from 6.1 to 7.5, one reaction for every 0.2 pH unit, were carried out while other conditions were the same. 1 M PIPES buffers were prepared at pH 6.1, 6.3, 6.5, 6.7, 6.9, 7.1, 7.3, and 7.5 by adjusting with 6 N NaOH. Eight helicase assays were done in the same way as described in the helicase assay section with 25 mM each of the above PIPES buffer substituting for the Tris.OAc buffer, pH 7.5.

3.3 Results

3.3.1 ssDNA-Dependent ATPase

We first tested the purified RecD protein for ATP hydrolysis activity. As predicted by the sequence alignment, the RecD protein exhibits efficient ATP hydrolysis activity in the presence of a single-stranded DNA oligonucleotide, with no detectable activity in the absence of DNA, as shown in figure 3.4. A low level of ATP hydrolysis was detected with linear dsDNA, and even less with circular dsDNA. The latter ATPase activity may result from a small amount of linear DNA contamination in the circular plasmid preparation.

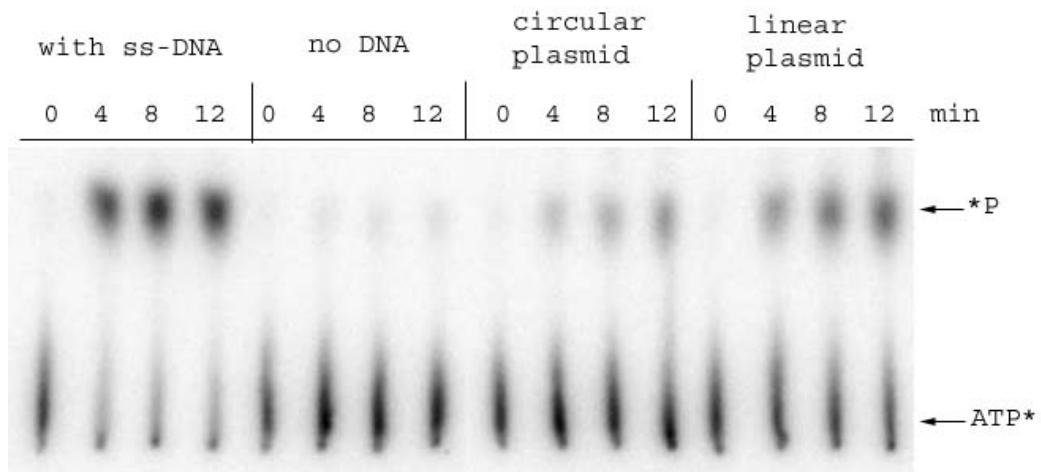


Figure 3.4 ATP hydrolysis by RecD on TLC membrane. Reaction mixtures contained 50 mM Tris-HCl, pH 7.5, 10 mM MgCl₂, 1 mM DTT, 5 % glycerol, 0.1 mg/ml BSA, 10 μM [γ-³²P]ATP, 0.2 nM RecD enzyme, and a 17 nt single-stranded oligonucleotide (first reaction), circular pTZ19R DNA (third reaction), pTZ19R linearized by cleavage with EcoR I (fourth reaction), or no DNA (second reaction). DNA concentration (when present) was 10 μM

3.3.2 DNA Helicase with Low Processivity

We then tested for DNA unwinding activity, as shown in figure 3.5. RecD unwound a 20 bp duplex with a 12 nt 5'-single-stranded extension (oligonucleotides I + II, figure 3.1), and the same duplex with a forked end (I + IV, 12 nt non-complementary extensions on both the 3'- and 5'-ends). There was no detectable unwinding of a 20 bp duplex with blunt ends nor of the duplex with the 3'-single-stranded tail. Thus the enzyme requires a DNA duplex with a 5'-single-stranded extension for helicase activity. While the forked substrate is unwound more rapidly than the tailed substrate, the enzyme does not require the fork, in contrast to some other helicases¹⁰⁹. There was no unwinding in the absence of ATP, magnesium ion, or RecD (data not shown).

The RecD protein was in excess over the DNA in the experiment shown in figure 3.5. Unwinding of the 5'-tailed and forked substrates was efficient even when the DNA was in 10-1000 – fold excess over the protein (figure 3.6 and figure 3.8). The fact that a substantial fraction of the DNA was unwound under these conditions suggests that the enzyme acts catalytically, with a single enzyme molecule unwinding several DNA (20-100), depending on the RecD concentration and the type of DNA substrate). The initial rates of the reactions were determined from the slopes of the linear part of the time courses. Each initial rate (figure 3.7 C and figure 3.9 C) was then divided by the corresponding RecD concentration used to determine that rate. The unwinding rates for each substrate were 6.0 (± 1.5) DNA molecules unwound/RecD/min, or 120 (± 30) bp/RecD/min (average and standard deviation of four determinations), for the 5'-tailed substrate (figure 3.7), and 48 (± 6) DNA molecules unwound/RecD/min, or 960 (± 120) bp/RecD/min (four determinations), for the forked substrate (figure 3.9).

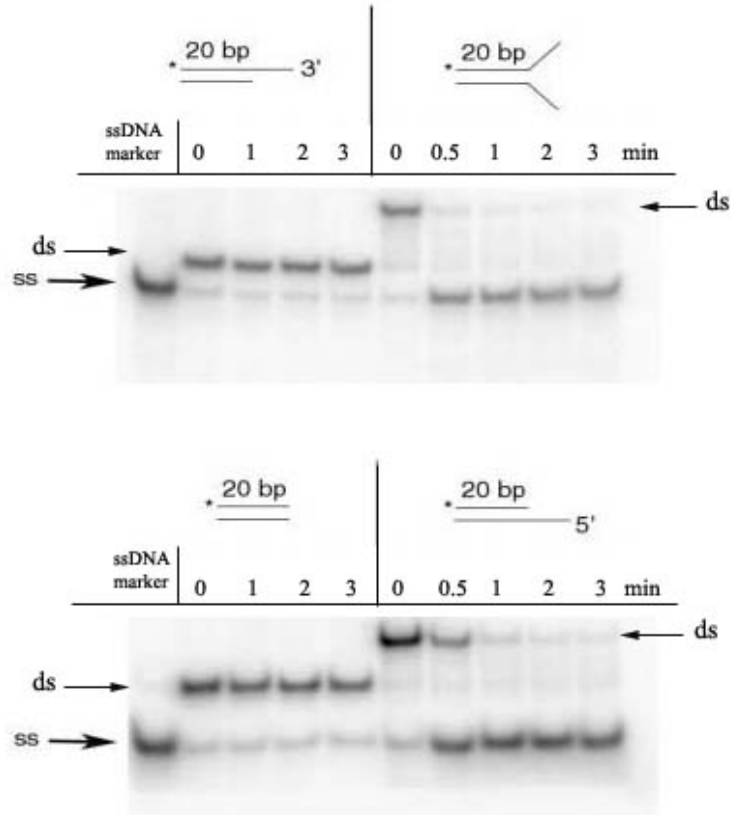


Figure 3.5 DNA unwinding by *D. radiodurans* RecD enzyme. Reaction mixtures contained 25 mM Tris-acetate, pH 7.5, 10 mM magnesium acetate, 1 mM ATP, 1 mM DTT, 0.1 mg/ml BSA, 1 nM (5% ^{32}P -labeled) double-stranded DNA substrate, and 5 nM RecD protein. The DNA substrates had 20 base pairs and 12 nt single-stranded tails where shown. Reactions were run at 30 °C and samples were analyzed on non-denaturing 15 % polyacrylamide gels as described in materials and methods. Samples in the first lane of each gel were taken before enzyme was added and were heated to 100 °C before loading, to provide a marker for the labeled single-strand.

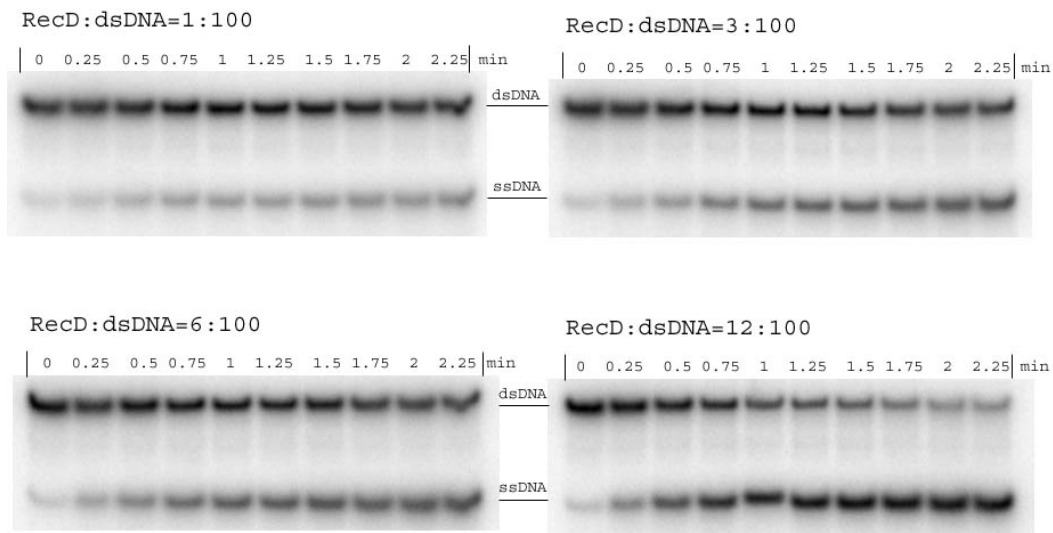


Figure 3.6 Unwinding at various RecD concentrations for the 20 bp 5'-tailed substrate. The DNA substrate (1 nM) was 20 bp with a 12 nt 5'-tail, with 0.01 nM RecD (first), 0.03 nM RecD (second), 0.06 nM RecD (third) and 0.12 nM RecD (fourth) in time-course reactions. Other conditions were as in figure 3.5. Samples were run on 15 % non-denaturing polyacrylamide gels and analyzed using a Phosphorimager as described in materials and methods.

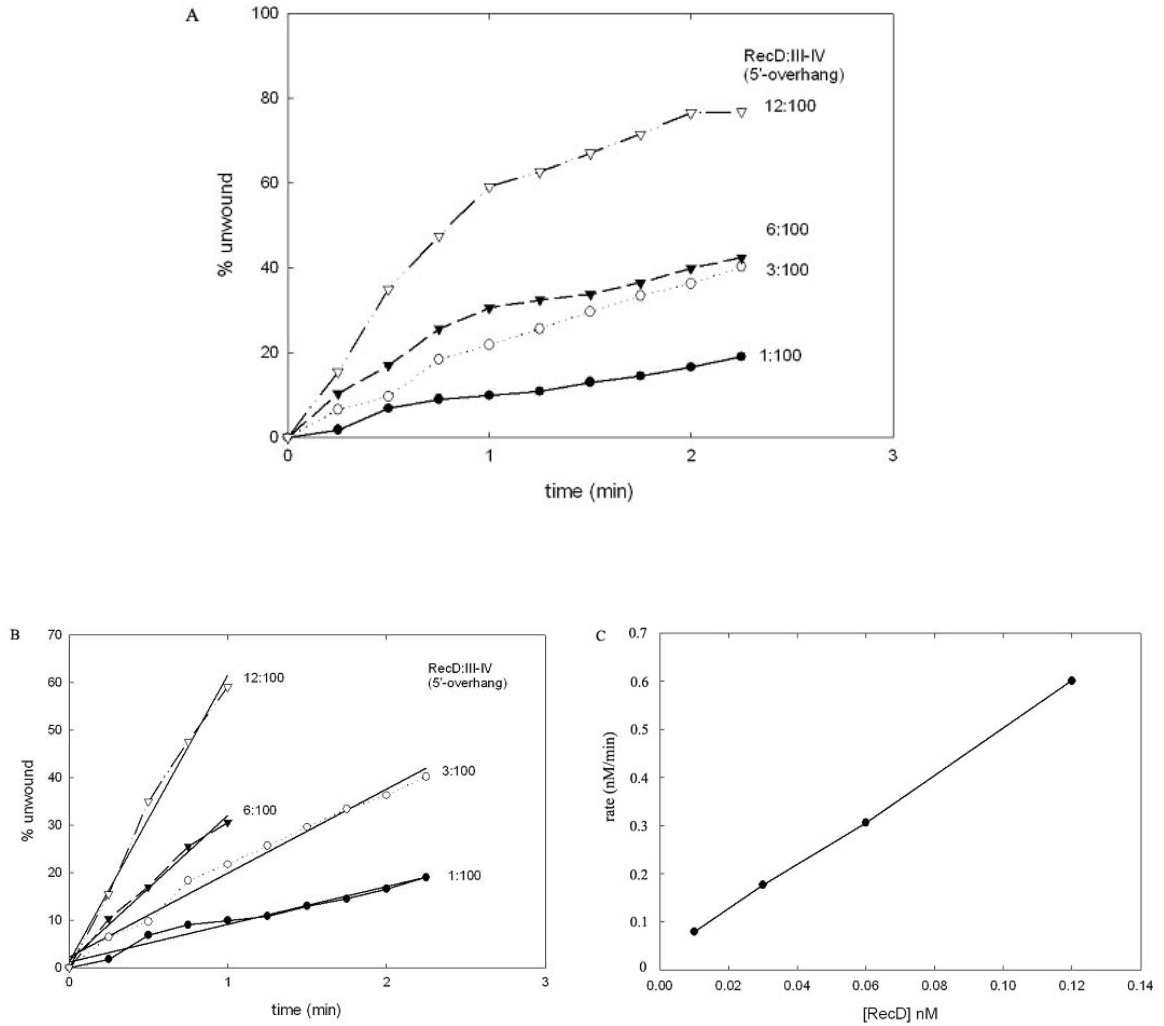


Figure 3.7 The calculation of the unwinding reaction rate for the 20 bp 5'-tailed substrate. (A) The reactions were with 0.01 nM RecD (closed circles), 0.03 nM RecD (open circles), 0.06 nM RecD (closed triangles) and 0.12 nM RecD (open triangles), as in figure 3.6. (B) The slope of the linear part of the time course was determined by linear regression for each reaction plot to calculate the initial rate. (C) Rate vs. RecD concentration plot.

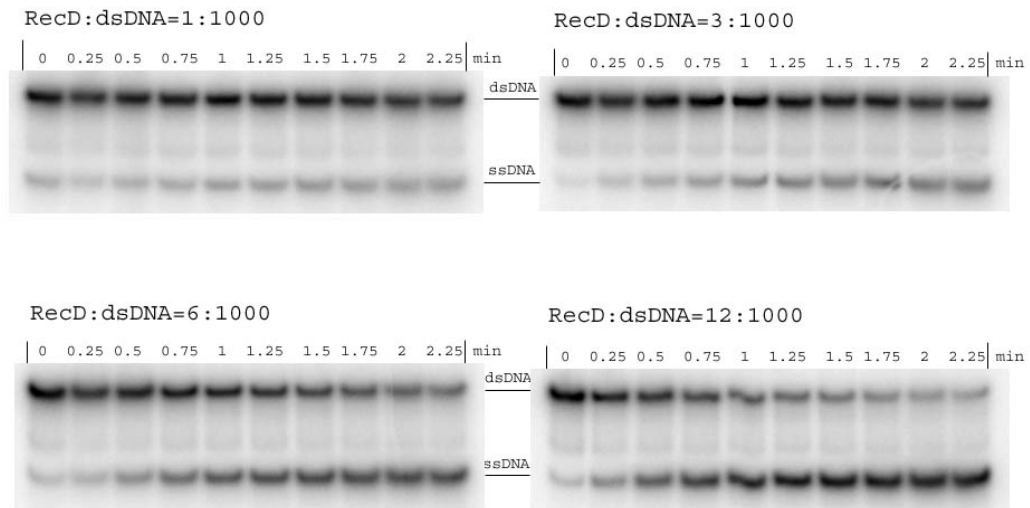


Figure 3.8 Unwinding at various RecD concentrations for the 20 bp fork-shaped substrate. The DNA substrate (1 nM) was 20 bp with a 12 nt single-stranded fork on one end, with 0.001 nM RecD (first), 0.003 nM RecD (second), 0.006 nM RecD (third) and 0.012 nM RecD (fourth) in time-course reactions. Other conditions were as in figure 3.5. Samples were run on 15 % non-denaturing polyacrylamide gels and analyzed using a Phosphorimager as described in materials and methods.

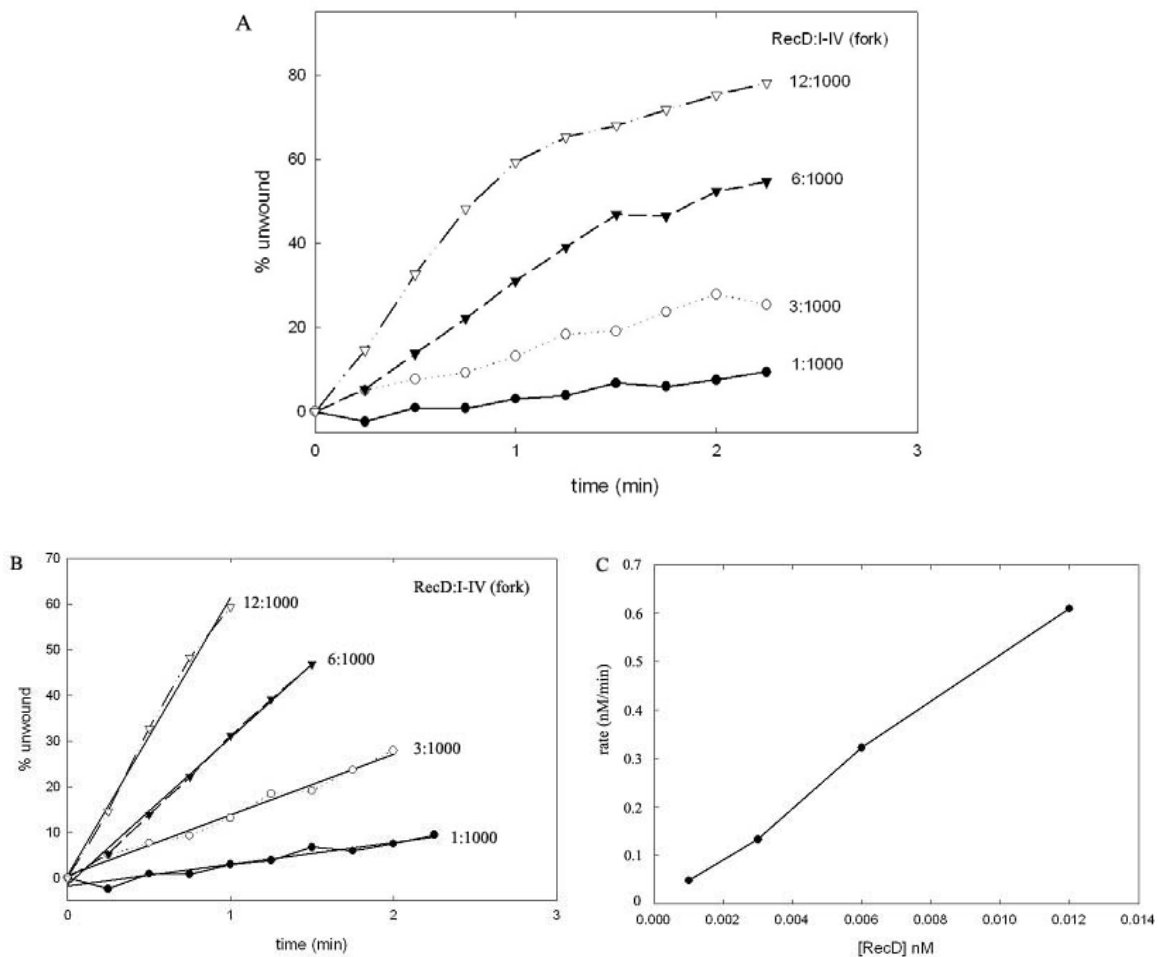


Figure 3.9 The calculation of the unwinding reaction rate for the 20 bp forked substrate. (A) The reactions were with 0.001 nM RecD (closed circles), 0.003 nM RecD (open circles), 0.006 nM RecD (closed triangles) and 0.012 nM RecD (open triangles), as in figure 3.8. (B) The slope of the linear part of the time course was determined by linear regression for each reaction plot to calculate the rate. (C) Rate vs. RecD concentration plot.

We tested next whether the enzyme can unwind duplex substrates with 5'-terminal extension shorter than 12 nt. We detected no unwinding of a 28 bp duplex with a 4 nucleotide 5'-single-stranded tail (oligomers IV + V, figure 3.1), with 1 nM DNA and 10 nM RecD (data not shown). 20 bp duplexes with 6 or 8-nucleotide 5'-tails (III + VI or III + VII, respectively) were very poor substrates under conditions where the substrates with a 10 or 12 nt overhang were unwound efficiently (figure 3.10). Greater unwinding of the 8 nt tailed substrate, and slight unwinding of the 6 nt tailed substrate, could be detected at higher enzyme concentration (10 nM; data not shown). These results suggest that the enzyme requires at least 10 nt of single-stranded DNA for tight binding to the DNA substrates.

We next asked whether the enzyme is able to unwind substrates longer than the 20 bp duplexes tested so far by using 52 and 76 bp substrates with a 12 nt 5'-single-stranded overhang, as shown in figure 3.2. In striking contrast to the results with the 20 bp substrates, a large molar excess of protein over DNA (10-100-fold) was required for significant unwinding of the 52 bp substrate (figure 3.12). There was little or no unwinding of the 52 bp substrate with enzyme concentrations equal to or less than the DNA (data not shown). The 76 bp substrate was unwound even less efficiently than the 52 bp substrate (figure 3.13).

The effects of different length of 5'-overhang

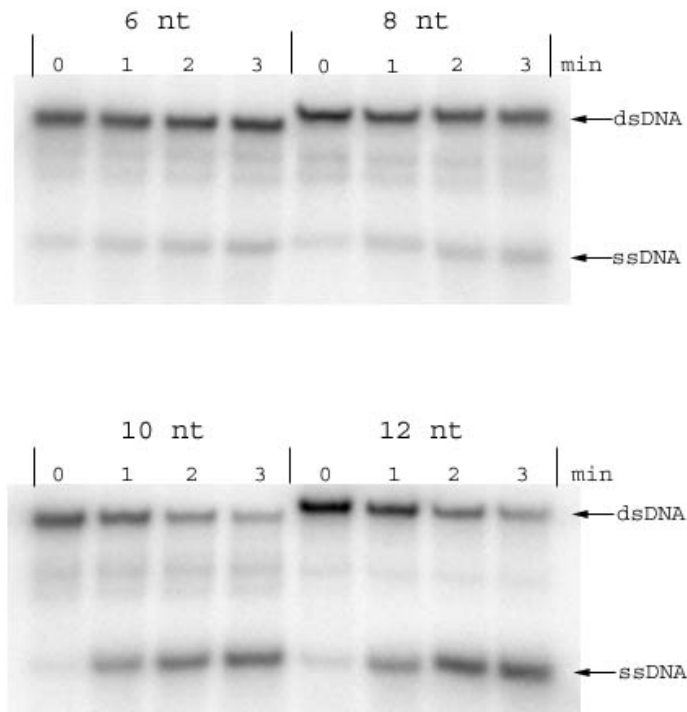


Figure 3.10 Effect of 5'-single-strand length on DNA unwinding. Reaction mixtures were as in figure 3.5, with 0.25 nM RecD and 1 nM [5'-³²P]DNA substrates consisting of 20-28 bp with 5'-single-stranded extensions of 6 nt, 8 nt, 10 nt, or 12 nt in a time course reaction. Samples were taken and analyzed on 15 % non-denaturing polyacrylamide gels as described in materials and methods.

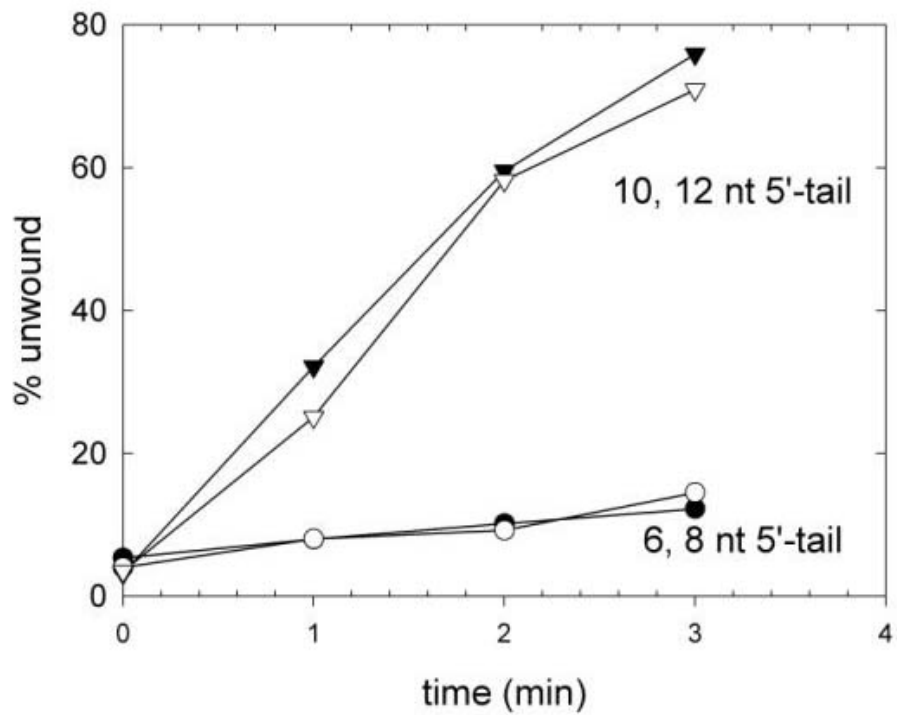


Figure 3.11 The % unwound vs. time plots for the effect of 5'-single-strand extension length on DNA unwinding. Reaction mixtures were as described in figure 3.10, with substrates consisting of 20 bp with 5'-single-stranded extensions of 6 nt (closed circles), 8 nt (open circles), 10 nt (closed triangles), or 12 nt (open triangles).

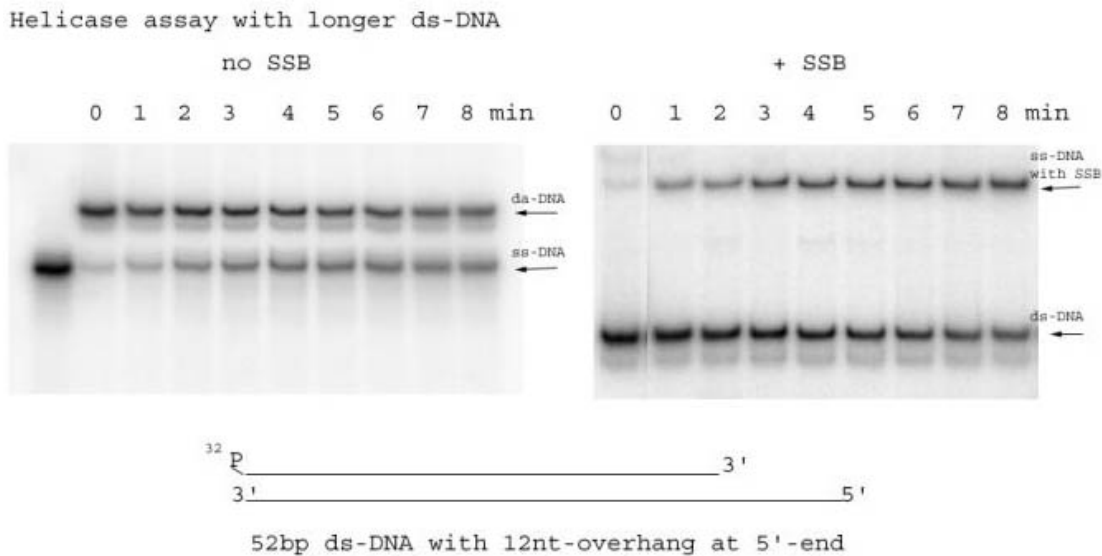


Figure 3.12 Time-course unwinding of 52 bp duplex. The reaction mixtures contained 1 nM of the 52 bp substrate with a 12 nt 5'-tail, 100 nM RecD, and other conditions as in figure 3.5, except the second reaction also contained *E. coli* SSB protein (20 nM). Samples containing EcSSB were quenched by the quenching buffer similar to the one used for regular helicase assay except that neither SDS nor unlabeled single-stranded DNA was included. Samples were taken and analyzed on 10 % non-denaturing polyacrylamide gels as described in materials and methods.

There are at least two possible explanations for the inefficient unwinding for the longer substrates compared to the 20 bp substrates. One is that the individual DNA strands might rewind behind the RecD as it travels along the DNA duplex. One way to prevent rewinding is to include a single-stranded DNA binding protein in the unwinding reaction mixtures, to grab the unwound strands before they can reanneal. The *E. coli* SSB

protein was able to bind to the unwound DNA strands (figure 3.12), but addition of EcSSB had little effect on the unwinding rate or extent for the 52 bp DNA (figure 3.13) and the 76 bp DNA (data not shown). (The EcSSB was in an amount sufficient to bind all of the ssDNAs in the reaction mixture, given a binding size of one EcSSB to 8 nt of ssDNA.) A second, likely, explanation for the inefficient unwinding of longer substrates is that RecD is a helicase with low processivity. The enzyme is able to unwind a short duplex (i.e., 20 bp) but it falls off before it can completely unwind the 52 bp dsDNA molecules.

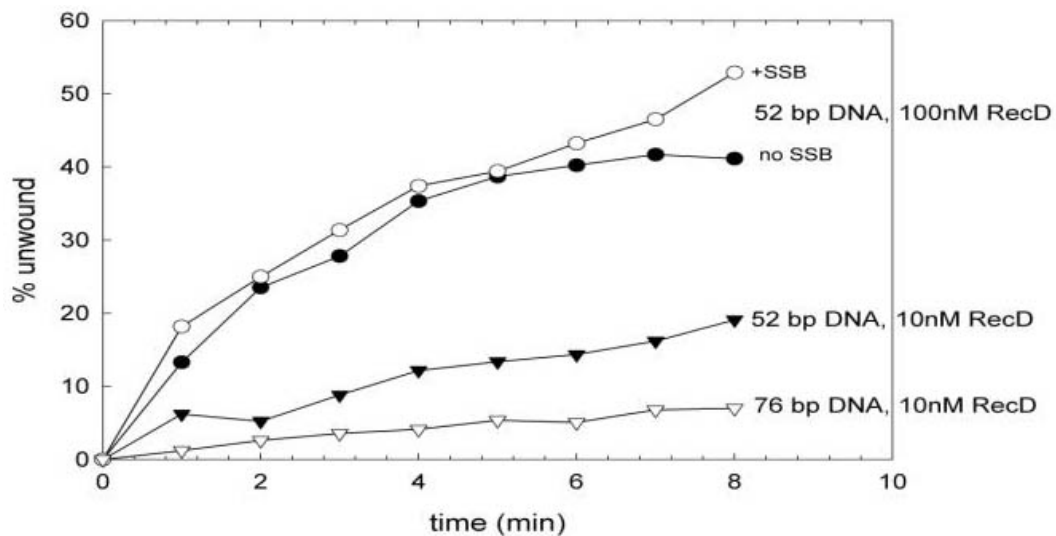


Figure 3.13 Unwinding of 52 and 76 bp duplexes at pH 7.5. The percent DNA unwound in the reactions shown in figure 3.12 was determined as described in materials and methods, for the 52 bp substrate, 100 nM RecD, no EcSSB (closed circles); 20 nM EcSSB (open circles). Other reactions (gels not shown) contained 52 bp substrate (1 nM), 10 nM RecD, no EcSSB (closed triangles); and 76 bp substrate (1 nM), 10 nM RecD, no EcSSB (open triangles).

3.3.2 The Binding of RecD to DNA Substrates

The theoretical basis for gel mobility shift experiment is that a small DNA molecule has a much higher mobility in gel electrophoresis than the same DNA does when it is bound to a protein. We measured the binding of RecD to hairpin oligonucleotides with various end structures, as shown in figure 3.14. The hairpin with a 12 nt forked end was bound tightly and two shifted complexes were observed. We presume that these complexes are DNA molecules with RecD bound to one or both ss-tails. Cooperative binding means that the second binding is easier than the first one, and complex I will not accumulate before complex II is present, as shown in figure 3.15 A. As shown in the figure 3.15 B, more than 50% of the DNA was formed into complex I while almost no complex II was present suggesting that there was no cooperativity for the binding of RecD to the forked hairpin. The slower mobility complex is likely that the two RecD proteins bind to the two tails individually, instead of binding to one tail upon dimerization.

The enzyme bound less tightly to the 5'-tailed DNA than to the fork. The hairpin with a 6 nt extension was bound weakest of all, with a large excess of protein required before a significant amount of DNA was shifted in the gel. Weak binding to this hairpin DNA is consistent with the fact that the duplex with a 6 nt 5'-tail is a very poor unwinding substrate (figure 3.10). This hairpin (at 20 nM) also did not inhibit the unwinding reaction of RecD (0.1 nM) with the 5'-tailed 20 bp substrate (1 nM) while other duplexes with longer ssDNA region showed significant inhibition (data not shown).

Interestingly, two shifted bands appeared at high protein concentrations for the 6 nt tailed hairpin. The slower mobility complex could result from additional enzyme

molecules binding to the DNA (non-specific binding, perhaps to the loop or to the double-stranded region in the hairpin), or from dimerization of the protein on the DNA. We do not know whether DNA unwinding requires the combined action of more than one RecD molecule on the DNA substrate, although the fact that the 5'-tailed substrate is unwound efficiently but only a single complex is observed in the binding experiment under the same RecD concentration suggests that the RecD enzyme may unwind these molecules as a monomer. Some Superfamily I helicases unwind DNA as dimers^{110, 111} while others apparently function as monomers^{112, 113}. Further experiments must be done to resolve this point for *D. radiodurans* RecD.

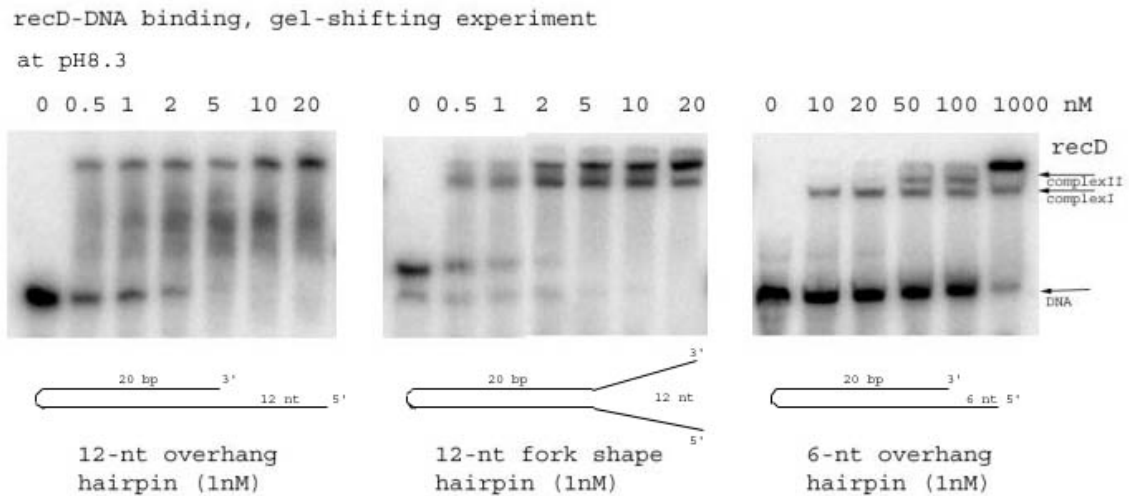


Figure 3.14 The binding between RecD and dsDNA hairpins with different ssDNA ends. The binding mixtures contained, in 5 μ l, 25 mM Tris-acetate, pH 7.5, 10 mM magnesium-acetate, 1 nM [5'-³²P] hairpin DNA and 1.25 μ l of appropriately diluted RecD. The samples were analyzed on non-denaturing 10 % polyacrylamide gels as described in materials and methods.

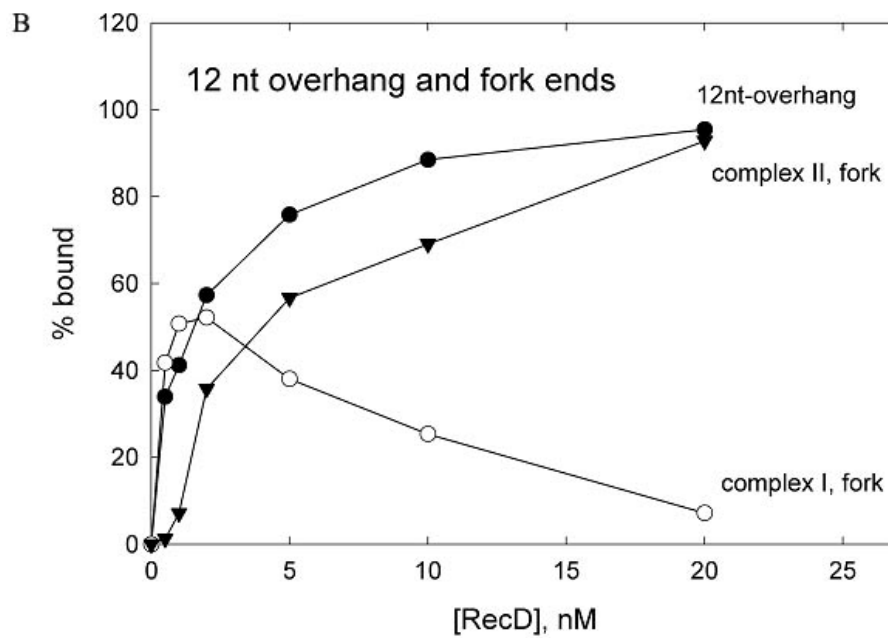
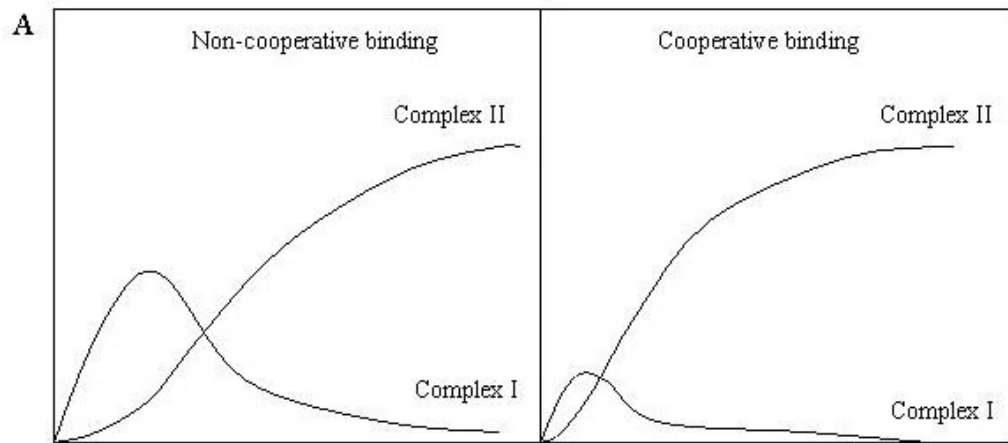


Figure 3.15 The quantitation of the gel shift experiment shown in figure 3.14. (A) The models of non-cooperative and cooperative binding. (B) The percent DNA bound in the reactions shown in figure 3.14 was determined as described in materials and methods, for the hairpin with 12 nt 5'-overhang, only one complex (closed circles); for the hairpin with 12 nt fork, the fast moving complex I (open circles) and the slower mobility complex II (closed triangles).

3.3.4 Lower pH (pH 6.5) Works Better Than pH 7.5

Since the unwinding of 52 and 76 bp dsDNA substrates were so inefficient, the question of whether the conditions we used in the helicase assay is optimal for RecD arose. Efforts were made to search for better reaction conditions for the helicase activity of RecD. It was shown that incubation temperature (37°C and 30°C, which is the growth temperature for *D. radiodurans*), didn't make any difference in the reaction rate. The rate of unwinding the 52 bp DNA was about 2-fold greater at lower magnesium ion concentration (1~3 mM) than at 10 mM Mg²⁺ as was used in previous experiments. The unwinding rate decreased slightly (<2-fold) at 5 or 10 mM ATP rather than 1 mM ATP, with Mg²⁺ concentration kept equal to the ATP. Added salt (NaCl or KCl) inhibited the reaction at all concentrations tested (25-400 mM) and was not included in further experiments.

Among all of the changes, pH change made the biggest difference. Substantially more 52 bp DNA was unwound at pH 6-6.5 than at pH 7.5, the conditions used in previous experiments, or at higher pH (pH 8-9, data not shown). Basically, the unwinding rate of the longer substrate increases while the reaction pH decrease in the range tested (pH 6.0-9.0) and reaches the peak at pH 6.5, as shown in figure 3.16. Thus, at pH 6.5 and 2 mM Mg²⁺, the 52 bp DNA was unwound at a rate of 0.194 (±0.017) DNA molecules unwound/RecD/min (10.1 (±0.9) bp/RecD/min, average of three individual rates), as compared to about 0.001 DNA molecules unwound/RecD/min (0.06 bp/RecD/min, average of three individual rates) at pH 7.5 and 10 mM Mg²⁺. The rate and extent of unwinding the 76 bp DNA was also enhanced at pH 6.5 vs. pH 7.5, but the 76 bp substrate was still unwound less efficiently than the 52 bp substrate in these conditions.

The SSB protein from *D. radiodurans* further enhanced the unwinding rate of the 52 bp substrate by about 2-fold at pH 6.5, as shown in figure 3.17 and figure 3.18, compared to the 30-50% increase (data not shown) in the presence of EcSSB.

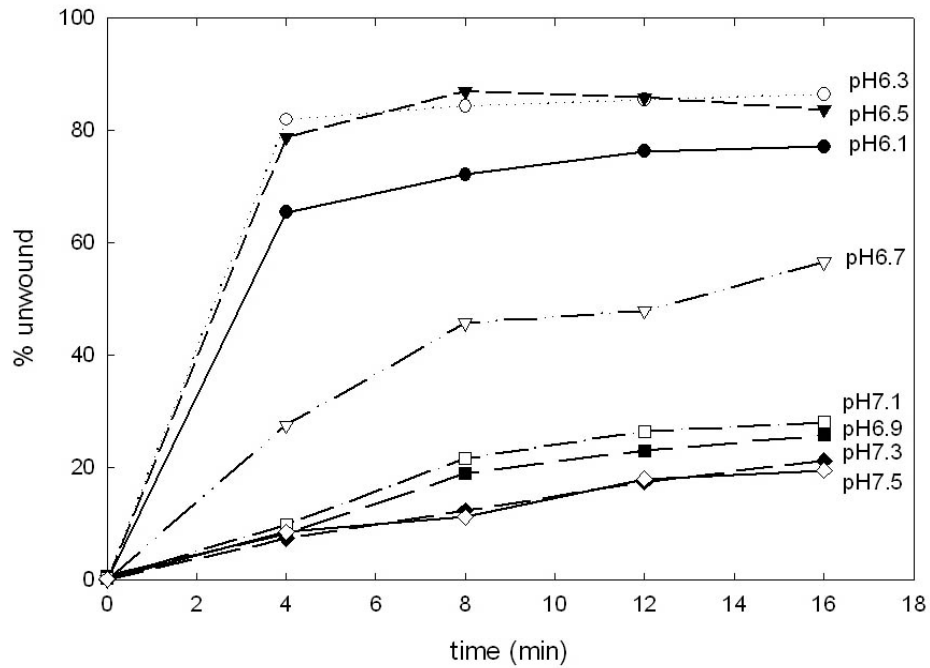


Figure 3.16 pH dependence of 52 bp substrate unwinding. Reaction mixtures contained 25 mM sodium PIPES buffer, adjusted to the indicated pH with NaOH, 2 mM magnesium acetate, 2 mM ATP, 1 nM of the 52 bp substrate, and 10 nM RecD. The samples were taken and analyzed on non-denaturing 15 % polyacrylamide gels and the percent DNA unwound was determined as described in materials and methods.

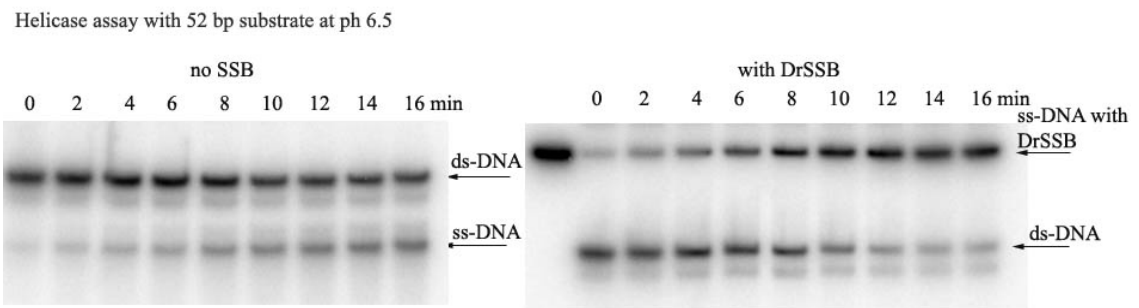


Figure 3.17 Time-course unwinding of 52 bp duplex at pH 6.5. The reaction mixtures contained 1 nM of the 52 bp substrate with a 12 nt 5'-tail, 25 mM sodium PIPES buffer, pH 6.5, 2 mM magnesium acetate, 2 mM ATP, and 0.1 nM RecD. The second reaction also contained *D. radiodurans* SSB protein (390 nM). Samples containing DrSSB were quenched without SDS and unlabeled single-stranded DNA. Samples were taken and analyzed on 10 % non-denaturing polyacrylamide gels as described in materials and methods.

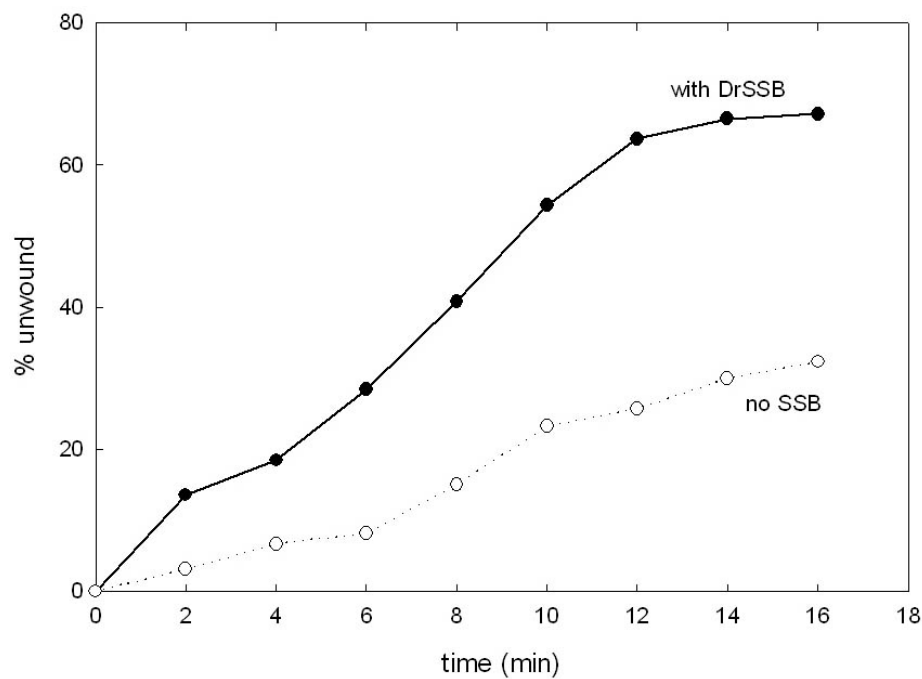


Figure 3.18 Unwinding of 52 bp duplex. The percent DNA unwound in the reactions shown in figure 3.17 was determined as described in materials and methods. For the 52 bp substrate, only 0.1 nM RecD was needed in reactions both without or with DrSSB, which is much smaller than 100 nM RecD needed in the same reactions under pH 7.5 without or with *E. coli* SSB in figure 3.12. Two reactions were either with 390 nM DrSSB (closed circles); or no DrSSB (open circle).

Surprisingly, the addition of SSB protein from *D. radiodurans* into the reaction at pH 7.5 showed significant increase of unwinding of the 52 bp duplex by RecD, as shown in figure 3.19. The increase was estimated at about 20-30 fold, compared to about 2-fold for the same reaction at pH 6.5 (figure 3.18). The fold number was the concentration difference of RecD used in the two reactions to get to the same extent in the same time course. In this way, instead of simply comparing the reaction extents for the two reactions with same amount of RecD, we can adjust for the product inhibition for RecD in the two reactions to the same level. The significant difference in the effect of DrSSB in unwinding the 52 bp duplex at pH 6.5 and pH 7.5 may suggest that DrSSB interacts with RecD to enhance its processivity by about 20-fold at pH 7.5. The interaction between DrSSB and RecD may not be as significant at pH 6.5 because another interaction between RecD molecules (dimerization, as will be discussed later) may be dominant and increase the processivity of RecD by about 200-fold.

We then compared other enzymatic activities of RecD at pH 6.5 and 7.5. The dramatic increase in unwinding efficiency of the longer DNA at pH 6.5 vs. 7.5 is not a result of enhanced ATP hydrolysis or intrinsic unwinding at lower pH. Thus, ATP hydrolysis was slightly greater at pH 7.5 (9.0 ATP hydrolyzed/RecD/sec, average of two individual reactions, 9.2 and 8.8 ATP hydrolyzed/RecD/sec, respectively) than at pH 6.5 (6.7 ATP/RecD/sec, average of two individual reactions, 6.5 and 6.8 ATP hydrolyzed/RecD/sec, respectively), with 0.2-1 nM RecD and 10 μ M of a 17 nt ssDNA co-factor, as shown in figure 3.20.

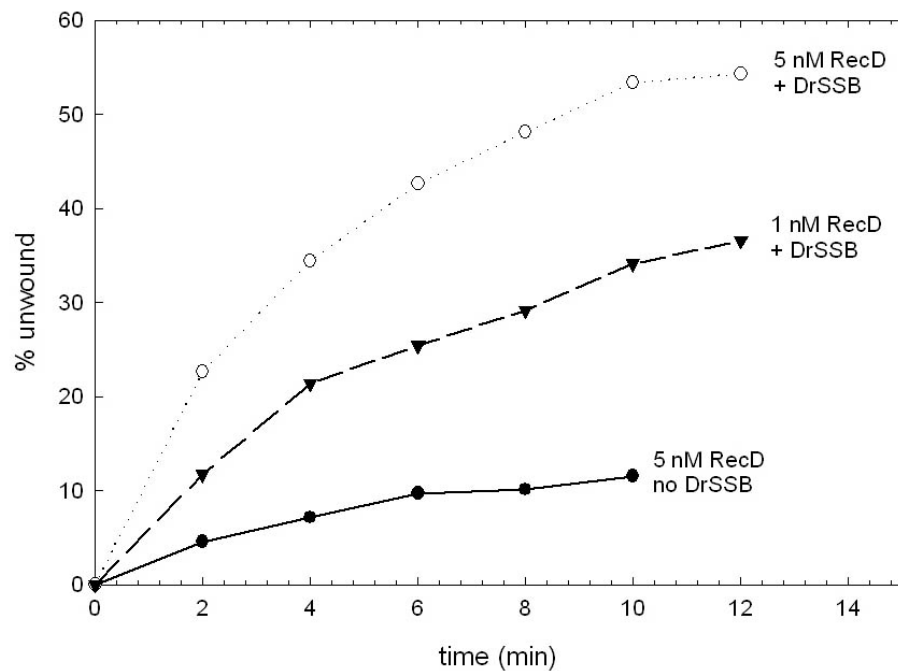


Figure 3.19 Unwinding of 52 bp duplex at pH 7.5, with SSB protein from *D. radiodurans*. Reaction mixtures contained 25 mM Tris-acetate, pH 7.5, 10 mM magnesium acetate, 1 mM ATP, 1 mM DTT, 0.1 mg/ml BSA, 1 nM 52 bp ds DNA. The percent DNA unwound was determined as described in materials and methods. The differences in each reaction are: 5 nM RecD, no DrSSB (closed circles); 5 nM RecD, 390 nM DrSSB (open circles); 1 nM RecD, 390 nM DrSSB (closed triangles).

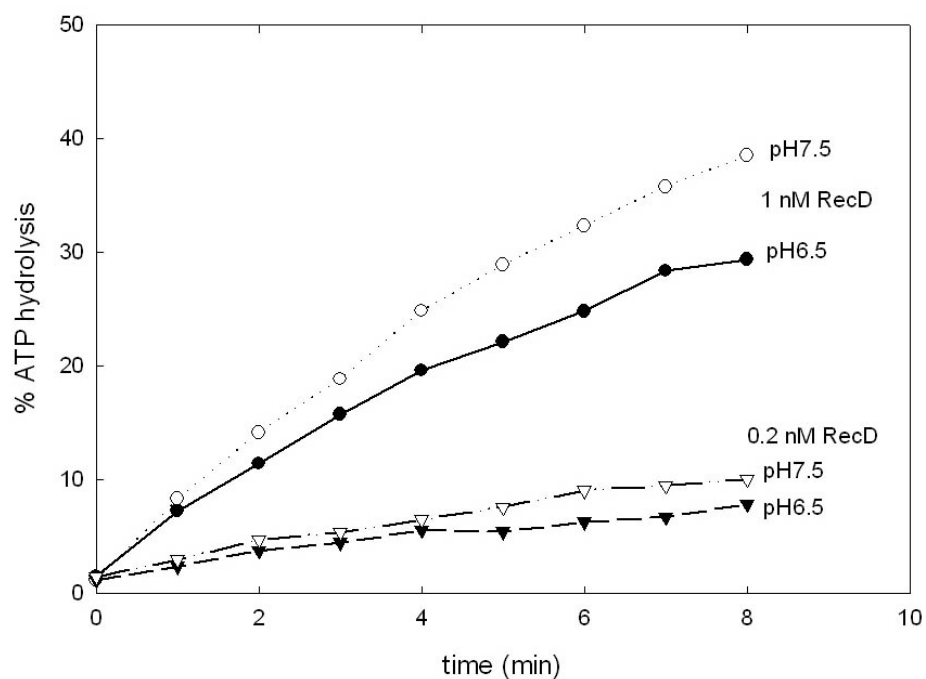


Figure 3.20 ATP hydrolysis by RecD at different pHs. Reaction mixtures contained 50 mM Tris-HCl, pH 7.5 and 10 mM MgCl₂, or 50 mM PIPES buffer, pH 6.5 and 2 mM MgCl₂, and 1 mM DTT, 5% glycerol, 0.1 mg/ml BSA, 10 μM ATP with 5% [γ-³²P]-labeled ATP, and 10 μM 17 nt single-stranded oligonucleotide. Both 0.2 and 1 nM RecD were used in the two reaction conditions and the samples were analyzed on TLC membranes as described in materials and methods.

When we tested the unwinding rates of 20 bp duplexes with either 12 nt 5'-overhang or 12 nt forked end at pH 6.5, we found that the effect of pH change was different on DNA substrates with different end structures. Unwinding of the 5'-tailed 20 bp substrate was about 2-fold faster at pH 6.5, with 2 mM Mg²⁺, 13.5 DNA molecules unwound/RecD/min (average of two reactions, 15.7 and 11.3 DNA molecules unwound/RecD/min, respectively) than at pH 7.5 and 10 mM Mg²⁺. Interestingly, the unwinding of the 20 bp DNA with a forked end was about 2-fold slower at pH 6.5, 22.2 DNA molecules unwound/RecD/min (average of two reactions, 25.9 and 18.5 DNA molecules unwound/RecD/min, respectively), than at pH 7.5, as shown in table 1 (each rate in this table is an average of two individual reactions). Apparently, lower pH increases the unwinding rate of substrate with a 5'-overhang and decreases the unwinding rate of substrate with a forked end.

A more striking observation is that binding of RecD to the 12 nt 5'-tailed hairpin DNA is much tighter at pH 6.5 than at pH 7.5, as shown in figure 3.21. Two complexes were observed for the 12 nt 5'-tailed hairpin at low RecD concentrations that unwound the 5'-tailed substrate efficiently and more than half of these complexes were the lower mobility complex. Stronger DNA binding at pH 6.5 is consistent with apparently higher processivity at pH 6.5 than at pH 7.5. The enzyme would be able to stay bound to the substrate until it is unwound completely and detected as separate single strands in the gel of unwinding assay at pH 6.5. Nevertheless, unwinding of the 52 and 76 bp substrates is significantly slower than for the 20 bp substrates under all conditions we tested.

A

Condition \ Substrates	Rate (DNA molecules/RecD/min)	
	5'-overhang	fork
2 mM Mg ²⁺ pH = 6.5	13.5	22.2
10 mM Mg ²⁺ pH = 6.5	12.5	30.4
10 mM Mg ²⁺ pH = 7.5	6.9	46.1

B

Substrate \ 2 mM Mg ²⁺ pH = 6.5	Rate (DNA molecules/RecD/min)
52 bp substrate	0.21
Reaction with SSB	0.25
76 bp substrate	0.03
Reaction with SSB	0.06

Table 1. Unwinding rates for 20 bp and longer substrates at different pHs. Every rate in the table is an average of rates from two individual reactions with different RecD concentrations. (A) For 20 bp substrate with 12 nt overhang, the reaction rate went down while increasing the Mg²⁺ concentration and/or increasing pH. For 20 bp substrate with 12 nt fork, the reaction rate went up while increasing the Mg²⁺ concentration and/or increasing pH. (B) The reaction rates for 52 and 76 bp substrates were about 200-fold slower at pH 7.5. The EcSSB in the reactions at pH 6.5 increased the rates a little bit.

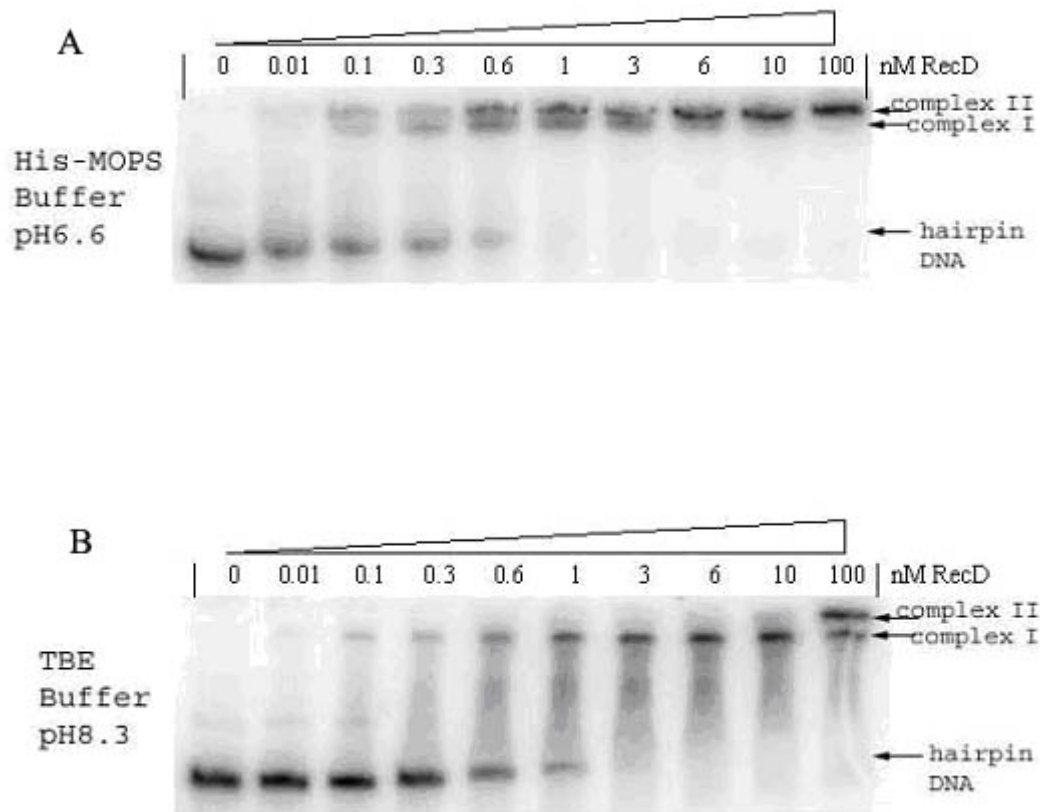


Figure 3.21 Effect of different pHs on DNA binding. The hairpin oligonucleotide with 12 nt 5'-single-stranded tail was used in this gel-shift experiment. (A) Top gel: Reaction mixtures contained 25 mM sodium PIPES, pH 6.5, 2 mM Mg-acetate, 1 nM 5'-³²P-labeled DNA and the indicated RecD concentrations. Samples were analyzed on non-denaturing 10 % polyacrylamide gels as described in materials and methods except using 1 × His-MOPS (30 mM) buffer, pH 6.6, instead of 1 × TBE buffer, pH 8.3, to run the gel. (B) Bottom gel: Reaction mixtures contained 25 mM Tris-acetate, pH 7.5, 10 mM Mg-acetate, and the rest was as in Figure 3.15.

3.3.5 K_d for the Binding at Different pH

The gel mobility shift experiment (figure 3.22) with low DNA concentration (0.0125 nM) was quantitated for assessment of the dissociation constant of RecD and DNA substrate. It can be estimated as: $K_d = [\text{DNA}] \times [\text{RecD}] / [\text{DNA-RecD}]$. In circumstances where the DNA concentration used in the reaction is much smaller than K_d , the dissociation constant is close to the RecD concentration at which half of the DNA is bound. The plot (as shown in figure 3.23 A) suggests that the K_d for RecD binding at both pHs are very small, which makes the presumption of $[\text{DNA}] \ll K_d$ invalid. We then tried to fit the data to the equation in figure 3.24 by using the non-linear regression function in Sigmaplot. However, the program could not fit the data, presumably because there are too few data points (RecD concentrations). We instead simulated the data by testing different values for K_d . The sum of squares $\Sigma = (\Delta_1)^2 + (\Delta_2)^2 + (\Delta_3)^2 + (\Delta_4)^2$ was used to determine how close the simulation was. The K_d of RecD at pH 8.3 was estimated to be 0.15 nM, while the K_d of RecD at pH 6.6 could not be done in the same way due to the absence of data at lower RecD concentrations, as shown in figure 3.23 A. Nevertheless, we can still see that the difference in binding affinity of RecD at different pHs was obvious, as shown in figure 3.23 B.

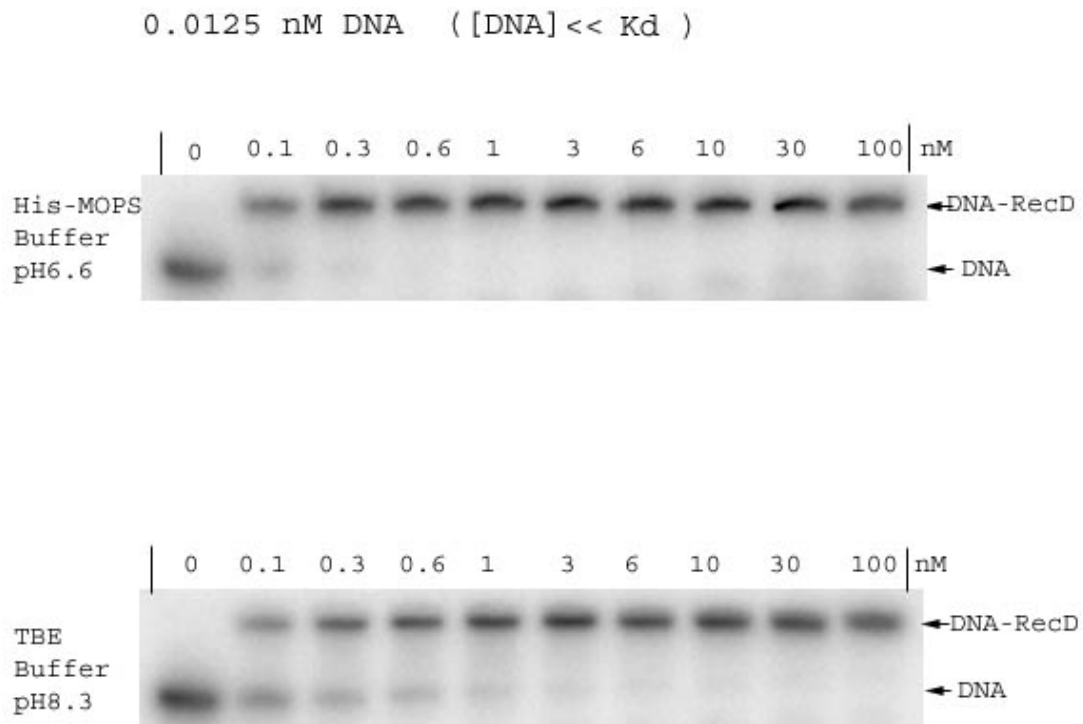


Figure 3.22 The binding of RecD to 12 nt hairpin DNA at different pHs. Reaction mixtures contained the same components as in the binding experiment as figure 3.21, except much less DNA (0.0125 nM DNA instead of 1 nM) was used. The samples were taken and analyzed on 10 % non-denaturing polyacrylamide gels as described in materials and methods except the gels were run for only about 10 min to prevent smearing in the lanes.

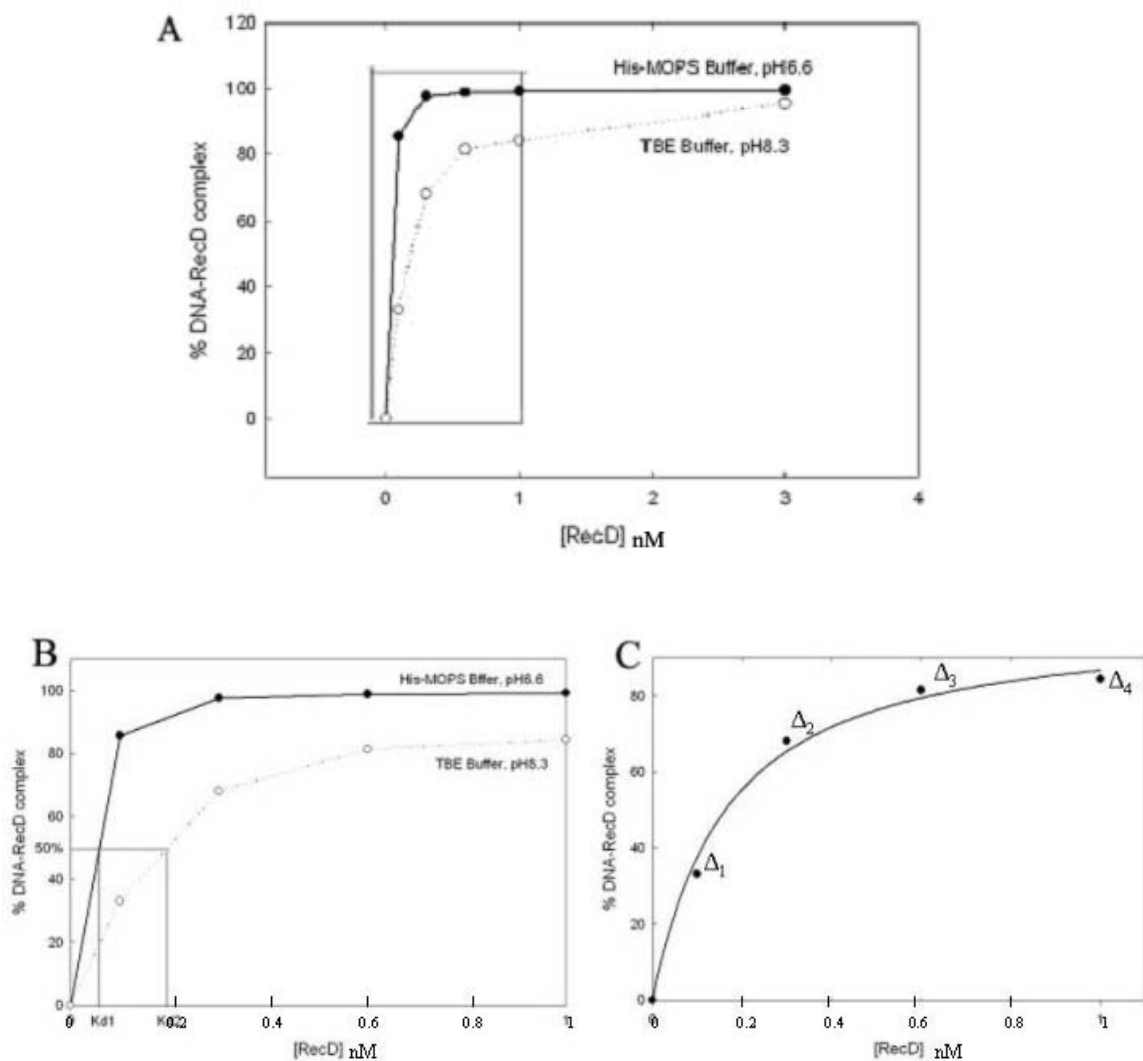
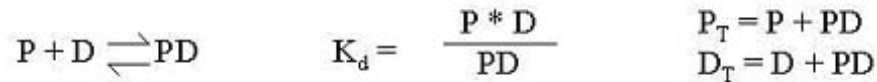


Figure 3.23 Assessment of K_d s at different pHs. The samples were taken and analyzed on 10 % non-denaturing polyacrylamide gels as shown in figure 3.22. (A) The percent DNA bound was analyzed by integrating the amount of radioactivity in the unbound dsDNA band, the DNA-protein complexes, and the radioactive material migrating intermediate between the two (shortening the gel-running time can prevent it happening). The amount of radioactivity in the two shifted DNA bands (not separated here due to short gel-running time) was summed for one total binding. (B) Part of the plot from (A). (C) The simulation by the equation for the reaction at pH 8.3. There are not enough data for reaction at pH 6.6 to do the simulation. The closest fit was from the K_d that gave the smallest $\Sigma = (\Delta_1)^2 + (\Delta_2)^2 + (\Delta_3)^2 + (\Delta_4)^2$, Δ was the Y axis distance (% DNA-RecD complex calculated and measured) at same RecD concentration.

$$\% \text{ DNA bound} = \frac{(K_d + P_T + D_T) - [(K_d + P_T + D_T)^2 - 4 * P_T * D_T]^{1/2}}{2 * D_T} * 100$$



P - protein, D - DNA, PD - protein-DNA complex
 P_T - total protein concentration,
 D_T - total DNA concentration.

Figure 3.24 The equation used for the simulation of the data from reaction at pH 8.3. This equation was used for the simulation in figure 3.23 C with the $K_d = 0.15$.

3.4 Discussion

The recombinant RecD protein showed a high level of biochemical activity *in vitro*. However, we are not sure what effect the C-terminal eight amino acid tag has on the activity. We cannot exclude the possibility that such a short tag could cause significant changes in the conformation and activity of RecD since the N-terminal His-tagged recombinant RecD protein acted as an extreme example. This could be addressed by expressing RecD protein without a tag. The biochemical study of the *D. radiodurans* RecD protein *in vitro* revealed that it is a DNA helicase moving along single-stranded DNA with 5'-3' polarity. It requires at least a 10 nt 5'-single-stranded tail, and does not unwind duplexes with blunt ends or a 3'-single-stranded tail. The fact that it unwinds 20

bp duplex efficiently but unwinds poorly with 52 and 76 bp substrates suggests it has low processivity.

3.4.1 Structure-Related Substrate Preference

The requirement of the substrate with at least 10 nucleotide 5'-single-stranded tail for RecD unwinding is different from the unwinding by RecBCD enzyme in *E. coli*, which requires blunt or near blunt ends^{114, 115}. The preference of RecD to fork-shaped substrate shows some similarity with a group of helicases involved in DNA replication. This group of helicases is distributed broadly in organisms - from viruses to human beings. For example, greater unwinding of a duplex with a forked end vs. with only one single-stranded tail was also observed with Pif1 helicase with 5'-3' polarity¹¹⁶ from yeast, which is a distant relative of RecD as shown in the COG tree (figure 1.4).

The low processivity of RecD, i.e., unwinding a short duplex efficiently, is also a commonly shared property in this group. Recent research found that the *pfh1* gene (Pif1 homolog) in fission yeast encodes an essential enzyme implicated in lagging strand DNA processing¹¹⁷. This enzyme has both DNA helicase and ATPase activities. The full-length Pfh1 protein is active as a monomer. It only displaces short (<30 bp) duplex DNA regions efficiently in a highly distributive manner and is markedly stimulated by the presence of a replication-fork-like structure in the substrate. The genetic and biochemical analyses of Pfh1 suggest its involvement in processing the single-stranded DNA flap generated *in vivo* by DNA polymerase-mediated lagging strand displacement during DNA synthesis (figure 3.25). The similarity shared by RecD and Pfh1 helicases may suggest a replication-related function of RecD.

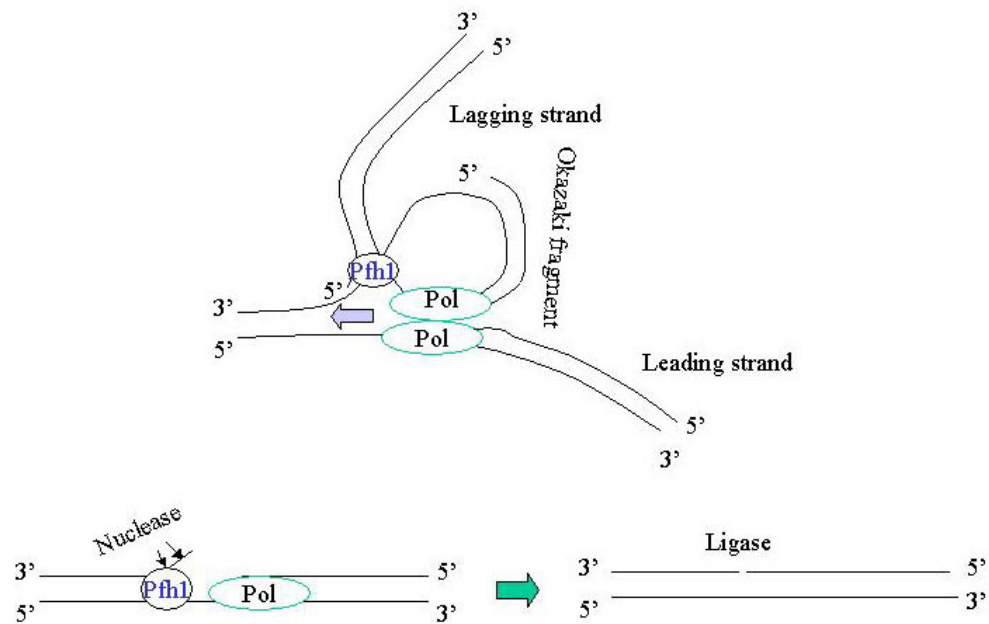


Figure 3.25 The schematic illustration of the possible role Pfh1 has in DNA replication¹¹⁷. The replication of the lagging strand generates short Okazaki fragments. Pfh1 helicase is responsible to unwind the 5'-end of the Okazaki fragments for the next 3'-DNA polymerase-containing strand to fill in, and then the nick is ligated by ligase.

3.4.2 Unwinding in Different Conditions

Under standard conditions, the RecBCD enzyme from *E. coli* can unwind an average of 30 +/- 3.2 kilobase pairs (kb)/DNA end before dissociation¹¹⁸. But for the RecD protein from *D. radiodurans*, the unwinding rates drop more than 20-fold for 20 bp vs. 52 bp substrates. If low processivity is the reason for the dramatic decrease in unwinding rate, we can assume that RecD can only unwind a duplex region shorter than 50 bp before it dissociates.

Another reason that may cause the decrease of unwinding rate was excluded by the addition of SSB protein into helicase reaction. The enhancement of unwinding 52 bp substrate with the addition of SSB protein from *E. coli* was about 30-60% at pH 6.5 or at pH 7.5. It can be simply explained that SSB protein binds to the unwound ssDNA product and prevents them from reannealing. However, the increases of unwinding the 52 bp substrate with the addition of SSB protein from *D. radiodurans* were significantly different at pH 6.5 and pH 7.5. The DrSSB markedly increased the unwinding of 52 bp substrate at pH 7.5 (>20-fold) while it only increased the unwinding by about 2-fold at pH 6.5. The effect of DrSSB in unwinding the longer substrate cannot be explained simply by the binding to the unwound ssDNA and preventing the rewinding. There must be some interaction between RecD and DrSSB, especially at pH 7.5. More experiments are needed to be done to get a conclusion.

3.4.3 The Rates Determined in Our Study

The helicase assay used in our study to determine the unwinding rate of RecD is an “all or none” DNA unwinding assay, detecting only fully unwound DNA. The low substrate concentration (1 nM) and enzyme concentration used in the assay also could not give us optimal rates since the binding of RecD enzyme to substrate is not complete in such low concentrations. We only measured the ssDNA product generated by the RecD molecules that bound to a DNA molecule. Since this method used a long time course, the unwinding we measured included the binding of RecD to dsDNA, unwinding, and dissociation from ssDNA to start over another round.

To avoid those problems and get a real rate, more sophisticated methods and instruments are needed. For example, single-turnover DNA unwinding uses excess enzyme to determine the rate of a single round of DNA unwinding. It measures the quantity of substrate that could be unwound in a single binding event. A DNA molecule that functions as a protein trap is needed in the reaction to prevent the rebinding of any enzyme molecule that dissociated from the substrate ¹¹⁹. Another good method is the pre-steady-state DNA unwinding. It requires excess substrate for the majority of the enzyme bind to DNA before initiation of the reaction to observe a burst of product formation ¹²⁰. A rapid chemical quench-flow instrument that measures reaction progress in as short as a few millisecond period can significantly increase the sensitivity of these methods.

3.4.4 Monomer or Dimer?

DNA helicases are an ubiquitous class of enzyme that use the binding and hydrolysis of nucleoside triphosphates to catalyze unwinding of duplex DNA to transiently form the single-stranded DNA intermediates required for replication, recombination, and repair. One of the central questions regarding helicase activity is whether the process of coupling ATP hydrolysis to DNA unwinding requires an oligomeric form of the enzyme.

As shown in figure 3.14, monomer is more likely the active state of the RecD protein during unwinding. There was only one single complex observed in the same condition (except no ATP was added) that the 5'-tailed substrate was unwound efficiently. The second complex with lower mobility could result from additional RecD molecules

binding to the loop or the double-stranded region of a hairpin DNA. This postulation is consistent with the property of Pfh1 helicase.

Meanwhile, a very interesting result was noticed during the experiment of helicase assay with two different substrates. Under exactly same condition, the unwinding rate for the substrate with fork shape (two ssDNA tails) at one end is almost eight times faster than the substrate with only one 5' - tail at one end. This observation brought up the question: does the two ssDNA region help RecD enzyme bind onto the substrate and how? Because as proved in the helicase assay that RecD enzyme could not unwind dsDNA with a 3' - tail, there is a possible explanation. The 3'-end ssDNA region in the fork-shaped substrate does not work as a platform for a RecD molecule to bind and start unwinding. Instead, it works as a scaffold to help the RecD protein step onto the 5' - end ssDNA region. Since the fork shape has equal length of both 3' - and 5' - ssDNA regions, the help cannot make such a big difference if only one RecD protein is needed to start the unwinding reaction. Only when more than one copy of RecD are needed, the RecD on the 3'-end ssDNA makes the dimerization step on 5'-end ssDNA much faster because it is in much closer vicinity than other RecD molecules in solution. Although lack of obvious cooperativity of the second RecD binding to the forked DNA substrate at pH 7.5 does not support the hypothesis of RecD dimer, the lower mobility complex on 5'-tailed hairpin at pH 6.5 suggests that DNA unwinding is not simply done by a RecD monomer. It is possible that RecD can function as a monomer with very unstable binding with DNA. Upon dimerization, which may be facilitated at pH 6.5, the RecD dimer stays more stably bound to the DNA and can unwind DNA with higher processivity. In fact,

most helicases work as oligomers (usually dimers or hexamers)¹⁵, which provide the helicase with multiple DNA binding sites.

The unwinding rates for 20 bp duplexes with 5'-overhang or forked end at pH 6.5 and pH 7.5 also supports the dimer theory, as shown in table 1. The unwinding rate of substrate with 5'-overhang increased at pH 6.5 vs. pH 7.5 because pH 6.5 favors the RecD binding and dimerization. As shown in figure 3.21, almost equal amount of RecD-DNA complex I and complex II were present at pH 6.5 with RecD concentration that unwound the 5'-tailed substrate efficiently. The fact that unwinding rate of substrate with fork end decreased at pH 6.5 vs. pH 7.5 because of the lower ATPase activity at pH 6.5, which is the speed-limit step for such a substrate. One experiment that we could have done would be to do binding with the forked DNA at pH 6.5, and look for cooperativity. If dimerization is enhanced at pH 6.5, it could turn up as cooperativity in binding to the forked DNA.

To finally address this question, more biophysical and biochemical measurements should be done. Sedimentation equilibrium and size-exclusion chromatography can be used to study the oligomeric state of the RecD protein by itself. A chemical crosslinking experiment that covalently link the DNA and protein when they are close enough to contact can be used to study the RecD state on the DNA substrate. However, these approaches may fail to provide evidence for oligomerization, because protein-protein interactions that are required for optimal activity may be transient in nature^{113, 120}.

Pre-steady-state analysis has proven to be an extremely powerful tool for studying enzymes that act on DNA. This method measures the first cycle of product formation in the presence of excess substrate. The “burst amplitude”, which refers to the quantity of

product formed during the first cycle, may indicate the quantity of active enzyme that is present in the reaction mixture. If a helicase can function as a monomer and is sufficiently processive, then the burst amplitude of product observed during DNA unwinding should be similar to the concentration of enzyme. If a helicase requires oligomerization or is highly nonprocessive, then the burst amplitude will be significantly less than the enzyme concentration^{113 121}. The studies on other helicases such as bacteriophage T4 Dda helicase, which is closely related to RecD, may give us some clue that how the RecD may work. Only after the biophysical and enzymatic studies are done, the oligomeric state of RecD for unwinding DNA can be revealed.

Chapter 4 BIOLOGICAL STUDY OF RECD FUNCTION *IN VIVO*

4.1 Introduction

Targeted insertional mutagenesis of the *Deinococcal recA* gene was used to prove that *recA* defect alone was responsible for the tremendous loss of radioresistance. This result is easy to understand since *recA* gene is an essential component in recombination repair pathway in most organisms. Repair of thousands of double strand breaks in *D. radiodurans* that appeared after exposure to radiation requires the RecA protein. To find out whether the RecD-like protein also plays some role in the DNA repair in *D. radiodurans*, a general and simple method that can inactivate any targeted gene in *D. radiodurans* was used to knock out the *recD* locus in chromosome I^{76, 105, 122}, as shown in figure 4.1. The plasmid pCR-blunt has a *recD* fragment inserted and can be integrated into the *D. radiodurans* chromosome I by insertional homologous recombination. The recombinant *D. radiodurans* cells that can grow on plates with the antibiotic kanamycin have their *recD* gene disrupted. Even though the polyploid nature (multiple copies of the genome) of *D. radiodurans* is a problem for this method, all of the *recD* gene copies in *D. radiodurans* cell can be disrupted by continuously growing transformed cells in media with antibiotics for several generations.

The phenotype of the *recD* mutants strains of *D. radiodurans*, such as growth curve, radiosensitivity to UV exposure, UV survival curve, and the ability to uptake exogenous DNA, were tested and compared with wild type *D. radiodurans*.

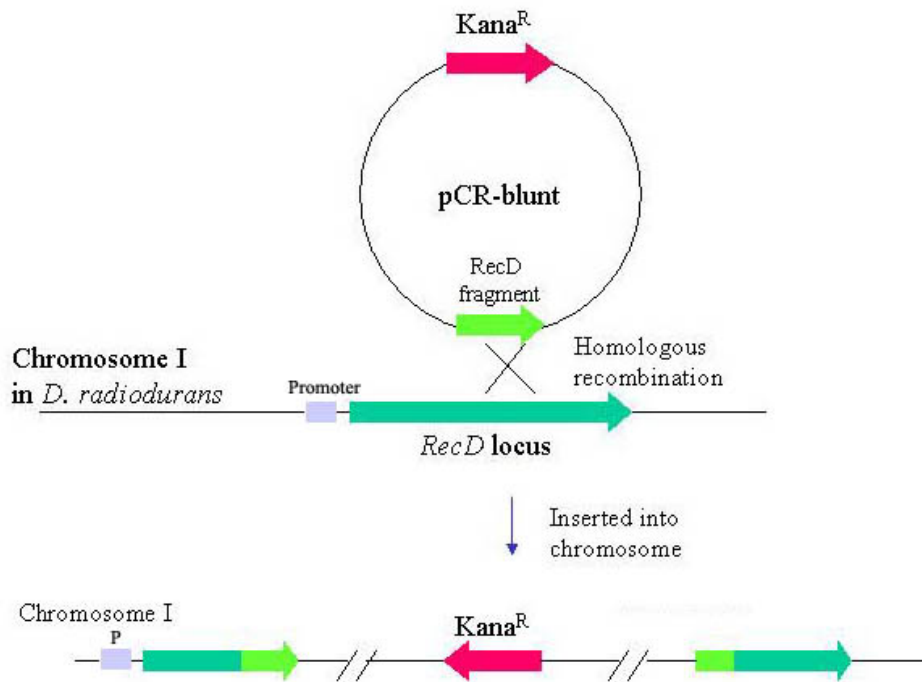


Figure 4.1 The schematic illustration of the method used to knockout targeted gene in *D. radiodurans*. The light green arrow is the *RecD* fragment (500-1500 bp) inserted in the plasmid pCR-blunt. The red arrow is the kanamycin resistance gene in the plasmid. The dark green arrow is the *recD* gene in chromosome I of *D. radiodurans* and the gray box at its left is its promoter.

4.2 Materials and Methods

4.2.1 pCR-blunt Plasmids with *recD* Fragment Insertions

Originally the pCR-blunt plasmid was designed to provide a highly efficient one-step cloning strategy for the direct insertion of blunt-end PCR products generated by a proofreading polymerase into a plasmid vector. In our study, besides PCR products, *recD* gene fragments from several double-digestions followed by mung bean nuclease digestion to produce blunt ends were also inserted into the pCR-blunt cloning vector to construct several plasmids that can be used to transform *D. radiodurans*. Competent *D. radiodurans* cells were transformed with those plasmids and the cells were screened for kanamycin resistance. Since the plasmid pCR-blunt is a ColE1 plasmid derivative and does not replicate as a plasmid in *D. radiodurans*, kanamycin resistance in *D. radiodurans* was produced by duplicated insertion of the plasmid into the chromosome by homologous recombination and subsequent replication of the plasmid with the genomic DNA.

As shown in Figure 4.2, the linearized plasmid vector (pCR[®]-Blunt II-TOPO[®]) (Invitrogen) has *Vaccinia virus* topoisomerase I covalently bound to the 3' ends. The ligation of the vector with a blunt-end DNA fragment is catalyzed by the topoisomerase efficiently. Indeed, the reaction occurs spontaneously within 5 minutes at room temperature, and then the product can be transformed into *E. coli* competent cells. In addition, it allows direct selection of recombinants via disruption of the lethal *E. coli* gene, *ccdB*. Ligation of a blunt-end DNA fragment disrupts expression of the *lacZα-ccdB* gene fusion permitting growth of only positive recombinants upon transformation.

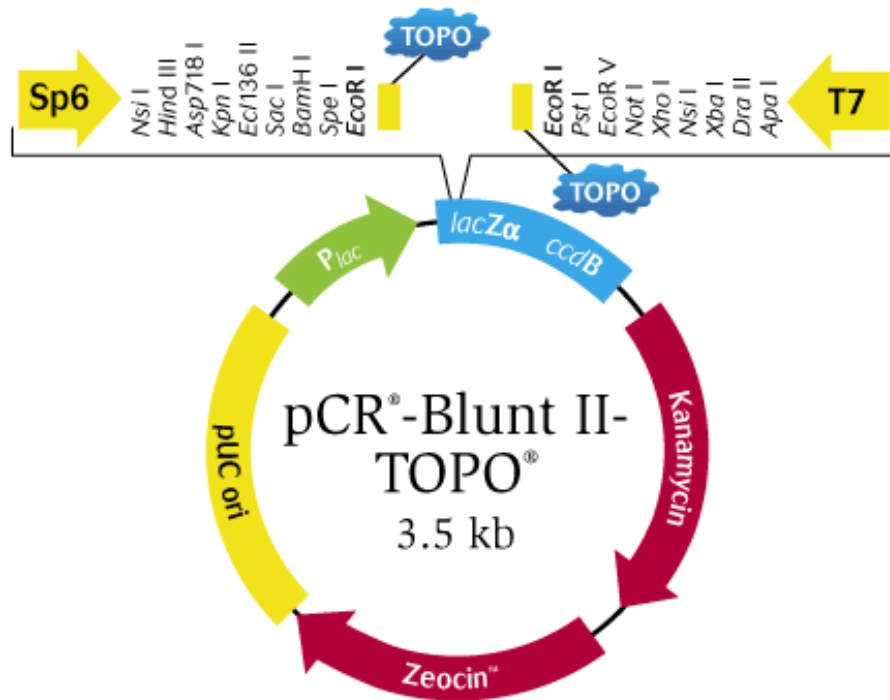


Figure 4.2 The schematic structure of plasmid pCR-blunt and the partial restriction map. It was taken from the company's website: <http://www.invitrogen.com>

According to the restriction map of the *recD* gene region (figure 4.3), three double-digested *recD* fragments, one PCR produced *recD* fragment and one *recC* fragment from the *E. coli recC* gene (as a negative control) were used to construct five pCR-blunt plasmid series. Since there is a stop codon right next to where the *recD*

fragment is inserted in the pCR-blunt vector, the following insertion of the plasmid into the *D. radiodurans* genome by homologous recombination will produce two incomplete copies of *recD* at the original *recD* locus, as shown in figure 4.1. The copy with *recD* gene promoter may be translated into a C-terminal truncated RecD protein by using the stop codon from the plasmid and the other copy without promoter cannot be translated.

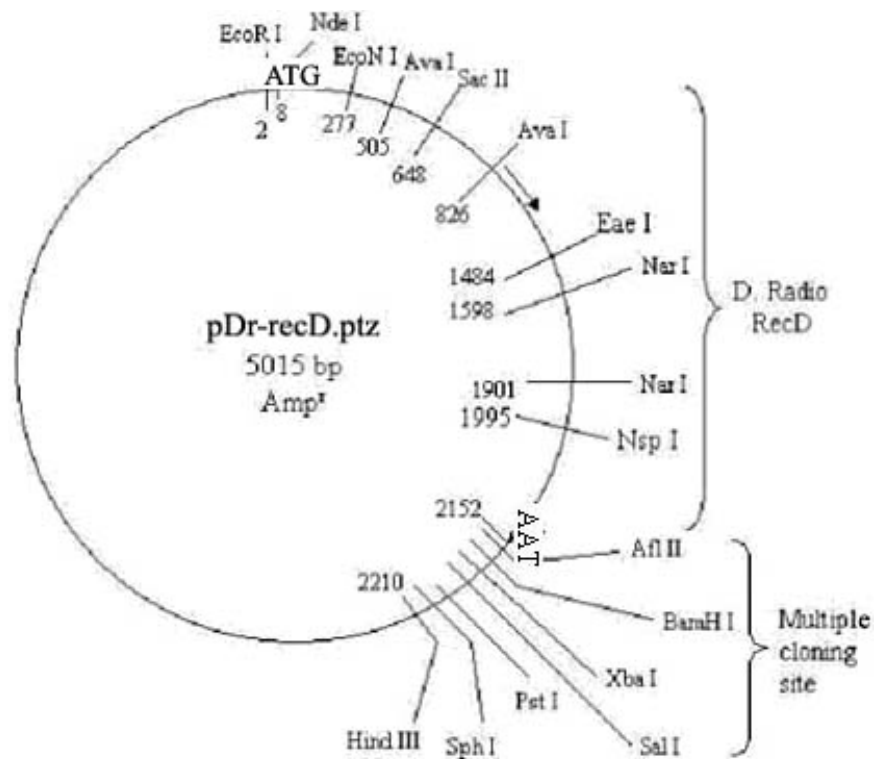


Figure 4.3 Part of the restriction map for plasmid pDR-recD.ptz. The 2150 bp *D. radiodurans* DNA fragment, encoding RecD, in vector pTZ19R starts at bp # 9 (*Nde I*) and ends at bp # 2154 (before *Afl II*). The restriction map in the *recD* gene region was determined by the web tool at: <http://www.firstmarket.com/cutter/cut2.html>

The five plasmids have the following insertions. Plasmid (1) has a 640 bp double digestion fragment (*Nde I* + *Sac II*, 8-648) of the *recD* 5'-end that may produce a N-terminal 200 amino acids peptide of RecD after insertion. Plasmid (2) has a 1476 bp double digestion fragment (*Nde I* + *Eae I*, 8-1484) close to the 5'-end that produces a 500 amino acid, C-terminal-truncated RecD. Plasmid (3) has a 1718 bp double digestion fragment (*EcoNI* + *Nsp I*, 277-1995) close to the 3'-end that produces a 670 amino acid RecD with C-terminal 45 amino acid truncated. Plasmid (4) has a 449 bp PCR product of the *recD* 3'-end including the stop codon so that an intact *recD* gene remains after insertion. Plasmid (5) has a 600 bp *recC* gene fragment from *E. coli* as a negative control for transformation efficiency. By using these plasmids to transform *D. radiodurans*, the corresponding colonies on kanamycin plates will have targeted insertions as designed.

The five DNA fragments were cloned into vector pCR-blunt as follows. The *recD* fragments for plasmids (1), (2) and (3) were from double-digestion with corresponding restriction enzymes followed by mung bean nuclease digestion to get blunt ends. Then, the products were run on 1.0 % 0.5 × TBE agarose gels, the desired DNA bands with correct sizes were cut out and the DNAs were recovered from the gels with QIAEX[®] II Gel Extraction Kit (Qiagen) as described before. The *recD* fragment for plasmid (4) was from a PCR product by using a pair of primers to amplify the 3'-end 449 bp *recD* gene fragment including the stop codon as described above. The *recC* fragment for plasmid (5) is a 600 bp *Ava I* digestion product from plasmid pPB500 treated the same way as for plasmids (1), (2) and (3). The DNA fragment and pCR-blunt vector were mixed at 1:1 ratio and ligated as described in the procedure coming with the pCR[®]-Blunt II-TOPO[®]. The ligation products were transformed into the *E. coli* XL-1 competent cells separately

followed by screening cells on LB plates with 30 µg/ml kanamycin. The colony with each type of recombinant plasmid was picked up and grown in LB media with 30 µg/ml kanamycin. The plasmids were isolated and the correct sizes of the insertions were verified by restriction digestion with *EcoR I* followed by electrophoresis on 1.0 % agarose gels.

4.2.2 The *Deinococcus radiodurans* Mutants with Different RecD Truncations by Homologous Recombination

D. radiodurans competent cells were prepared as described¹²³ with some modification: (1) Middle exponential culture (OD₆₀₀ is about 2) was harvested by centrifugation at 4 °C, 4,500 × g for 10 min. (2) The cells were washed with distilled water two times. (3) The cell pellet was then resuspended at 10⁹ cells per ml with an appropriate volume of a mixture (20: 8: 3) of TGY broth (0.8 % Tryptone, 0.4 % Yeast extract, and 0.1 % glucose), 0.1 M CaCl₂, and glycerol. (4) The aliquots of cells (100 µl/each) were frozen on powdered dry ice, and stored at –80 °C until needed.

The five pCR-blunt plasmid series were used to transform *D. radiodurans* as follows. 4 µg/each plasmid was added into corresponding 100 µl/each of *D. radiodurans* competent cells and kept on ice for 15 minutes followed by 32 °C water bath for 45 minutes with agitation. Then, 5 ml TYG media /each sample was added and incubated in 30 °C for 18 hours with aeration. The next day, the cells were collected from the media and spread onto kanamycin (30 µg/ml) plates. After more than two days incubation in 30 °C the colony numbers were counted and one or two colonies for each transformation were picked up and used to do further tests.

The positive colonies from each transformation of (1), (2), and (3) were grown in TYG broth with kanamycin for three generations. Since after the insertion of plasmid (4), the mutant *D. radiodurans* cells still retain an intact *recD* gene, this mutant was not used for the verification and phenotype study. It was only used for the comparison of transformation efficiency with different length of *recD* fragments in the plasmids. The third generation cells were used to isolate their genomic DNAs. The correct genomic insertion of the plasmid for each *D. radiodurans* mutant was verified by PCR with two pairs of primers amplifying sequences with partial genomic and partial plasmid DNAs. PCR reactions were carried out in 100 µl/each tube with 0.5 µg/each genomic DNA as template from *D. radiodurans* mutants and wild type control, 0.2 mM/each dNTP, 1 µM/each of the two primers in 1× Pfu Turbo polymerase (Stratagene) buffer. 2.5 unit of the Pfu Turbo polymerase was added to start the PCR reaction. Incubation for 4 min at 96 °C was used as initial step, followed by 25 cycles of 1 min at 96 °C for template DNA denaturation, 1 min at 61 °C for primer annealing, and 6 min at 72 °C for the primer extension. An extra 10 min at 72 °C was added to the end of 25 cycles to make sure the extension was completed. The PCR products were then directly loaded onto a 1.0 % agarose gel.

4.2.3 The Phenotype of the Mutants

The comparison of growth curves⁷⁸ for wild type and mutants (1) and (3) was done by inoculating 200ml/each fresh TYG media (with 30 µg/ml kanamycin for mutant cells) with stationary phase wild type or mutant *D. radiodurans* cells and incubating the media at 30 °C. The OD₆₀₀ absorptions were measured every three hours by taking 1 ml

culture out, and appropriate dilution was applied if necessary until the absorption didn't go up for each sample. The reason for using mutants (1) and (3) is that mutant (1) has the longest C-terminal truncation (>500 aa) and mutant (3) has the shortest C-terminal truncation (45 aa) and may be partially functional.

The UV-sensitivity change of the wild type and mutant (1) were done by exposing the TYG plates streaked with wild type or mutant cells to UV radiation. Antibiotics kanamycin was added into the TYG plates for the mutant. The streaked cell lines were equally divided into four parts and each part was corresponding to one of the four exposure times: 0, 3, 6 10 minutes. The unexposed parts were protected by thick black cardboard. The irradiated plates were incubated at 30 °C until the colonies reached the regular size.

The UV survival experiment ⁷⁹ was done by exposing the same amount of exponential or stationary phase cells of wild type and mutants to UV radiation in a time course. 2 µl of exponential or stationary phase cultures from each of *D. radiodurans* wild type and mutants was added into 10 ml 0.1 M MgSO₄ solution. The cell solution was kept under UV exposure (106 µw/cm²) in a glass plate. 50 µl cell solution was taken out, mixed with 50 µl TYG broth and spread onto corresponding plates every 2 minutes. All of the plates were then incubated in 30 °C for at least two days until the colonies reached the regular size. Then, the colony number on each plate was counted and survival numbers vs. the time curves were drawn.

The exogenous DNA uptake ability of wild type and mutant *D. radiodurans* were compared by using plasmid pACYC184 inserted with a genomic DNA fragment ¹²³ of *D. radiodurans* digested with *BamH I*. Some studies found that plasmid pACYC184 can

also bring the drug-resistance to *D. radiodurans* by using the duplication insertion of homologous recombination similar to pCR-blunt¹²⁴. There are two drug-resistances (tetracycline and chloramphenicol-resistance) in pACYC184. Restriction enzyme *BamH I* was chosen because it is located within the tetracycline-resistance gene. The recombinant plasmids will lose its tetracycline resistance after a positive insertion. The number of *BamH I* cleavage sites in the *D. radiodurans* genomic DNA was calculated by the distribution of A T G C in *D. radiodurans*. In the *D. radiodurans* genome, there might be a *BamH I* site every 2928 bp length. The same amount of *BamH I* digested genomic DNA (end concentration) was added into plasmid pACYC184 digested with the same enzyme and then T4 ligase. The ligation product was then used to transform HB101 competent cells. The plasmids from colonies which can grow on chloramphenicol but not tetracycline plates, were isolated and the sizes of insertions were detected by *BamH I* digestion followed by a 1.0% agarose gel. The recombinant plasmids were then used to transform *D. radiodurans* competent cells as described before for pCR-blunt plasmid. The efficiencies of the transformations in wild type and *recD* mutants were compared.

4.3 Results

4.3.1 The Five pCR-blunt Plasmids with Various Insertions

As shown in figure 4.4, the five plasmids have correct insertions. More digestions were done for the plasmids (1), (2), and (3) to decide the orientations of the inserted *recD* fragments (data not shown). Two pairs of primers were designed to check the plasmid insertion in genomic DNA after homologous recombination, as shown in figure 4.5 and figure 4.6.

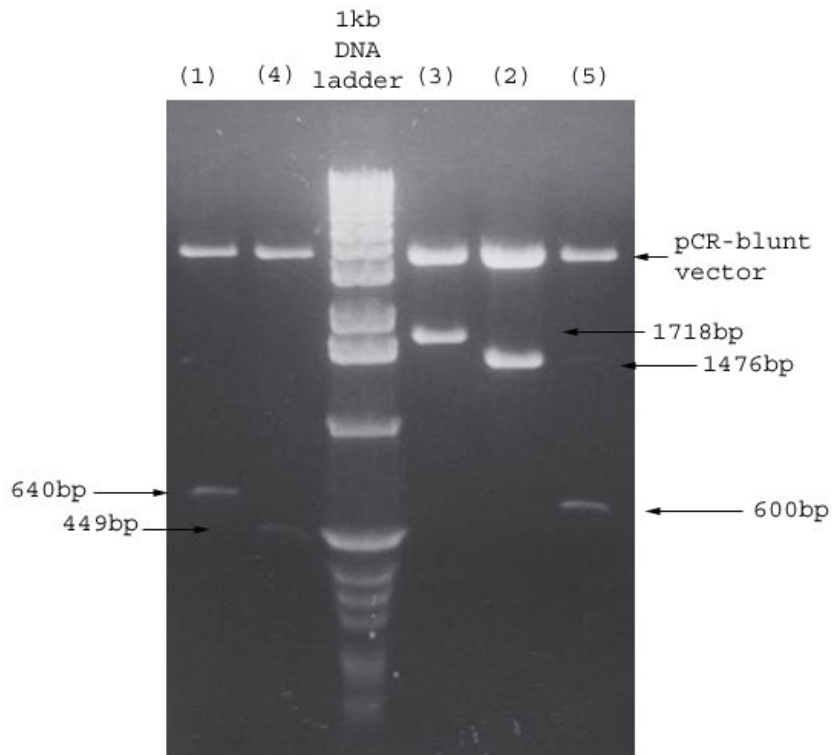


Figure 4.4 The *EcoRI* digestion products from the five newly constructed pCR-blunt plasmids. Plasmid (1) has a 640 bp fragment from the 5'-terminus of the *recD* gene. Plasmid (2) has a 1476 bp fragment from the 5'-end region of the *recD* gene. Plasmid (3) has a 1718 bp fragment from the 3'-end region of the *recD* gene. Plasmid (4) has a 449 bp fragment from the 3'-terminus of the *recD* gene including the stop codon. Plasmid (5) has a 600 bp fragment from the *E. coli recC* gene.

4.3.2 The *recD* Locus Disrupted Mutants of *Deinococcus radiodurans*

The transformation efficiencies for the five plasmids used showed length-dependence (table 2). The plasmid with longer *recD* fragment inserted showed higher efficiency. The plasmid (5) with a 600 bp DNA fragment from *recC* of *E. coli* as a negative control showed no colonies on the selective plates.

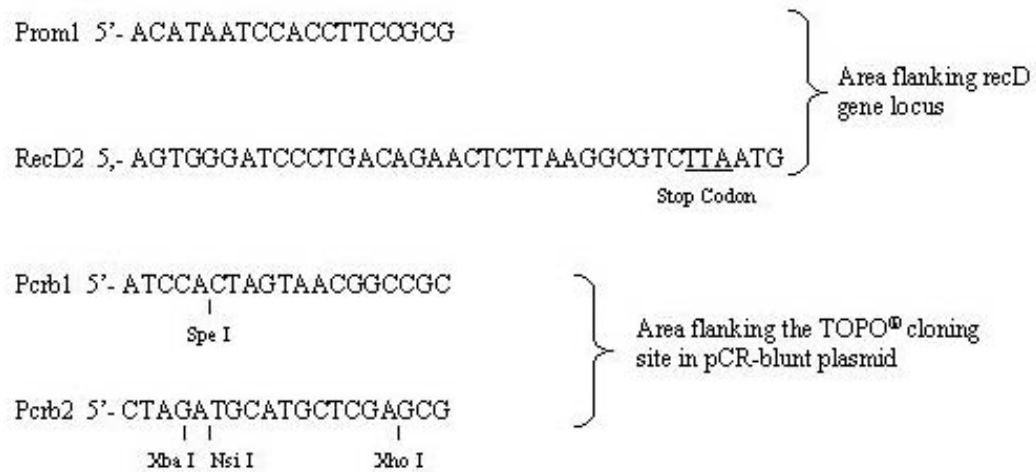


Figure 4.5 The four primers designed to verify the insertion of plasmids into the genome of *D. radiodurans*. According to the orientation of the *recD* gene fragments in the plasmids, the designed primer pairs Prom1 & Pcrb1, Pcrb2 & RecD2 can produce specific lengths of PCR products from the genomic DNA of corresponding *D. radiodurans* mutants.

Four primers (figure 4.5) were designed to amplify the two joint regions in the *D. radiodurans* chromosome I with plasmid insertion by homologous recombination. Since the three *recD* fragments in plasmids (1), (2), and (3) have the same orientation (figure 4.6), the primers were used in two pairs (one black and one green arrows as one pair, as shown in figure 4.7).

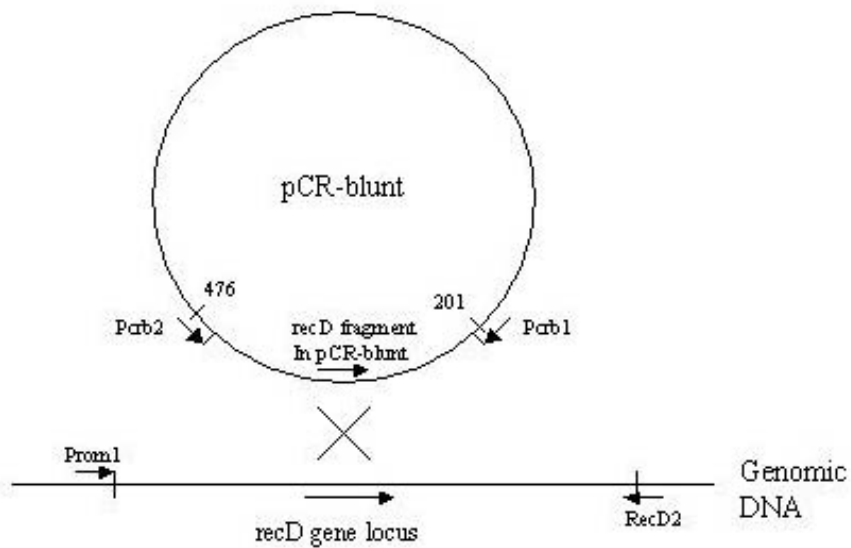


Figure 4.6 The locations of the four primers designed to verify the plasmid insertion. The four primers, as shown by four short arrows, are complementary to the regions in the plasmid and genomic DNA next to the arrows.

The calculated PCR products from mutants (1), (2), and (3) by two pairs of primers:

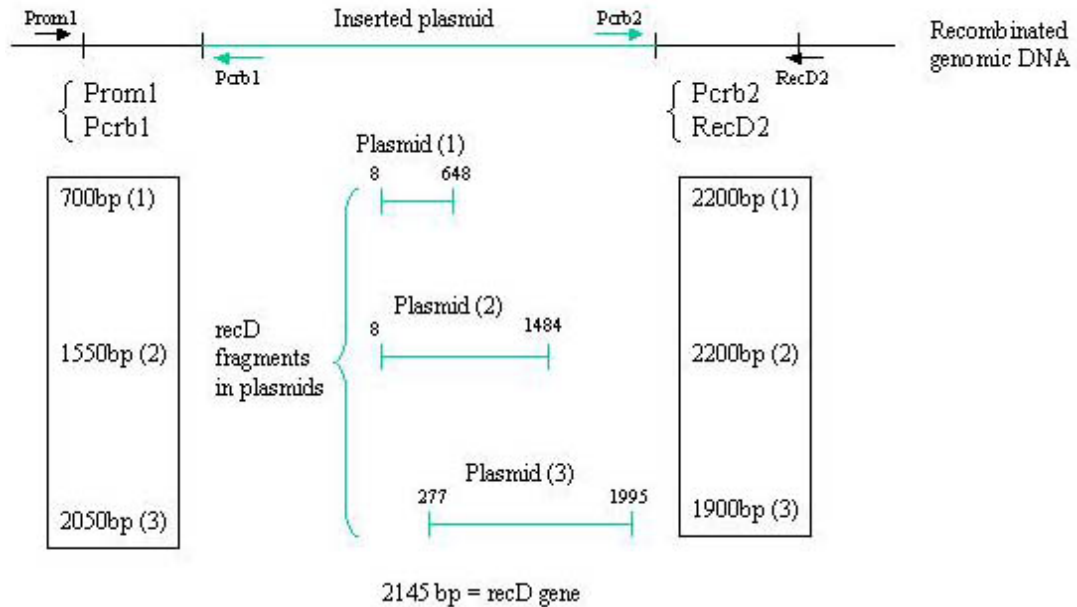


Figure 4.7 The lengths for the expected PCR products from mutant (1), (2) and (3) amplified by the designed two pairs of primers. Since mutant (4) has an intact *recD* gene copy after insertion, the PCR products will be the same as wild type *D. radiodurans*.

As shown in figure 4.8, the 5'-end PCR with primers Prom1 and Pcrb1 showed the PCR bands with expected sizes (figure 4.7). The 3'-end PCR with primers Pcrb2 and RecD2 also showed the correct sizes (figure 4.9, left gel). Because of the polyploid nature of *D. radiodurans*, the PCR reactions with primers flanking the original *recD* gene (Prom1 and RecD2) were also done to make sure all the *recD* copies were disrupted in the genome of mutant *D. radiodurans* (figure 4.9, right gel). The mutants (1), (2), and (3) with no intact *recD* left were used to do the phenotype studies. The presence of the PCR

products from the joint region of the plasmid and chromosome I and the absence of the PCR product from the whole *recD* gene in the *D. radiodurans* mutants suggested that each pCR-blunt plasmid was integrated in each type of *D. radiodurans* mutant and there was no intact *recD* gene copy left in the cells after three generations under kanamycin selective pressure.

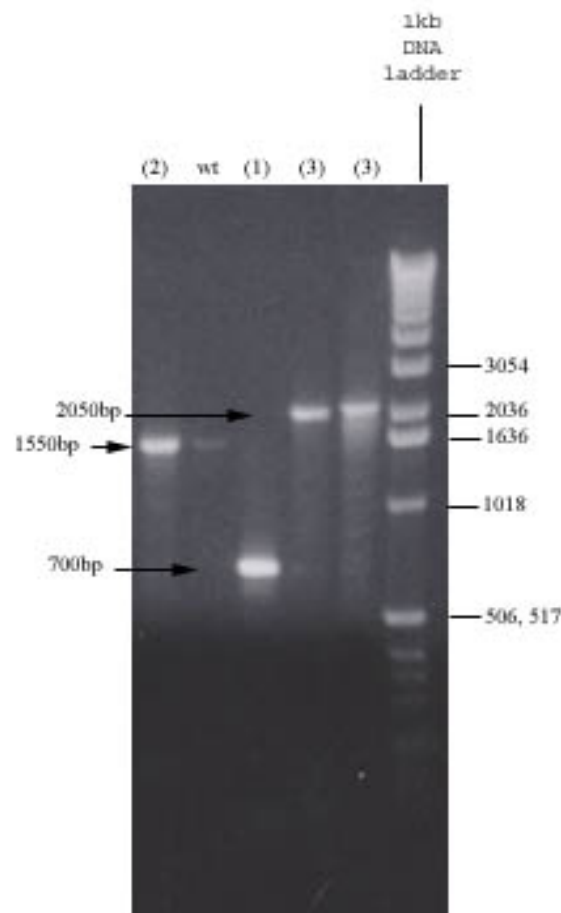


Figure 4.8 5'-end PCR products from genomic DNAs of *D. radiodurans* wild type and mutants. The reactions (100 μ l/each) were done as described in figure 2.3 by using 0.5 μ g genomic DNA from the corresponding *D. radiodurans* cells and 1 μ M/each primers: Prom1 and Pcrb1. The PCR products were run on a 1% agarose gel with 1 kb DNA ladder.

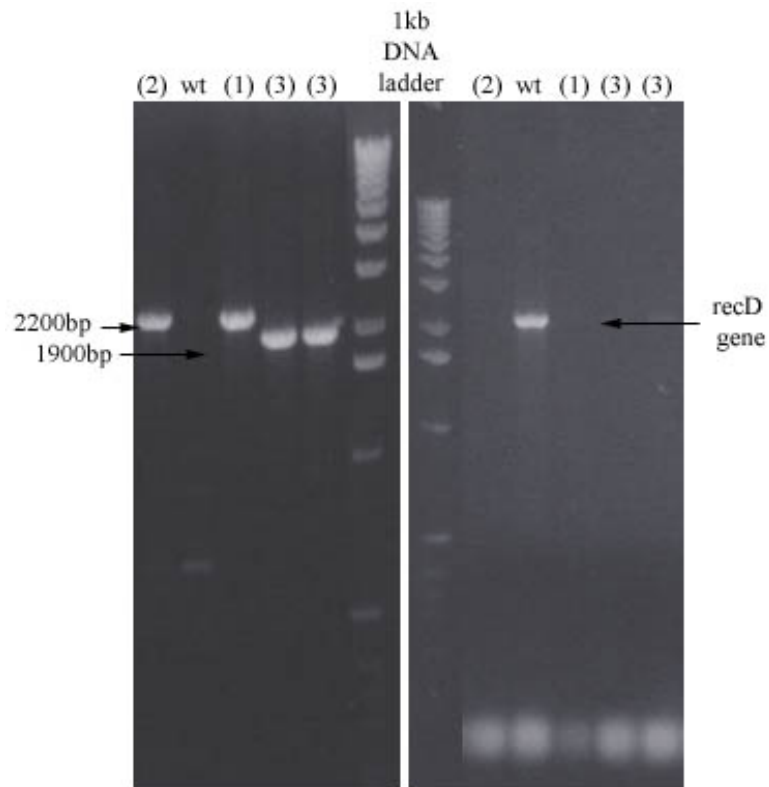


Figure 4.9 3'-end and whole *recD* gene PCR products from genomic DNAs of *D. radiodurans* wild type and mutants. The reaction (100 μ l/each) was done as described in figure 2.3 by using 0.5 μ g/each genomic DNA from the corresponding *D. radiodurans* cells. Each reaction on the left gel had 1 μ M/each primers: Pcrb2 and RecD2. Each reaction on the right gel had 1 μ M/each primers: Prom1 and RecD2 that amplify the whole *recD* region. The PCR products were run on a 1% agarose gel with 1 kb DNA ladder.

4.3.3 The phenotype changes of mutants (1) and (3)

The growth curves of wild type, mutant (1) with more than 500 amino acids truncated from the C-terminus, and mutant (3) with only about 45 amino acids truncated from the C-terminus are shown in figure 4.10. The differences between the wild type and mutants are the lengths of their lagging phases and the steepness of the slopes in their exponential phases. Since we had to include kanamycin in the TYG broth for the two mutants (otherwise the kanamycin resistance in the mutant cells will be lost by the cells ejecting the plasmid insertion from their genomes), we are not sure whether the longer lagging phase for the mutants is because of loss of RecD activity or kanamycin inhibiting cell growth.

The fact that the mutant (1) with RecD mostly truncated has a longer lag time than the mutant (3) with only a small part of RecD truncated, which may be partially functional, suggests that *recD* disruption is related to the change of growth curve for the *D. radiodurans* mutants. The RecD protein may be involved in the checkpoint regulation in *D. radiodurans* before the cells can start exponential growth since the absence of RecD protein causes a longer lag time. The RecD protein also might be involved in DNA replication in *D. radiodurans* since the mutants grew slower than the wild type. Since we used stationary cells to inoculate fresh TYG broth and start the growth curves, the cells at the zero time point of the growth curves had to express the kanamycin resistance gene first, which might also contribute to the longer lagging phase. The slightly slower growth during exponential phase for the mutants, especially the mutant (1) as shown in figure 4.11, may suggest that RecD functions in cell division. Interestingly, the logOD₆₀₀ vs. time curves of both mutants showed a pattern that there was a slower growing phase in

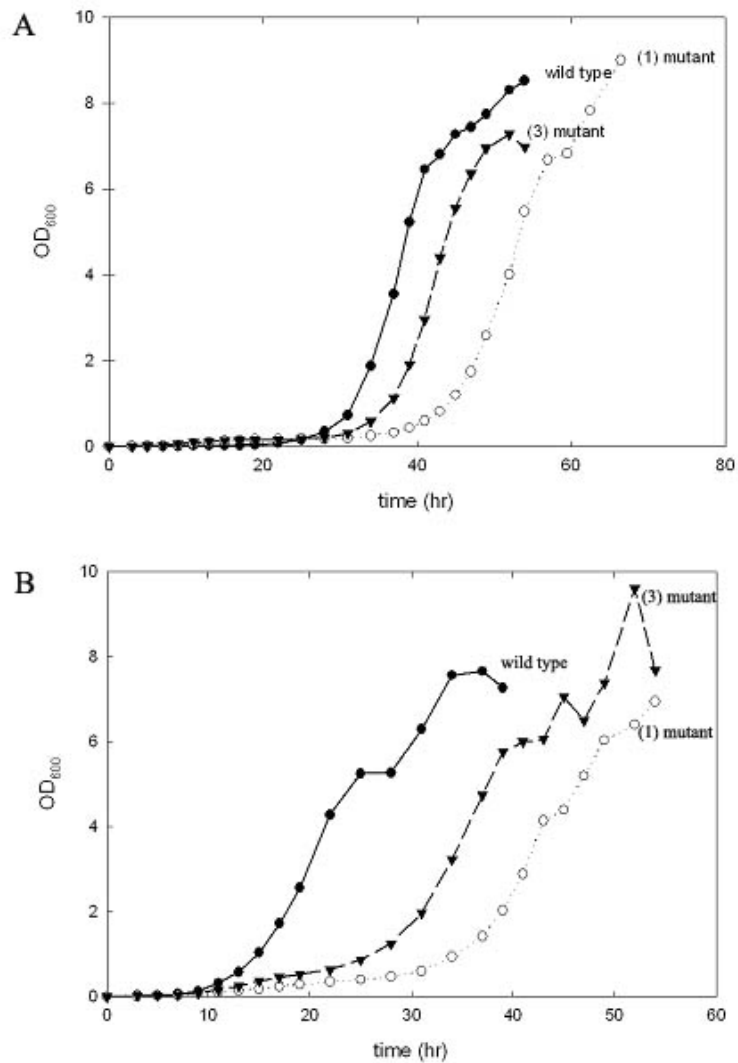


Figure 4.10 The growth curves for *D. radiodurans* wild type and mutants (1) and (3). The cells were grown in TYG media, with 30 mg/l kanamycin for the mutants, and incubated at 30 °C for about three days. About every three hours, 1 ml culture of each was taken out and diluted if necessary to measure the OD₆₀₀ until the reading didn't go up anymore. A and B were repetitive experiments with wild type(closed circles), (1) mutant (open circles) and (3) mutant (closed triangles).

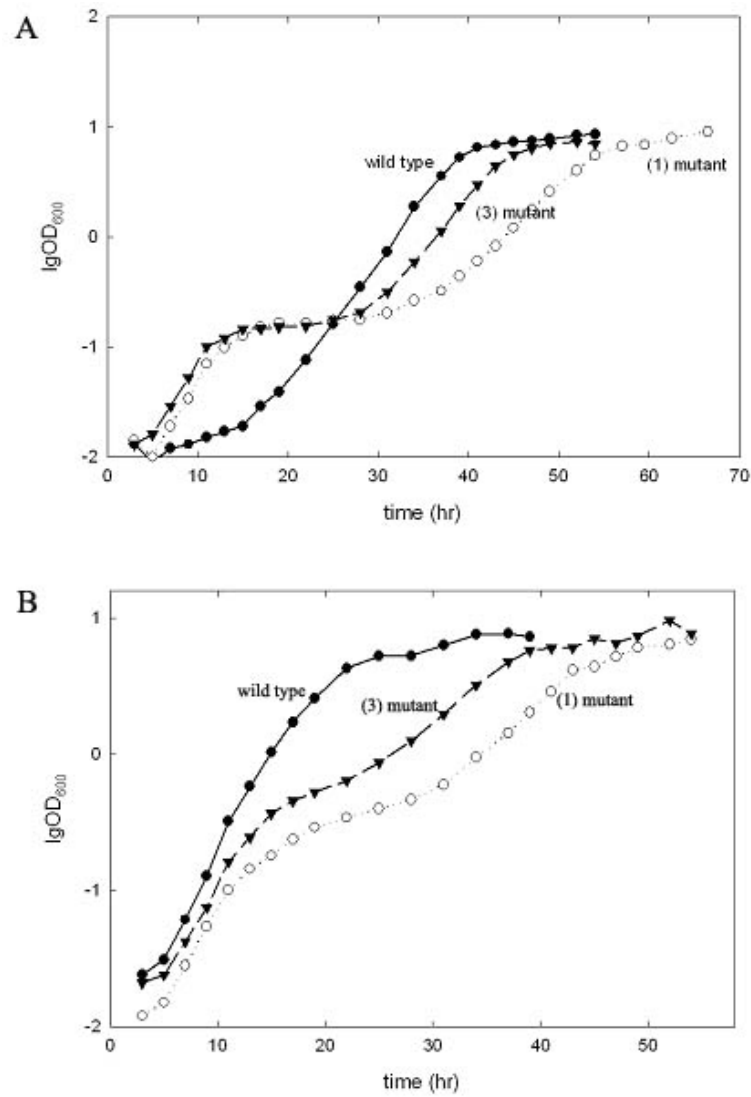


Figure 4.11 The $\log OD_{600}$ vs. time plot for the growth curves shown in figure 4.10. The difference in exponential phase between *D. radiodurans* wild type and mutants is amplified by drawing the plot in this way.

the middle of the curves, which may suggest that something complex is going on there. More experiments, such as inoculating with more cells and with cells in exponential phase, are needed to be done to get a conclusion.

We then tested whether there is a radiosensitivity change caused by *recD* mutation through the comparison of the wild type and mutant (1) cells to ultraviolet light exposure. As shown in figure 4.12, the mutant (1) growing on TYG plates with kanamycin was slightly more sensitive to ultraviolet exposure. Next, we tested the UV survival curves for wild type and mutants from both the exponential and stationary phases, as shown in figure 4.13 and figure 4.14. The results were consistent with each other in that mutants from both exponential and stationary phases are slightly less UV-resistant compared to wild type. More specifically, the decrease of the UV resistance of the mutants is larger in exponential phase cells than in stationary phase cells, which is consistent with the postulation from growth curves that RecD is involved in cell division. The result that the decrease of the UV resistance is larger in mutant (1) than in mutant (3) is consistent with the fact that mutant (1) is the mutant with the most severely truncated RecD and has a longer lagging phase than mutant (3).

We actually didn't finish the exogenous uptake experiment as we designed since its extremely low transformation efficiency. The uptake of exogenous plasmid pACYC184 by *D. radiodurans* was based on the same procedure by which the pCR-blunt plasmids were integrated in the genome through homologous recombination. The efficiencies of transformations with pCR-blunt plasmid series gave us a reasonable result as shown in table 2. However, the same transformation done with pACYC184 plasmid series showed almost no positive colonies on the chloramphenicol selective plates.

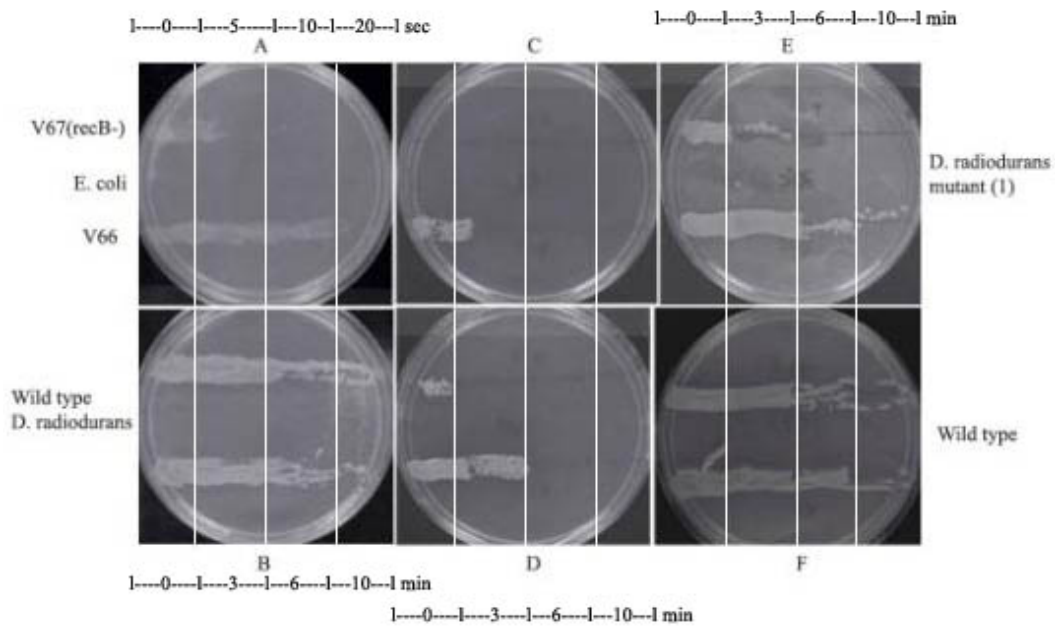


Figure 4.12 The comparison of UV-sensitivity of *E. coli* and *D. radiodurans* wild type and mutant (1). The plates were drawn and streaked with the corresponding cell cultures as described in materials and methods. Plate A has *E. coli* V67 (*recB*⁻, top) and V66 (wild type, bottom). Plates C and E have *D. radiodurans* mutant (1). Plates B, D, and F have *D. radiodurans* wild type. Each cell line was equally divided into four parts. The exposure time course for *E. coli* cells (A) was 0, 5, 10 and 20 seconds and 341 $\mu\text{w}/\text{cm}^2$ UV intensity. The exposure time course for *D. radiodurans* cells (B-F) was 0, 3, 6 and 10 minutes and various UV intensities: 345 $\mu\text{w}/\text{cm}^2$ for (B), 650 $\mu\text{w}/\text{cm}^2$ for (C and D), and 350 $\mu\text{w}/\text{cm}^2$ for (E and F). B and F were almost the same but done at different times.

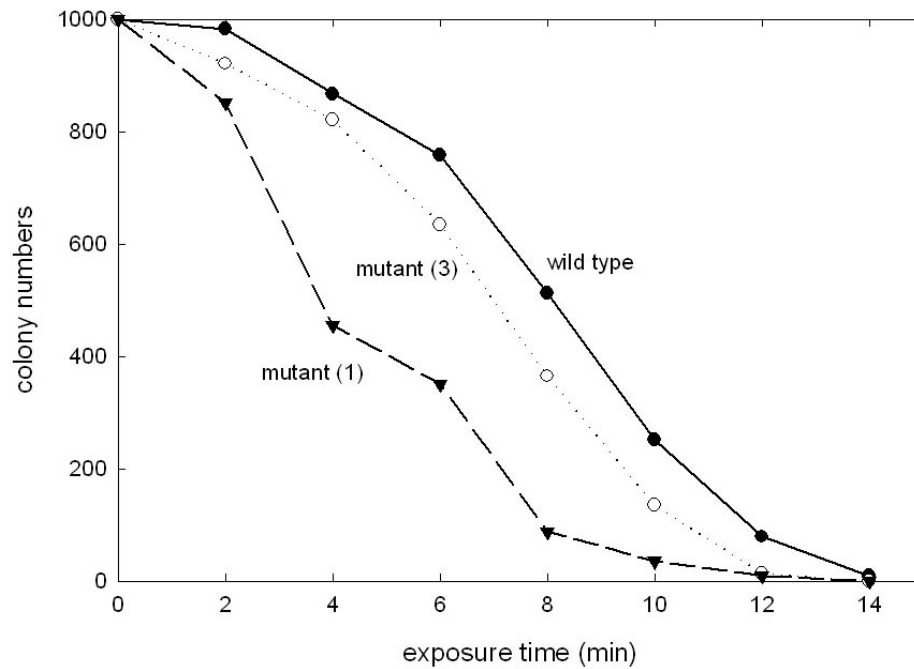


Figure 4.13 The UV survival curves for *D. radiodurans* wild type and mutant (1) and (3) from exponential phase. About the same amount of exponential phase cells were kept in 10 ml of 50 mM magnesium sulfate solution in a plate and exposed to UV radiation with $106 \mu\text{w}/\text{cm}^2$ intensity. $50 \mu\text{l}$ solution was taken out at each time point and $50 \mu\text{l}$ TYG media was added before it was spread onto TYG plates (with kanamycin for the mutant cells). The plates were incubated at 30°C for 2-3 days before the colonies were counted.

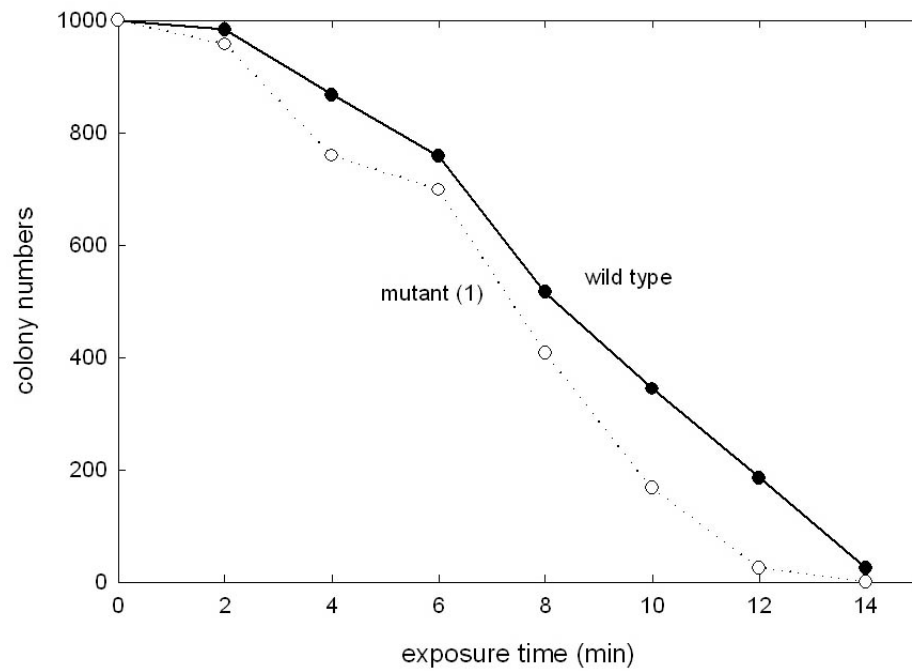


Figure 4.14 The UV survival curves for *D. radiodurans* wild type and mutant (1) from stationary phase. The experiment was done in the same way as described in figure 4.13.

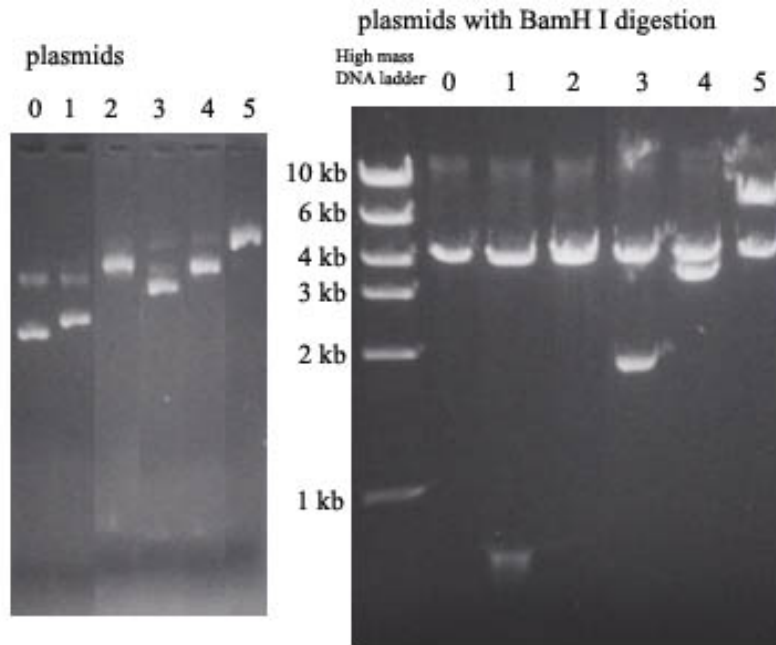


Figure 4.15 The five pACYC184 plasmids prepared for the exogenous DNA uptake experiment. The gel on the left shows the circular plasmids pACYC184 (0) and the five newly constructed plasmids (1-5) with various lengths of genomic DNA insertion from *D. radiodurans* as described in materials and methods. The gel on the right shows the *BamHI* digestion products of the plasmids on a 1% agarose gel with high mass DNA ladder. Plasmid (0) is pACYC184 alone without any insertion. Plasmid (1) has < 1 kb genomic DNA fragment inserted. Plasmid (2) is a plasmid with two copies of vectors ligated together. Plasmid (3) has a ~ 2 kb genomic DNA fragment inserted. Plasmid (4) has a ~ 3.6 kb genomic DNA fragment inserted. Plasmid (5) has a ~ 6.5 kb genomic DNA fragment inserted.

pCR-blunt plasmid	Length of <i>recD</i> Fragment insertion (bp)	Number of colonies
(1)	640	10
(2)	1476	50
(3)	1718	60
(4)	449	10
(5)	600 <i>recC</i> fragment	0 as negative control

pACYC184 plasmid	Length of genomic DNA fragment insertion (kb)	Number of colonies
(1)	< 1	0
(2)	4.1 another vector	0 as negative control
(3)	2	2
(4)	3.6	1

Table 2 Efficiencies of transformation with pCR-blunt and pACYC184 plasmid series. (A) Transformation efficiency of *D. radiodurans* wild type cells with pCR-blunt plasmids showed length-dependence. (B) Transformation efficiency of *D. radiodurans* wild type cells with pACYC184 plasmids were extremely low.

Since the transformation efficiency for pACYC184 is too low even for wild type *D. radiodurans*, the transformation efficiencies for *D. radiodurans recD* mutants was not done. Some research showed that the cross-link repair in *D. radiodurans* induced by mitomycin C was inhibited in cells post-incubated in the presence of chloramphenicol¹²⁵. The incapacity of resolving the cross-links that appeared during insertional recombination by plasmid pACYC184 may be the reason that the transformation efficiency is extremely low in *D. radiodurans* competent cells growing on chloramphenicol (10 µg/ml) selective

plates. Some other plasmids with antibiotic resistance genes other than chloramphenicol, such as pCR-blunt used before, may be useful in this experiment.

4.6 Discussion

Repair of DNA damage in *D. radiodurans* follows an ordered series of events^{60, 78}. While growth-promoting conditions are essential for removal of lesions from cellular DNA, the cells themselves do not immediately divide. Indeed, there is a dramatic inhibition of growth for extended durations following acute exposure to nonlethal (or partially lethal) DNA damage. This growth lag is associated with limited degradation of chromosomal DNA intrinsic to the DNA repair processes⁵⁹. Studies showed that following a nonlethal exposure of stationary-phase *D. radiodurans* to 1.5 megarads under anoxic conditions, dilute liquid cultures of *D. radiodurans* show no growth for about 10 hours and then resume rapid exponential growth⁶⁷. The delay of the onset of cellular replication in *D. radiodurans* is dose-dependent. It suggests that there is a checkpoint mechanism in *D. radiodurans* that not only monitors the progress of DNA damage repair but also correspondingly controls the initiation of replicative DNA synthesis⁶⁰. As shown in the result, the growth curve for the *recD* mutant of *D. radiodurans* has longer growth lag before the exponential phase than the wild type. It may suggest that the events happening during the lag phase require the *recD* gene product or the mutant cells need longer time before cells can divide, which is consistent with the fact that the mutants grow slightly slower than wild type *D. radiodurans*.

Both UV sensitivity experiments we did showed that the *recD* mutants are only slightly less UV resistant than wild type compared to the dramatic loss of UV resistance

in *recA*⁶⁸ and *uvrA*⁸⁰ mutants of *D. radiodurans*. Since the products of *recA* and *uvrA* genes were proven to be very important in DNA damage repair, the slight UV sensitivity caused by *recD* disruption may suggest that the RecD protein is not involved in DNA repair in *D. radiodurans*. It was part of the reason that we did not pursue the mutant study further. We might have done more experiments with it if there had been a dramatic effect of the mutation.

The design for the exogenous DNA uptake experiment was good even though it didn't get finished. We should try it with other plasmids. So far the phenotype studies of the *recD* mutants didn't show a significant change. However, we have not tested the *recD* mutants for double-stranded DNA break repair in *D. radiodurans* yet. *D. radiodurans* is resistant to DNA damage caused by many different sources with different types of DNA damage produced, such as gamma radiation, desiccation, and chemical agents. It is possible that RecD is involved in the repair pathway of a type of DNA damage that we didn't study yet.

Chapter 5 DISCUSSION AND CONCLUSION

By cloning and expressing the *D. radiodurans* *recD*-like gene in *E. coli*, we studied its biochemical function. The RecD protein exhibits single-stranded DNA-dependent ATPase and DNA helicase activities. The helicase substrates are 20 base pair duplexes with blunt ends, with a 12 nucleotide single-stranded tail on either the 3' or 5'-end, or with a 12 nucleotide single-stranded fork on one end. The RecD protein unwinds only the 5'-tailed and forked substrates and the unwinding rate is seven times faster for the forked substrate.

The helicase assay shows that the *D. radiodurans* RecD protein unwinds 20 bp double-stranded DNA substrates catalytically (i.e., most of DNA was unwound, even at 100:1 = DNA:enzyme ratio). The unwinding rate is about 7 DNA molecules per minute (140 bp/min) for 5'-overhang DNA and about 48 DNA molecules per minute (950 bp/min) for forked DNA. When using longer DNA (52 bp), the unwinding rate is much slower - only about 0.39 DNA molecule per minute (20 bp/min) and a little bit faster when single-stranded DNA binding (SSB) protein from *E. coli* is added. The significant increase of unwinding efficiency with SSB from *D. radiodurans* suggests an interaction between RecD and DrSSB. These results show that the *D. radiodurans* RecD protein is a DNA helicase that moves with 5'-3' polarity on single-stranded DNA. Keeping in mind that the *E. coli* RecD protein was shown recently to unwind dsDNA with the same 5'-3' polarity, the low processivity of the *D. radiodurans* RecD protein, which is different from the processive RecBCD enzyme in *E. coli*⁵, suggests that it may function in a complex with other proteins.

5.1 The RecD-Like Protein Compared to RecD Subunit

Our study of the RecD protein is the first examination of the family of RecD-like proteins that are found in *D. radiodurans* and in some Gram-positive bacteria. Part of the motivation for the present study was to have a RecD protein that could be studied biochemically. The *E. coli* RecD protein is largely insoluble when overexpressed and must be purified in denatured form and then renatured in order to detect its enzymatic activity. The RecD protein from *D. radiodurans* is soluble when overexpressed and purified, has high enzymatic activity, and retains activity during prolonged storage. Thus it may be suitable for structure-function study of a RecD-like helicase.

The RecD protein is a DNA helicase whose substrate specificity indicates that it moves with 5'-3' polarity along single-stranded DNA. It requires at least a 10 nt length of 5'-single-stranded tail, and does not unwind duplexes with blunt end or a 3'-single stranded tail. The best substrate that we have tested has a forked end. Greater unwinding of a duplex with a forked end vs. one with only one single-stranded tail was also observed with Pif1 from yeast, a helicase included in the COG0507 RecD helicase family. Unwinding of the longer substrates (52 and 76 bp) is always much less efficient than the 20 bp substrates, indicating that the RecD unwinds DNA with low processivity. Low processivity could indicate that its function is to unwind DNA only over short distances, or there may be other proteins that enhance its processivity, as observed for the RecB helicase subunit in RecBCD and the PcrA helicase¹²⁶.

The RecD subunit of the *E. coli* RecBCD enzyme is also a helicase with apparent 5'-3' polarity, and it is thought to act as a helicase during RecBCD enzyme activity⁴⁰. However, RecD is dispensable for unwinding, since RecBC enzyme is already a

helicase²⁶, and the major effect of removing RecD from RecBCD is on the nuclease activity of RecBCD^{127, 128}. Although the nuclease active site resides in RecB, loss of the RecD subunit reduces the nuclease activity to very low levels that are not biologically relevant^{36, 46}. ATP hydrolysis by RecD is not required for its role in stimulating the nuclease activity. Thus, the phenotypes of *E. coli recD* null mutants are quite different from those of *recB* or *recC* null mutants as discussed before. Cells with null mutations in *recB* or *recC*, and *recBCD* deletion mutants, are deficient in homologous recombination, sensitive to various DNA-damaging agents, and susceptible to infection by certain mutant bacteriophages that are normally destroyed by the RecBCD nuclease activity^{1, 129}. The *recD* null mutants are recombination proficient and resistant to DNA damaging agents, presumably due to activity of RecBC in these mutants³³. The *recD* mutants are however susceptible to phage infections due to the low level of nuclease activity in the mutants⁴⁶.

5.2 The Characteristics of C-Terminal His-Tagged RecD for Its Binding to Resin and Solubility May Reveal Some Structural Properties of RecD

The fact that the N-terminal His-tagged RecD protein had problems to stay soluble after it was overexpressed in *E. coli* host cells and also to bind to the Ni²⁺-NTA resin might reveal some structural characteristics of the RecD protein. The N-terminus of RecD is likely folded into either the core of protein or the hydrophobic interface between protein subunits (dimerization) so that the attached His-tag tail is not accessible to the nickel resin. The insolubility of RecD protein while overexpressed might reveal the importance of the N-terminus in the folding process after the polypeptide is translated. The attached 20 amino acid sequence on the N-terminus has a fairly big volume and

cannot be folded into the protein core or a complementary interface with another protein subunit so that the newly synthesized polypeptide cannot automatically fold into its native structure. The misfolded or partially folded protein will then polymerize and form insoluble inclusion bodies in the host cell. When the His-tag is attached to the C-terminus of RecD protein, even though the 8 amino acid tag has smaller volume compared to the 20 amino acid on N-terminus, it is much more accessible to the nickel resin. And, since the C-terminal His-tag does not cause any structural disfiguration, the C-terminus of RecD protein is likely more flexible and stays on the outer surface of the protein.

5.3 Difference in Helicase Activities with Short (20 bp) and Longer (52 or 76 bp) dsDNA Substrates and the Requirement for the ss DNA 5'-overhang

The unwinding rates that we found for RecD with the 20 bp substrates are comparable to rates reported for similar substrates with some other helicases, including the bacteriophage T4 Dda helicase^{121, 130}, the bacteriophage T7 helicase¹³¹, and the *E. coli* rep helicase¹³². The rates that we have measured are initial reaction rates determined at low DNA substrate concentrations, and thus they may be less than the maximal unwinding rate of which the enzyme is capable. The DNA binding measurements showed that little RecD protein bound to the DNA under conditions similar to the unwinding reactions (except that ATP was not present in the binding mixtures). Greater unwinding rates might be observed either at higher DNA concentrations (V_{\max} conditions), or at higher protein concentrations under single-turnover conditions. Some helicases unwind DNA much more rapidly than does RecD, including RecBCD⁵ and *E. coli* UvrD¹³³.

The RecD protein is not alone regarding its requirement of at least a 10-nucleotide ssDNA overhang at the 5'-end, the preference for the fork-shaped substrates, its low processivity and unwinding polarity. Studies showed that some helicases involved in replication have some similarity with the RecD protein. A chloroplast DNA helicase II from pea (*Pisum sativum*) is an ssDNA-dependent ATPase. Its helicase activity was markedly stimulated by DNA substrates with replication fork-like structure and a 5'-tailed fork was more active than the 3'-tailed fork. Its activity was also inhibited by KCl or NaCl while requiring divalent cation ($Mg^{2+} > Mn^{2+} > Ca^{2+}$). It was suggested that this helicase could be involved in the replication of ctDNA¹³⁴. Another example is the human DNA helicase IV. Besides the need of a divalent cation ($Mg^{2+} = Mn^{2+} = Zn^{2+}$) and ATP or dATP hydrolysis for its activity, this enzyme requires more than 84 bases of single-stranded DNA overhang and moves in the 5' to 3' direction along the bound strand. Similar to human DNA helicase I and the nuclear DNA helicase II from calf thymus nuclei, which both have opposite polarity¹³⁵, this enzyme can also unwind a RNA-DNA hybrid¹³⁶. This property suggests the possible role in unwinding the RNA primer from the template in the lagging strand while the replication fork moves forward.

Some other helicases also show some level of similarity to RecD, such as the RepA protein of the mobilizable broad host range plasmid RSF1010. The RepA helicase has 5' to 3' polarity with a preference for a 3'-tailed substrate. Its optimal unwinding activity was achieved at the remarkably low pH of 5.5 and the presence of *E. coli* SSB protein stimulates unwinding 2-3 fold. It has a key function in its replication¹³⁷. An important property of these replicative helicases is that they usually unwind DNA duplexes or RNA-DNA hybrid with a short annealed portion (<32 bp for human DNA

helicase VI¹³⁸) and prefer a replication fork-like structure of the substrate, which are exactly what the RecD protein showed.

5.4 The Lack of Apparent Difference in the Phenotypes between Wild Type and *recD* Mutants of *Deinococcus radiodurans*

The biological function of RecD in *D. radiodurans* is not known. The *recD* mRNA was detected in an experiment that measured global gene expression in *D. radiodurans* using a DNA microarray. It showed that at least at one time point during the recovery following acute irradiation (15 kGy), 832 genes (28 % of the genome) were induced and 451 genes (15 %) were repressed 2-fold or more. The *recD* mRNA expression level did not increase after gamma irradiation of a stationary phase culture (in fact, it decreased slightly)¹³⁹. This may suggest that the *D. radiodurans* RecD protein is not involved in DNA repair. However, transcription of genes encoding proteins involved in DNA repair does not necessarily increase in response to DNA damage. For example, the *recB*, *recC*, and *recD* genes of *E. coli* are not induced after UV irradiation. The mRNAs from the two *recD* genes were also detected in the transcriptome of *C. trachomatis*. The RecD protein itself was detected in the *D. radiodurans* proteome by mass spectrometry, but only in cells grown under certain conditions (e.g., stationary phase cells or mid-log phase cells in rich media)¹⁴⁰.

The *recD* knockout mutant studies in *D. radiodurans* revealed a longer lagging phase before the cells started exponential growth and the mutants were slightly more sensitive under UV exposure compared to the wild type. There are two possible explanations for the lack of apparent change in its phenotype. First, there are other types

of DNA damage repair we didn't investigate. Second, the RecD protein, instead of a role in DNA repair, is involved some housekeeping pathway such as DNA replication. The second possibility is actually consistent with the slightly decreased expression level of RecD after induction of DNA damage because the DNA replication in cells with DNA damage pauses and resumes after the damage is repaired.

5.5 Conclusion

The ability to recognize and repair abnormal DNA structure is common to all forms of life. Studies in a variety of species have identified an incredible diversity of DNA repair pathways. Documenting and characterizing the similarities and differences in repair between species has important value for understanding the origin and evolution of repair pathways as well as for improving our understanding of phenotypes affected by repair (e.g., mutation rates, lifespan, tumorigenesis, survival in extreme environments). So far, the study on the DNA damage repair pathways in *D. radiodurans* is very limited. There is not a conclusive explanation for its significant DNA damage tolerance. Since there is also no existing model bacterium that has similar level of UV resistance as does *D. radiodurans*, the research will have a long way to go.

According to the orthologous groups of RecD, we can find some similarity that *D. radiodurans* shares with other much less UV resistant bacteria. But can RecD in *D. radiodurans* be related to some DNA repair proteins in species apparently far from its group? The horizontal gene transfer and domain shuffling during evolution played an important role in providing the genetic diversity in organisms¹⁰¹. Many of the eukaryotic repair proteins clearly can be traced to bacterial and archaeal roots. Some organellar

(mitochondrial or chloroplast) repair proteins are good examples. They are relatively independent and only involved in the DNA metabolism of organellar genomes. They entered the eukaryotic ancestor once and stayed there as the organellar genomes. Vice versa, some repair proteins in prokaryotes such as *Chlamydia trachomatis*, which is grouped with *D. radiodurans* (*C. trachomatis* RecD1), have evolutionary origins in eukaryotic lineages¹⁴¹. The phylogenetic mosaic of *Chlamydial* genes, including a large number of genes with phylogenetic origins from eukaryotes, implies a complex evolution to adapt to specific habitats⁹⁸.

The properties of the purified RecD protein *in vitro* are: (1) it is a DNA helicase with 5'-3' polarity; (2) it unwinds dsDNA substrates with a 5'-single-stranded terminal extension and prefers the fork-shaped ssDNA at the end; and (3) it has low processivity. The similarities shared by the RecD protein we studied from *D. radiodurans* and replicative helicases as mentioned before found from some viruses, prokaryotes, and organelles of eukaryotes might shed some light on finding out its biological function *in vivo*. Considerable further research and study need to be directed towards the detection of its interaction component *in vivo* and its mutant study before we can completely reveal the role it plays in the extreme radioresistance of *Deinococcus radiodurans*.

BIBLIOGRAPHY:

1. Amundsen, S. K., Neiman, A. M., Thibodeaux, S. M. & Smith, G. R. (1990). Genetic dissection of the biochemical activities of RecBCD enzyme. *Genetics* 126, 25-40.
2. Chedin, F. & Kowalczykowski, S. C. (2002). A novel family of regulated helicases/nucleases from Gram-positive bacteria: insights into the initiation of DNA recombination. *Mol. Microbiol.* 43, 823-34.
3. Kuzminov, A., Schabtach, E. & Stahl, F. W. (1994). Sites in combination with RecA protein increase the survival of linear DNA in *Escherichia coli* by inactivating *exoV* activity of RecBCD nuclease. *EMBO J.* 13, 2764-2776.
4. Kowalczykowski, S. C., Dixon, D. A., Eggleston, A. K., Lauder, S. D. & Rehrauer, W. M. (1994). Biochemistry of homologous recombination in *Escherichia coli*. *Microbiol. Rev.* 58, 401-465.
5. Bianco, P. R., Brewer, L. R., Corzett, M., Balhorn, R., Yeh, Y., Kowalczykowski, S. C. & Baskin, R. J. (2001). Processive translocation and DNA unwinding by individual RecBCD enzyme molecules. *Nature* 409, 374-8.
6. Cox, M. M. (1998). A broadening view of recombinational DNA repair in bacteria. *Genes Cells* 3, 65-78.
7. Michel, B. (2000). Replication fork arrest and DNA recombination. *Trends Biochem. Sci.* 25, 173-178.
8. George, J. W., Stohr, B. A., Tomso, D. J. and Kreuzer, K. N. (2001). The tight linkage between DNA replication and double-strand break repair in bacteriophage T4. *Proc. Natl. Acad. Sci. USA* 98, 8290-7.
9. Cox, M. M. (2001). Recombinational DNA repair of damaged replication forks in *E. coli*. *Annu. Rev. Genet.* 35, 53-82.
10. Cox, M. M., Goodman, M. F., Kreuzer, K. N., Sherratt, D. J., Sandler, S. J. & Marians, K. J. (2000). The importance of repairing stalled replication forks. *Nature* 404, 37-41.
11. Kowalczykowski, S. C. (2000). Initiation of genetic recombination and recombination-dependent replication. *Trends Biochem. Sci.* 25, 156-165.

12. Smith, G. R. (1989). Homologous recombination in *E. coli*: multiple pathways for multiple reasons. *Cell* 58, 807-809.
13. El Karoui, M., Ehrlich, S. D. & Gruss, A. (1998). Identification of the *lactococcal* exonuclease/recombinase and its modulation by the putative Chi sequence. *Proc. Natl. Acad. Sci. USA* 95, 626-631.
14. Smith, G. R. (1990). RecBCD Enzyme. In *Nucleic Acids and Molecular Biology* (Eckstein, F. & Lilley, D. M. Jr., eds.), Vol. 4, pp. 78-98. Springer-Verlag, Berlin, Heidelberg.
15. Lohman, T. M. & Bjornson, K. P. (1996). Mechanism of Helicase-Catalyzed DNA Unwinding. *Annu. Rev. Biochem.* 65, 169-214.
16. Dixon, D. A. & Kowalczykowski, S. C. (1991). Homologous pairing *in vitro* stimulated by the recombination hotspot, Chi. *Cell* 66, 361-371.
17. Dixon, D. A. & Kowalczykowski, S. C. (1993). The recombination hotspot χ is a regulatory sequence that acts by attenuating the nuclease activity of the *E. coli* RecBCD enzyme. *Cell* 73, 87-96.
18. Anderson, D. G. & Kowalczykowski, S. C. (1997). The recombination hot spot χ is a regulatory element that switches the polarity of DNA degradation by the RecBCD enzyme. *Genes & Devel.* 11, 571-581.
19. Bianco, P. R. & Kowalczykowski, S. C. (1997). The recombination hotspot Chi is recognized by the translocating RecBCD enzyme as the single strand of DNA containing the sequence 5'-GCTGGTGG-3'. *Proc. Natl. Acad. Sci. USA* 94, 6706-6711.
20. Cheng, K. C. & Smith, G. R. (1987). Cutting of Chi-like sequences by the RecBCD enzyme of *Escherichia coli*. *J. Mol. Biol.* 194, 747-750.
21. Taylor, A. & Smith, G. R. (1980). Unwinding and rewinding of DNA by the RecBC enzyme. *Cell* 22, 447-457.
22. Anderson, D. G. & Kowalczykowski, S. C. (1997). The translocating RecBCD enzyme stimulates recombination by directing RecA protein onto ssDNA in a Chi-dependent manner. *Cell* 90, 77-86.
23. Taylor, A. F., Schultz, D. W., Ponticelli, A. S. & Smith, G. R. (1985). RecBC enzyme nicking at Chi sites during DNA unwinding: location and orientation-dependence of the cutting. *Cell* 41, 153-163.
24. Amundsen, S. K., Taylor, A. F. & Smith, G. R. (2000). The RecD subunit of the *Escherichia coli* RecBCD enzyme inhibits RecA loading,

- homologous recombination, and DNA repair. *Proc. Natl. Acad. Sci. USA* 97, 7399-404.
25. Myers, R. S., Kuzminov, A. & Stahl, F. W. (1995). The recombination hotspot χ activates RecBCD recombination by converting *Escherichia coli* to a *recD* mutant phenocopy. *Proc. Natl. Acad. Sci. USA* 92, 6244-6248.
 26. Dixon, D. A., Churchill, J. J. & Kowalczykowski, S. C. (1994). Reversible inactivation of the *Escherichia coli* RecBCD enzyme by the recombination hotspot χ *in vitro*: evidence for functional inactivation or loss of the RecD subunit. *Proc. Natl. Acad. Sci. USA* 91, 2980-2984.
 27. Taylor, A. F. & Smith, G. R. (1999). Regulation of homologous recombination: Chi inactivates RecBCD enzyme by disassembly of the three subunits. *Genes & Devel.* 13, 890-900.
 28. Dixon, D. A. & Kowalczykowski, S. C. (1995). Role of the *Escherichia coli* recombination hotspot, χ , in RecABCD-dependent homologous pairing. *J. Biol. Chem.* 270, 16360-16370.
 29. Taylor, A. F. & Smith, G. R. (1992). RecBCD enzyme is altered upon cutting DNA at a Chi recombination hotspot. *Proc. Natl. Acad. Sci. USA* 89, 5226-5230.
 30. Spies, M., Bianco, P. R., Dillingham, M. S., Handa, N., Baskin, R. J. & Kowalczykowski, S. C. (2003). A molecular throttle: the recombination hotspot Chi controls DNA translocation by the RecBCD helicase. *Cell* 114, 647-54.
 31. Arnold, D. A. & Kowalczykowski, S. C. (2000). Facilitated loading of RecA protein is essential to recombination by RecBCD enzyme. *J. Biol. Chem.* 275, 12261-5.
 32. Anderson, D. G. & Kowalczykowski, S. C. (1998). SSB protein controls RecBCD enzyme nuclease activity during unwinding: a new role for looped intermediates. *J. Mol. Biol.* 282, 275-285.
 33. Churchill, J. J., Anderson, D. G. & Kowalczykowski, S. C. (1999). The RecBC enzyme loads RecA protein onto ssDNA asymmetrically and independently of χ , resulting in constitutive recombination activation. *Genes & Devel.* 13, 901-911.
 34. Finch, P. W., Storey, A., Chapman, K. E., Brown, K., Hickson, I. D. & Emmerson, P. T. (1986). Complete nucleotide sequence of the *Escherichia coli recB* gene. *Nucleic Acids Res.* 14, 8573-8582.

35. Finch, P. W., Storey, A., Brown, K., Hickson, I. D. & Emmerson, P. T. (1986). Complete nucleotide sequence of *recD*, the structural gene for the α subunit of Exonuclease V of *Escherichia coli*. *Nucleic Acids Res.* 14, 8583-8594.
36. Amundsen, S. K., Taylor, A. F., Chaudhury, A. M. & Smith, G. R. (1986). *recD*: the gene for an essential third subunit of exonuclease V. *Proc. Natl. Acad. Sci. USA* 83, 5558-5562.
37. Chen, H. -W., Randle, D. E., Gabbidon, M. & Julin, D. A. (1998). Functions of the ATP hydrolysis subunits (RecB and RecD) in the nuclease reactions catalyzed by the RecBCD enzyme from *Escherichia coli*. *J. Mol. Biol.* 278, 89-104.
38. Chen, H. -W., Ruan, B., Yu, M., Wang, J. & Julin, D. A. (1997). The RecD subunit of the RecBCD enzyme from *Escherichia coli* is a single-stranded DNA-dependent ATPase. *J. Biol. Chem.* 272, 10072-10079.
39. Phillips, R. J., Hickleton, D. C., Boehmer, P. E. & Emmerson, P. T. (1997). The RecB protein of *Escherichia coli* translocates along single-stranded DNA in the 3' to 5' direction: a proposed ratchet mechanism. *Mol. Gen. Genet.* 254, 319-329.
40. Dillingham, M. S., Spies, M. & Kowalczykowski, S. C. (2003). RecBCD enzyme is a bipolar DNA helicase. *Nature* 423, 893-7.
41. Taylor, A. F. & Smith, G. R. (2003). RecBCD enzyme is a DNA helicase with fast and slow motors of opposite polarity. *Nature* 423, 889-93.
42. Boehmer, P. E. & Emmerson, P. T. (1992). The RecB subunit of the *Escherichia coli* RecBCD enzyme couples ATP hydrolysis to DNA unwinding. *J. Biol. Chem.* 267, 4981-4987.
43. Eggleston, A. K. & Kowalczykowski, S. C. (1993). Biochemical characterization of a mutant RecBCD enzyme, the RecB²¹⁰⁹CD enzyme, which lacks χ -specific, but not non-specific, nuclease activity. *J. Mol. Biol.* 231, 605-620.
44. Schultz, D. W., Taylor, A. F. & Smith, G. R. (1983). *Escherichia coli* RecBC pseudorevertants lacking Chi recombinational hotspot activity. *J. Bacteriol.* 155, 664-680.
45. Arnold, D. A., Bianco, P. R. & Kowalczykowski, S. C. (1998). The reduced levels of recognition by the RecBC¹⁰⁰⁴D enzyme reflect its recombination defect *in vivo*. *J. Biol. Chem.* 273, 16476-16486.

46. Chaudhury, A. M. & Smith, G. R. (1984). A new class of *Escherichia coli* *recBC* mutants: implications for the role of RecBC enzyme in homologous recombination. . *Proc. Natl. Acad. Sci. USA* 81, 7850-7854.
47. Yu, M., Souaya, J. & Julin, D. A. (1998). The 30-kDa C-terminal domain of the RecB protein is critical for the nuclease activity, but not the helicase activity, of the RecBCD enzyme from *Escherichia coli*. *Proc. Natl. Acad. Sci. USA* 95, 981-986.
48. Dupureur, C. M. & Dominguez, M. A. Jr. (2001). The PD...(D/E)XK motif in restriction enzymes: a link between function and conformation. *Biochemistry* 40, 387-394.
49. Selent, U., Ruter, T., Kohler, E., Liedtke, M., Thielking, V., Alves, J., Oelgeschlager, T., Wolfes, H., Peters, F. & Pingoud, A. (1992). A site-directed mutagenesis study to identify amino acid residues involved in the catalytic function of the restriction endonuclease *EcoRV*. *Biochemistry* 31, 4808-15.
50. Wang, J., Chen, R. & Julin, D. A. (2000). A single nuclease active site of the *Escherichia coli* RecBCD enzyme catalyzes single-stranded DNA degradation in both directions. *J. Biol. Chem.* 275, 507-513.
51. Yu, M., Souaya, J. & Julin, D. A. (1998). Identification of the nuclease active site in the multifunctional RecBCD enzyme by creation of a chimeric enzyme. *J. Mol. Biol.* 283, 797-808.
52. Churchill, J. J. & Kowalczykowski, S. C. (2000). Identification of the RecA protein-loading domain of RecBCD enzyme. *J. Mol. Biol.* 297, 537-42.
53. Anderson, D. G., Churchill, J. J. & Kowalczykowski, S. C. (1999). A single mutation, RecB(D1080A), eliminates RecA protein loading but not Chi recognition by RecBCD enzyme. *J. Biol. Chem.* 274, 27139-44.
54. Hsieh, S. & Julin, D. A. (1992). Alteration by site-directed mutagenesis of the conserved lysine residue in the consensus ATP-binding sequence of the RecB protein of *Escherichia coli*. *Nucleic Acids Res.* 20, 5647-5653.
55. Rinken, R., Thoms, B. & Wackernagel, W. (1992). Evidence that *recBC*-dependent degradation of duplex DNA in *Escherichia coli* *recD* mutants involves DNA unwinding. . *J. Bacteriol.* 174, 5424-5429.
56. Thaler, D. S., Sampson, E., Siddiqi, I., Rosenberg, S. M., Stahl, F. W. & Stahl, M. (1988). A hypothesis: Chi-activation of RecBCD enzyme involves removal of the RecD subunit. In *Mechanisms and Consequences*

of DNA Damage Processing (Friedberg, E. & Hanawalt, P., eds.), pp. 413-422. Alan R. Liss, Inc., New York.

57. Makarova, K. S., Aravind, L., Wolf, Y., Tatusov, R. L., Minton, K. W., Koonin, E. V. & Daly, M. J. (2001). Genome of the extremely radiation-resistant bacterium *Deinococcus radiodurans* viewed from the perspective of comparative genomics. *Microbiol. and Mol. Biol. Rev.* 65, 44-79.
58. Daly, M. J., Ouyang, L., Fuchs, P. & Minton, K. W. (1994). *In vivo* damage and *recA*-dependent repair of plasmid and chromosomal DNA in the radiation-resistant bacterium *Deinococcus radiodurans*. *J. Bacteriol.* 176, 3508-17.
59. Battista, J. R. (1997). Against all odds: the survival strategies of *Deinococcus radiodurans*. *Annu. Rev. Microbiol.* 51, 203-24.
60. Minton, K. W. (1994). DNA repair in the extremely radioresistant bacterium *Deinococcus radiodurans*. *Mol. Microbiol.* 13, 9-15.
61. Daly, M. J., Ling, O. & Minton, K. W. (1994). Interplasmidic recombination following irradiation of the radioresistant bacterium *Deinococcus radiodurans*. *J. Bacteriol.* 176, 7506-15.
62. Daly, M. J. & Minton, K. W. (1995). Interchromosomal recombination in the extremely radioresistant bacterium *Deinococcus radiodurans*. *J. Bacteriol.* 177, 5495-505.
63. Daly, M. J. & Minton, K. W. (1997). Recombination between a resident plasmid and the chromosome following irradiation of the radioresistant bacterium *Deinococcus radiodurans*. *Gene* 187, 225-9.
64. Battista, J. R., Earl, A. M. & Park, M. J. (1999). Why is *Deinococcus radiodurans* so resistant to ionizing radiation? *Trends Microbiol.* 7, 362-5.
65. Kuzminov, A. (1999). Recombinational repair of DNA damage in *Escherichia coli* and bacteriophage lambda. *Microbiol. Mol. Biol. Rev.* 63, 751-813.
66. Lin, J., Qi, R., Aston, C., Jing, J., Anantharaman, T. S., Mishra, B., White, O., Daly, M. J., Minton, K. W., Venter, J. C. & Schwartz, D. C. (1999). Whole-genome shotgun optical mapping of *Deinococcus radiodurans*. *Science* 285, 1558-62.
67. Grimsley, J. K., Masters, C. I., Clark, E. P. & Minton, K. W. (1991). Analysis by pulsed-field gel electrophoresis of DNA double-strand

- breakage and repair in *Deinococcus radiodurans* and a radiosensitive mutant. *Int. J. Radiat. Biol.* 60, 613-26.
68. Sweet, D. M. & Moseley, B. E. (1974). Accurate repair of ultraviolet-induced damage in *Micrococcus radiodurans*. *Mutat. Res.* 23, 311-8.
 69. Battista, J. R. (2000). Radiation resistance: the fragments that remain. *Curr. Biol.* 10, R204-5.
 70. Krasin, F. & Hutchinson, F. (1977). Repair of DNA double-strand breaks in *Escherichia coli*, which requires *recA* function and the presence of a duplicate genome. *J. Mol. Biol.* 116, 81-98.
 71. Harsojo, Kitayama, S. & Matsuyama, A. (1981). Genome multiplicity and radiation resistance in *Micrococcus radiodurans*. *J. Biochem. (Tokyo)* 90, 877-80.
 72. Punita, S. J., Reddy, M. A. & Das, H. K. (1989). Multiple chromosomes of *Azotobacter vinelandii*. *J. Bacteriol.* 171, 3133-38.
 73. Bauche, C. & Laval, J. (1999). Repair of oxidized bases in the extremely radiation-resistant bacterium *Deinococcus radiodurans*. *J. Bacteriol.* 181, 262-9.
 74. Hansen, M. T. (1980). Four proteins synthesized in response to deoxyribonucleic acid damage in *Micrococcus radiodurans*. *J. Bacteriol.* 141, 81-6.
 75. Tanaka, A., Hirano, H., Kikuchi, M., Kitayama, S. & Watanabe, H. (1996). Changes in cellular proteins of *Deinococcus radiodurans* following gamma-irradiation. *Radiat. Environ. Biophys.* 35, 95-9.
 76. Markillie, L. M., Varnum, S. M., Hradecky, P. & Wong, K. K. (1999). Targeted mutagenesis by duplication insertion in the radioresistant bacterium *Deinococcus radiodurans*: radiation sensitivities of catalase (*katA*) and superoxide dismutase (*sodA*) mutants. *J. Bacteriol.* 181, 666-9.
 77. White, O., Eisen, J. A., Heidelberg, J. F., Hickey, E. K., Peterson, J. D., Dodson, R. J., Haft, D. H., Gwinn, M. L., Nelson, W. C., Richardson, D. L., Moffat, K. S., Qin, H., Jiang, L., Pamphile, W., Crosby, M., Shen, M., Vamathevan, J. J., Lam, P., McDonald, L., Utterback, T., Zalewski, C., Makarova, K. S., Aravind, L., Daly, M. J., Fraser, C. M. & et al. (1999). Genome sequence of the radioresistant bacterium *Deinococcus radiodurans* R1. *Science* 286, 1571-7.

78. Moseley, B. E. & Copland, H. J. (1975). Isolation and properties of a recombination-deficient mutant of *Micrococcus radiodurans*. *J. Bacteriol.* 121, 422-8.
79. Gutman, P. D., Carroll, J. D., Masters, C. I. & Minton, K. W. (1994). Sequencing, targeted mutagenesis and expression of a *recA* gene required for the extreme radioresistance of *Deinococcus radiodurans*. *Gene* 141, 31-7.
80. Agostini, H. J., Carroll, J. D. & Minton, K. W. (1996). Identification and characterization of *uvrA*, a DNA repair gene of *Deinococcus radiodurans*. *J. Bacteriol.* 178, 6759-65.
81. Carroll, J. D., Daly, M. J. & Minton, K. W. (1996). Expression of *recA* in *Deinococcus radiodurans*. *J. Bacteriol.* 178, 130-5.
82. Narumi, I., Satoh, K., Kikuchi, M., Funayama, T., Kitayama, S., Yanagisawa, T., Watanabe, H. & Yamamoto, K. (1999). Molecular analysis of the *Deinococcus radiodurans* *recA* locus and identification of a mutation site in a DNA repair-deficient mutant, *rec30*. *Mutat. Res.* 435, 233-43.
83. Kim, J. I. & Cox, M. M. (2002). The RecA proteins of *Deinococcus radiodurans* and *Escherichia coli* promote DNA strand exchange via inverse pathways. *Proc. Natl. Acad. Sci. USA* 99, 7917-21.
84. Satoh, K., Narumi, I., Kikuchi, M., Kitayama, S., Yanagisawa, T., Yamamoto, K. & Watanabe, H. (2002). Characterization of RecA⁴²⁴ and RecA⁶⁷⁰ proteins from *Deinococcus radiodurans*. *J. Biochem. (Tokyo)* 131, 121-9.
85. Daly, M. J. & Minton, K. W. (1996). An alternative pathway of recombination of chromosomal fragments precedes *recA*-dependent recombination in the radioresistant bacterium *Deinococcus radiodurans*. *J. Bacteriol.* 178, 4461-71.
86. Karlin, S. & Mrazek, J. (2001). Predicted highly expressed and putative alien genes of *Deinococcus radiodurans* and implications for resistance to ionizing radiation damage. *Proc. Natl. Acad. Sci. USA* 98, 5240-5245.
87. Karlin, S. & Mrazek, J. (2000). Predicted highly expressed genes of diverse prokaryotic genomes. *J. Bacteriol.* 182, 5238-50.
88. Gupta, R. S. (1998). Protein phylogenies and signature sequences: a reappraisal of evolutionary relationships among archaeobacteria, eubacteria, and eukaryotes. *Microbiol. Mol. Biol. Rev.* 62, 1435-91.

89. Olsen, G. J. & Woese, C. R. (1993). Ribosomal RNA: a key to phylogeny. *FASEB J.* 7, 113-23.
90. Mattimore, V. & Battista, J. R. (1996). Radioresistance of *Deinococcus radiodurans*: functions necessary to survive ionizing radiation are also necessary to survive prolonged desiccation. *J. Bacteriol.* 178, 633-7.
91. Lennon, E., Gutman, P. D., Yao, H. L. & Minton, K. W. (1991). A highly conserved repeated chromosomal sequence in the radioresistant bacterium *Deinococcus radiodurans* SARK. *J. Bacteriol.* 173, 2137-40.
92. Udupa, K. S., O'Cain, P. A., Mattimore, V. & Battista, J. R. (1994). Novel ionizing radiation-sensitive mutants of *Deinococcus radiodurans*. *J. Bacteriol.* 176, 7439-46.
93. Boling, M. E. & Setlow, J. K. (1966). The resistance of *Micrococcus radiodurans* to ultraviolet radiation. 3. A repair mechanism. *Biochim. Biophys. Acta.* 123, 26-33.
94. Minton, K. W. & Daly, M. J. (1995). A model for repair of radiation-induced DNA double-strand breaks in the extreme radiophile *Deinococcus radiodurans*. *Bioessays* 17, 457-64.
95. Levin-Zaidman, S., Englander, J., Shimoni, E., Sharma, A. K., Minton, K. W. & Minsky, A. (2003). Ringlike structure of the *Deinococcus radiodurans* genome: a key to radioresistance? *Science* 299, 254-6.
96. Tatusov, R. L., Koonin, E. V. & Lipman, D. J. (1997). A Genomic perspective on protein families. *Science* 278, 631-637.
97. Tatusov, R. L., Fedorova, N. D. & Jackson, J. D. (2003). The COG database: an updated version includes eukaryotes. *BMC Bioinformatics* 4(1), 41.
98. Stephens, R. S. & Kalman, S. (1998). Genome sequence of an obligate intracellular pathogen of humans: *Chlamydia trachomatis*. *Science* 282, 754-759.
99. Chedin, F., Ehrlich, S. D. & Kowalczykowski, S. C. (2000). The *Bacillus subtilis* AddAB helicase/nuclease is regulated by its cognate Chi sequence *in vitro*. *J. Mol. Biol.* 298, 7-20.
100. Chedin, F., Noirot, P., Biaudet, V. & Ehrlich, S. D. (1998). A five-nucleotide sequence protects DNA from exonucleolytic degradation by AddAB, the RecBCD analogue of *Bacillus subtilis*. *Mol. Microbiol.* 29, 1369-1377.

101. Aravind, L., Walker, D. R. & Koonin, E. V. (1999). Conserved domains in DNA repair proteins and evolution of repair systems. *Nucleic Acids Res.* 27, 1223-1242.
102. Sambrook, J., Fritsch, E. F. & Maniatis, T. (1989). *Molecular Cloning: A Laboratory Manual*. 2nd edit. 3 vols, Cold Spring Harbor Laboratory Press, Cold Spring Harbor, NY.
103. Maniatis, T., Fritsch, E. F. & Sambrook, J. (1982). *Molecular Cloning: A Laboratory Manual*, Cold Spring Harbor Laboratory, Cold Spring Harbor, NY
104. Driedger, A. A. & Grayston, M. J. (1970). Rapid lysis of cell walls of *Micrococcus radiodurans* with lysozyme: effects of butanol pretreatment on DNA. *J. Microbiol.* 16, 889-93.
105. Lennon, E. & Minton, K. W. (1990). Gene fusions with *lacZ* by duplication insertion in the radioresistant bacterium *Deinococcus radiodurans*. *J. Bacteriol.* 172, 2955-61.
106. Thomas, J. G., Ayling, A. & Baneyx, F. (1997). Molecular chaperones, folding catalysts, and the recovery of active recombinant proteins from *E. coli*. To fold or to refold. *Appl. Biochem. Biotechnol.* 66, 197-238.
107. Korangy, F. & Julin, D. A. (1992). A mutation in the consensus ATP-binding sequence of the RecD subunit reduces the processivity of the RecBCD enzyme from *Escherichia coli*. *J. Biol. Chem.* 267, 3088-3095.
108. Eggington, J. M., Haruta, N., Wood, E. A. & Cox, M. M. (2004). The single-stranded DNA-binding protein of *Deinococcus radiodurans*. *BMC Microbiol.* 4, 2.
109. Patel, S. S. & Picha, K. M. (2000). Structure and function of hexameric helicases. *Annu. Rev. Biochem.* 69, 651-97.
110. Cheng, W., Hsieh, J., Brendza, K. M. & Lohman, T. M. (2001). *E. coli* Rep oligomers are required to initiate DNA unwinding *in vitro*. *J. Mol. Biol.* 310, 327-50.
111. Maluf, N. K., Fischer, C. J. & Lohman, T. M. (2003). A dimer of *Escherichia coli* UvrD is the active form of the helicase *in vitro*. *J. Mol. Biol.* 325, 913-35.
112. Velankar, S. S., Soultanas, P., Dillingham, M. S., Subramanya, H. S. & Wigley, D. B. (1999). Crystal structures of complexes of PcrA DNA

- helicase with a DNA substrate indicate an inchworm mechanism. *Cell* 97, 75-84.
113. Nanduri, B., Byrd, A. K., Eoff, R. L., Tackett, A. J. & Raney, K. D. (2002). Pre-steady-state DNA unwinding by bacteriophage T4 Dda helicase reveals a monomeric molecular motor. *Proc. Natl. Acad. Sci. USA* 99, 14722-7.
 114. Ganesan, S. & Smith, G. R. (1993). Strand-specific binding to duplex DNA ends by the subunits of the *Escherichia coli* RecBCD enzyme. *J. Mol. Biol.* 229, 67-78.
 115. Farah, J. A. & Smith, G. R. (1997). The RecBCD enzyme initiation complex for DNA unwinding: enzyme positioning and DNA opening. *J. Mol. Biol.* 272, 699-715.
 116. Lahaye, A., Leterme, S. & Foury, F. (1993). Pif1 DNA helicase from *Saccharomyces cerevisiae*. Biochemical characterization of the enzyme. *J. Biol. Chem.* 268, 26155-61.
 117. Ryu, G. H., Tanaka, H., Kim, D. H., Kim, J. H., Bae, S. H., Kwon, Y. N., Rhee, J. S., MacNeill, S. & Seo, Y. (2004). Genetic and biochemical analyses of Pfh1 DNA helicase function in fission yeast. *Nucleic Acids Res.* 32, 4205-16.
 118. Roman, L. J., Eggleston, A. K. & Kowalczykowski, S. C. (1992). Processivity of the DNA helicase activity of *Escherichia coli* RecBCD enzyme. *J. Biol. Chem.* 267, 4207-4214.
 119. Cheng, W., Brendza, K. M., Gauss, G. H., Korolev, S., Waksman, G., & Lohman, T. M. (2002). The 2B domain of the *Escherichia coli* Rep protein is not required for DNA helicase activity. *Proc. Natl. Acad. Sci. USA* 99, 16006-11.
 120. Maluf, N. K., Ali, J. A. & Lohman T. M. (2003). Kinetic mechanism for formation of the active, dimeric UvrD helicase-DNA complex. *J. Biol. Chem.* 278, 31930-40.
 121. Nanduri, B., Eoff, R. L., Tackett, A. J. & Raney, K. D. (2001). Measurement of steady-state kinetic parameters for DNA unwinding by the bacteriophage T4 Dda helicase: use of peptide nucleic acids to trap single-stranded DNA products of helicase reactions. *Nucleic Acids Res.* 29, 2829-35.
 122. Smith, M. D., Masters, C. I., Lennon, E., McNeil, L. B. & Minton, K. W. (1991). Gene expression in *Deinococcus radiodurans*. *Gene* 98, 45-52.

123. Masters, C. I., Smith, M. D., Gutman, P. D. & Minton, K. W. (1991). Heterozygosity and instability of amplified chromosomal insertions in the radioresistant bacterium *Deinococcus radiodurans*. *J. Bacteriol.* 173, 6110-7.
124. Masters, C. I. & Minton, K. W. (1992). Promoter probe and shuttle plasmids for *Deinococcus radiodurans*. *Plasmid* 28, 258-61.
125. Kitayama, S. (1982). Adaptive repair of cross-links in DNA of *Micrococcus radiodurans*. *Biochim. Biophys. Acta.* 697, 381-4.
126. Anand, S. P. & Khan, S. A. (2004). Structure-specific DNA binding and bipolar helicase activities of PcrA. *Nucleic Acids Res.* 32, 3190-97.
127. Korangy, F. & Julin, D. A. (1993). Kinetics and processivity of ATP hydrolysis and DNA unwinding by the RecBC enzyme from *Escherichia coli*. *Biochemistry* 32, 4873-4880.
128. Bianco, P. R. & Kowalczykowski, S. C. (2000). Translocation step size and mechanism of the RecBC DNA helicase. *Nature* 405, 368-372.
129. Chaudhury, A. M. & Smith, G. R. (1984). *Escherichia coli* recBC deletion mutants. *J. Bacteriol.* 160, 788-791.
130. Raney, K. D., Sowers, L. C., Millar D. P. & Benkovic, S. J. (1994). A fluorescence-based assay for monitoring helicase activity. *Proc. Natl. Acad. Sci. USA* 91, 6644-8.
131. Jeong, Y. J., Levin, M. K. & Patel, S. S. (2004). The DNA-unwinding mechanism of the ring helicase of bacteriophage T7. *Proc. Natl. Acad. Sci. USA* 101, 7264-69.
132. Bjornson, K. P., Amaratunga, M., Moore, K. J. & Lohman, T. M. (1994). Single-turnover kinetics of helicase-catalyzed DNA unwinding monitored continuously by fluorescence energy transfer. *Biochemistry* 33, 14306-16.
133. Dessinges, M. N., Lionnet, T., Xi, X. G., Bensimon, D. & Croquette, V. (2004). Single-molecule assay reveals strand switching and enhanced processivity of UvrD. *Proc. Natl. Acad. Sci. USA* 101, 6439-44.
134. Tuteja, N & Phan, T. N. (1998). A chloroplast DNA helicase II from pea that prefers fork-like replication structures. *Plant Physiology.* 118, 1029-38.
135. Zhang, S. S. & Grosse, F. (1991). Purification and characterization of two DNA helicases from calf thymus nuclei. *J. Biol. Chem.* 266, 20483-90.

136. Tuteja, N., Rahman, K., Tuteja, R. & Falaschi, A. (1991). DNA helicase IV from HeLa cells. *Nucleic Acids Res.* 19, 3613-8.
137. Scherzinger, E., Ziegelin, G., Barcena, M., Carazo, J. M., Lurz, R. & Lanka, E. (1997). The RepA protein of plasmid RSF1010 is a replicative DNA helicase. *J. Biol. Chem.* 272, 30228-36.
138. Tuteja, N., Ochem, A., Taneja, P., Tuteja, R., Skopac, D. & Falaschi, A. (1995). Purification and properties of human DNA helicase VI. *Nucleic Acids Res.* 23, 2457-63.
139. Liu, Y., Zhou, J., Omelchenko, M. V., Beliaev, A. S., Venkateswaran, A., Stair, J., Wu, L., Thompson, D. K., Xu, D., Rogozin, I. B., Gaidamakova, E. K., Zhai, M., Makarova, K. S., Koonin, E. V. & Daly, M. J. (2003). Transcriptome dynamics of *Deinococcus radiodurans* recovering from ionizing radiation. *Proc. Natl. Acad. Sci. USA* 100, 4191-6.
140. Lipton, M. S., Pasa-Tolic, L., Anderson, G. A., Anderson, D. J., Auberry, D. L., Battista, J. R., Daly, M. J., Fredrickson, J., Hixson, K. K., Kostandarithes, H., Masselon, C., Markillie, L. M., Moore, R. J., Romine, M. F., Shen, Y., Stritmatter, E., Tolic, N., Udseth, H. R., Venkateswaran, A., Wong, K. K., Zhao, R. & Smith, R. D. (2002). Global analysis of the *Deinococcus radiodurans* proteome by using accurate mass tags. *Proc. Natl. Acad. Sci. USA* 99, 11049-54.
141. Belland, R. J., Zhong, G., Crane, D. D., Hogan, D., Sturdevant, D., Sharma, J., Beatty, W. L. & Caldwell, H. D. (2003). Genomic transcriptional profiling of the developmental cycle of *Chlamydia trachomatis*. *Proc. Natl. Acad. Sci. USA* 100, 8478-8483.